Gelation and Hardening Mechanisms in a Model Polyester Resin and Related Systems.

A thesis submitted to Glasgow University in fulfilment of the requirements for the Degree of Doctor of Philosophy

by

Brian M. Grieveson.

April 15th. 1957.

The author is greatly indebted to Dr.M. Gordon for the suggestions and encouragement given during the course of this work. Thanks are also due to Professor P.D. Ritchie of the Royal College of Science and Technology, Glasgow, and Professor R.H. Peters of the College of Science and Technology, Manchester, in whose departments the work was carried out.

Contents.

Summary.

Widespread industrial use of unsaturated polyester "contact" resins has led to speculation concerning the mechanism of their hardening reaction. Model compounds for the commercial polyesters were therefore prepared, and their hardening reaction with methyl methacrylate was studied using an original combined viscometer-dilatometer.

Investigations into the effect of variations in the amount and type of free radical initiator showed that the gelation of the model system occurred through a conventional addition copolymerisation between the two types of unsaturation present, and also provided confirmation for the proposed kinetic scheme for the pre-gelation reaction mechanism. Preliminary investigations were made into the change in the reaction rate curve in the region of the gel point when passing from a linear to a related polyfunctional (non-linear) polymerisation, and a theoretical explanation is given for the sharpening of the gradual rate increase into a definite kink occurring at the gel point. Infrared examination of the model polyesters prepared from maleic anhydride showed that almost complete isomerisation of the unsaturated linkage from the cis to the trans form took place during the polycondensation reaction.

The final stages in the curing of a polyester resin, which are of direct technical interest because of their

effect on the high temperature properties of laminating resins, were studied using a ball rebound relaxation technique which produced mechanical "spectra" of the polymer. Second order transition phenomena were shown to give rise to strong absorption peaks, the positions of which were used to follow curing reactions. An "isoelastic rate principle" is proposed for the final decay of the curing rate based on the supposition that curing mechanisms in this phase of the reaction are diffusion controlled relaxation processes. The applicability of the principle to resin systems in general was successfully illustrated by experiments on a base-catalysed epoxide system and an acid-catalysed urea-formaldehyde polycondensation as well as on the vinyl copolymerisation of the model polyester. Observations were made on the relationship between the final state of cure reached in the model polyester system and its original composition.

Incidental measurements involved in the evaluation of the ball rebound relaxation technique led to the detection of unusual characteristics in the melting behaviour of linear polyethylenes and isotactic polypropylenes.

1. Introduction.

In a patent applied for in 1936[1], there was a reference to polymers of ethylene glycol maleate copolymerised with monomeric styrene, which marked the approximate beginning of present day unsaturated alkyd "contact" resins. Commercial development of unsaturated polyester resins began in the United States in 1941 when an allyl casting resin (allyl diglycol carbonate) was introduced. Contact resins, usually used as glass fabric reinforced laminates, are now widely used in industry in a number of applications such as car and bus bodies, boat hulls, helmets, corrugated roofing lights, and several types of military equipment. These widespread uses, which accounted for an annual production in the United Kingdom of about 1500 tons in 1955, have lead to speculation[2 & 3] concerning the mechanism of their hardening reaction.

The belief has found acceptance that the reactions are conventional copolymerisations between the two types of unsaturation present, the vinyl or allyl monomers and the unsaturated linear polyester crosslinker components. However, although several investigations (e.g. reference 3) have been made into the effect of the chemical structure on the physical properties and the thermal stability of the fully cured polyester resin, little or no work has so far been reported concerning the more fundamental aspects of the polymerisation reaction.

Commercial unsaturated polyester resins are usually composed of a glycol "maleate" polyester modified with varying proportions of saturated dibasic acids in order to improve the flexibility of the final product (i.e. the double bonds are spaced out by flexible saturated groups). This polyester is dissolved in a vinyl or allyl monomer of which the most common is styrene. The other monomers which are used include methyl methacrylate, vinyl acetate, diallyl phthalate, vinylidene chloride and triallyl cyanurate. Before use, a free radical initiator such as benzoyl peroxide or methyl ethyl ketone peroxide is added to the resin syrup which then "cures" to form a hard crosslinked polymer.

The model system chosen to represent the "contact resin" polyesters in this study of their reaction mechanisms was a condensation product of ethylene glycol and maleic anhydride This was a low molecular weight unsaturated polyester which thus embodied the essential properties of the commercial products. The saturated acid component was ommitted from the model compound since it plays no part in the hardening reaction being merely a means of modifying the final physical properties. The absence of this component also greatly simplified the characterisation of the model. The unmodified glycol-maleic anhydride condensation product was found to be insoluble in styrene and therefore methyl methacrylate, the next most widely used in commercial practice, was chosen as comonomer.

The range of model polyesters of different molecular weights used in this work were characterised by number average molecular weight determinations, measurements of density and refractive index and infrared spectroscopic examination. The infrared examination incidentally showed that during the polycondensation reaction, the maleic double bond underwent cis-trans isomerisation. Therefore, although the model resins were in fact prepared from maleic anhydride, they are alluded to throughout this thesis as polyethylene fumarate resins (PEF).

The bulk polymerisation reaction of vinyl compounds may be divided into three stages. In the first stage, reaction takes place in a low viscosity medium in which relatively low monomer to polymer conversions exist. Here, the mechanism may be treated by classical mass law theories involving the assumption of the main steps of initiation, propagation, termination, and possibly such subsidiary steps as chain transfer. The two later stages arise from the fact that the elementary steps are liable to become rate controlled by diffusion due to the increasing viscosity. In the second stage, diffusion control affects the termination step which may result in an exponential increase in the rate of monomer consumption (the Trommsdorf or Gel Effect), and the reaction rate at these intermediate conversions can be treated in terms of diffusion control of termination alone. In the third phase, the propagation rate, transfer rates, and

eventually also the initiation rate may be become diffusion controlled and the kinetic characteristics are least dependent on the chemical nature of the system. Near equilibrium, the rate decays to zero under the sway of diffusion control in a rubbery or glassy system.

In the work reported here, investigations have been made into the first and final stages of the copolymerisation of the model "contact resin" system. The results obtained, together with the results from an independent study[4] of the intermediate second stage, shed some light on the reaction mechanisms involved.

In the study of the initial stages of the polyethylene fumarate/methyl methacrylate (PEF/MMA) reaction, it was assumed that the reaction was an addition copolymerisation to which the classical network theory of gelation due to Flory[5] and Stockmayer[6] could be applied. Flory[5a] postulated that the gel point in polyfunctional reactions occurs when the weight average molecular weight (and hence also the viscosity) becomes infinite; i.e. when, in an infinite sample of the reaction mixture, the weight fraction of infinite networks first excedes zero. A general equation has been deduced in various ways [5a,6b,7]. for determining this critical condition (denoted throughout this thesis by the subscript $_c$) in terms of the fraction ϕ of the functionalities which have reacted, viz

$$\phi_c = 1/(f_w - 1) \qquad (1)$$

where f_w is the weight average functionality of the molecules present initially i.e. when $\phi = 0$. A generalised form of equation (1) is in this work, applied to the PEF/MMA system, and the theoretical gelation behaviour thus predicted is compared with experimental observations. Simultaneous and continuous measurements of the viscosity and the reaction rate (via the shrinkage in the volume of the reaction mixture) have been made using an original combined viscometer-dilatometer or viscodilatometer. These measurements have shown substantial agreement with the postulated simple addition-copolymerisation theory.

While this work was in progress, measurements were published concerning gelation phenomena in a series of diallyl monomers. Simpson and Holt[8] claimed that these results were not in accordance with the gelation theory of polyfunctional additions, and since the PEF/MMA system had been shown to conform to the theory, it was decided to reinvestigate the diallyl gelations using the viscodilatometric technique in order to establish whether the reported discrepancies were real and significant.

In the third stage of the PEF/MMA bulk polymerisation, the reaction rate decays to zero under the sway of diffusion control as the system approaches its equilibrium state of cure. The kinetic characteristics in this phase are least dependent on the chemical nature of the system, and it was therefore thought desirable to widen the scope of the

investigation so as to embrace a range of resin curing reactions in which a curing rate decays to zero.

An understanding of the nature of curing reactions is of great interest to industry[9], and many methods have been evolved for the measurement of "cure", especially for following the last stages of the reaction. A torsion pendulum method has been used to investigate the cross-linking reaction in phenol-formaldehyde novolacs[10], and the Schmidt-Bisterfeld hot needle test[11] is used for the evaluation of the final state of cure in phenolic resins. Measurements of ultrasonic wave propagation[12], electrical conductivity[13], density[13], and infrared radiation absorption characteristics[14] have been used to study a variety of curing reactions, but all the data thus obtained is vague. The object has been to find a quick precise method of measuring the rate of curing and to obtain absolute values which can be correlated to the chemical structure of individual polymers.

Recent developments have shown the usefulness of relaxation methods for studying the kinetics of rapid molecular processes in a remarkable diversity of phenomena. Leonard[15] used ultrasonic measurements to study relaxation in the gas phase, Schultz-Grünow and Weyman[16] investigated relaxation effects in the non-Newtonian viscosity behaviour of liquids, Zener[17] has described a whole spectrum of relaxation processes in metals, and nuclear magnetic resonance studies[18] have been used to measure the various kinds of relaxation

shown by magnetic dipoles in solids. In the field of polymer chemistry, relaxation methods have been extensively used for various purposes (e.g. Ferry[19], Tobolsky[20], Müller[21], Stavermann[22], Bueche[23], Wolf[24], and Chuikin[25].), but the main accent has been on the relationships between chemical structure and mechanical behaviour. The use of such parameters as dielectric constant, mechanical modulus, or stress relaxation rate for the study of second order transition temperatures is partly due to the fact that the practical importance of such transitions lies chiefly in the associated changes in these electrical and mechanical properties, and partly also because their measurement allows the use of powerful experimental and analytical techniques. This has led to the description of mechanically observed transitions in terms of spectra of relaxation times[26] based on Maxwell's treatment of viscosity[27], and the interpretation of dielectric transitions in terms of Debye's molecular relaxation theory[28 & 29]. Since however, mechanical dispersion is quite analogous to dielectric dispersion, the mechanical results have also been interpreted in terms of an extension of Debye's theory.

The study of curing reactions is essentially a study of the rate at which the segments of the polymer chains diffuse towards each other through the rubbery mass in order to become crosslinked. They diffuse in virtue of their rotational modes of motion, and for the investigation

of the speed of segmental rotations, relaxation methods (which match an applied frequency with the internal frequency of the molecular motion) are particularly suitable.

It was therefore decided to use an appropriate relaxation technique for measurements of rates of curing by scanning the energy absorption characteristics over a range of temperatures at some suitable deformation frequency. The characteristics required by the scanning apparatus were:

a) It should have accurate temperature control of the polymer specimen together with rapid temperature adjustment over a wide range.

b) Measurements should be rapid to enable changes in state of cure to be accurately followed.

c) It should have facility for testing in vacuo or in an inert atmosphere.

d) Only a small polymer specimen should be required, and the test should be non-destructive.

These requirements were all embodied in the ball rebound relaxation apparatus which was developed and which was used for investigations into the curing mechanisms of the last stages of the PEF/MMA model polyester hardening reaction and also an epoxide resin curing reaction. The aim of the work was to demonstrate that the final stage of the curing was a diffusion controlled relaxation process, and as a result of the study of these and other resin curing systems, a general "isoelastic rate principle" is proposed. The

succesful verification of this principle showed that the reaction rates were dependent on rates of interchange of position between segments of the polymer chains in that two apparently different properties - chemical rates and elasticity, were correlated (i.e. both depended on the segmental relaxation rate). Incidental measurements involved in the evaluation of the experimental data produced by the ball rebound apparatus also led to the detection of hitherto unknown phenomena in the melting characteristics of linear polyethylenes and isotactic polypropylenes.

2. Experimental Techniques and Materials.

2.1 The Viscodilatometer.

Because of the importance of polymerisation rates, viscosities and the interconnections between these two quantities in polymerising systems in general, and in the model polyester resin system in particular, it was felt that some means of making simultaneous measurements of them was required. Menary, Ubbelohde and Wright[30] have described a densitometer-viscometer using a steel cored glass float. To determine the density of the polymerisate, this float could be brought to rest in it electomagnetically with a coil acting as a current balance. Relative viscosities were obtained from the density and the time of rise of the float between fixed marks on the reaction tube. It was decided that a simpler instrument, more convenient to use, was needed.

The requirements were met by the development of a viscometer-dilatometer (or viscodilatometer) which is continuous rather than intermittent in its use. This instrument combines the normal dilatometer with a plug viscometer, which takes certain trends in the design of capillary micro-viscometers to their logical conclusion. Signer and Berneis[31] have described such a capillary instrument. It evaluates viscosities <u>via</u> Poiseuille's law applied to the gravity flow rate of a column of solution bounded by two menisci through a narrow capillary making

a low angle with the horizontal. As is desirable in polymerisation work, the viscosity is thus measured at extremely low rates of shear. To eliminate end corrections, Umstätter[32] prefers to confine the two menisci in capillaries of much wider bore, while the hydrodynamic resistance is furnished by a connecting narrow bore capillary. He considers that this method should be applicable down to capillary diameters of 0.1μ. A plug of sintered glass is roughly equivalent to a number of very fine capillary elements mounted in parallel, and it is more easily made than a single uniform capillary. The flow rate through a porous plug follows Darcy's law[33] rather than Poiseuille's law, and though these laws lead to precisely the same dependence of flow rate on viscosity and pressure, it must be admitted that Poiseuille's law has a theoretical, and Darcy's law only an empirical status. This point however does not detract from the usefulness of the viscodilatometer. The consistency of the results obtained is illustrated below (**Table 2 and Appendix II**).

Details of the Pyrex viscodilatometer and the brass stand on which it was mounted are shown in Fig.1. The porous plugs of the viscodilatometers were made from crushed Pyrex, the fraction collected between 60 and 80 mesh in a B.S. sieve being used (cf. Gordon and Macnab[34]). A 0.5 to 1.0 cm. column of the dry crushed glass was formed about 1cm. from the end of an 8cm. length of precision bore capillary

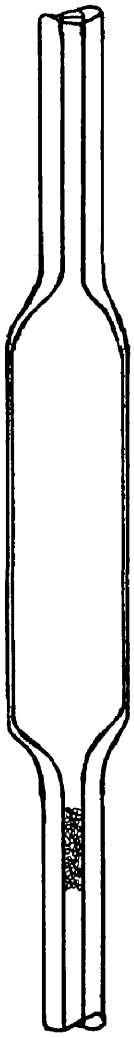

Detail of the
Viscodilatometer

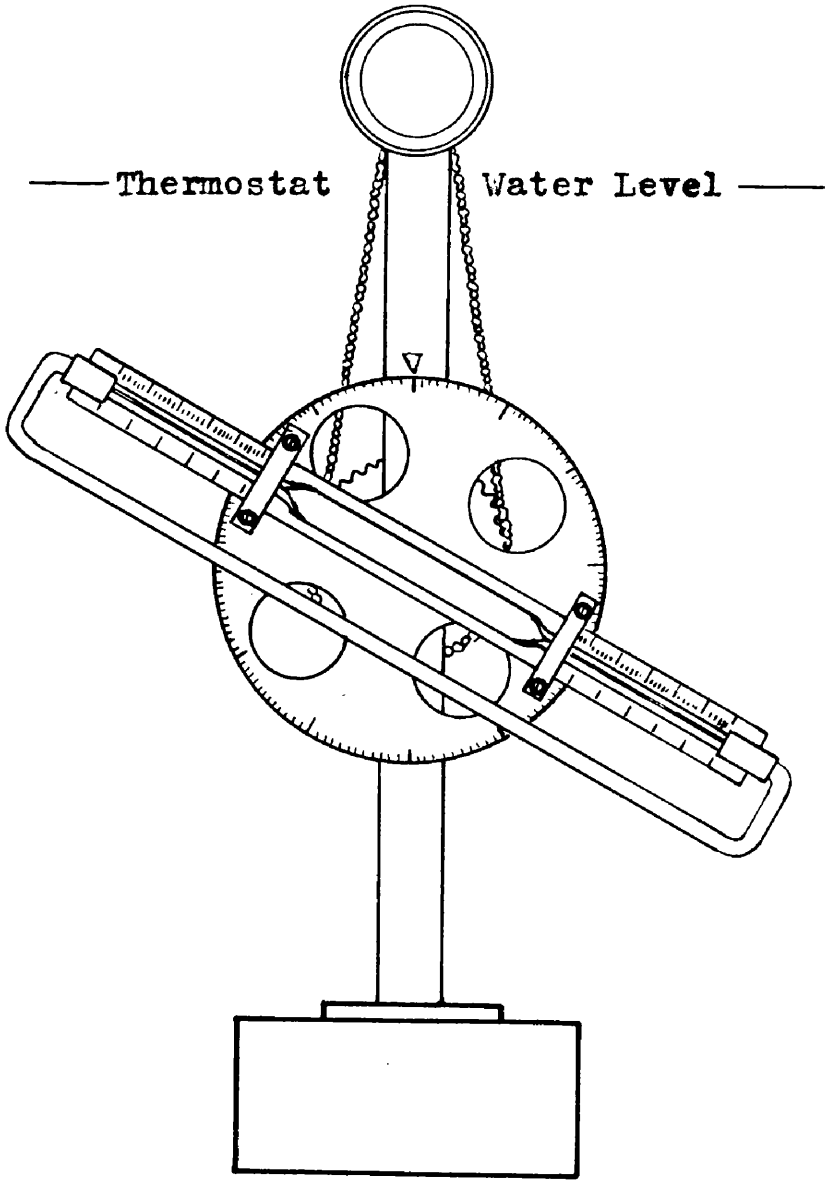

A viscodilatometer
mounted on its stand.

Figure 1.

tubing (1·5 mm. internal diameter), using a fine glass rod to hold the powder in position. The column was heated in a batswing flame until the powder sintered to form a porous plug. Any slight shrinkage of the sintered mass was corrected by adding further powder and resintering. The plugs used in this work had an average maximum pore size of 90 microns as determined by the method described in B.S.S. 1752.1952. The pore size could be controlled by using crushed glass of a different fineness and by varying the amount of sintering. The capillary tubing was then sealed to the dilatometer bulb as shown in Fig.1. Care was taken to ensure that the capillary containing the plug and the plug-free capillary sealed to the other end of the dilatometer bulb were colinear. This was achieved by rotating the viscodilatometer in a brass jig during the sealing operation. The instrument was calibrated for volume by measuring the lengths of columns of known weights of distilled water at 20°C, and for viscosity by measurements of the rate of flow of these columns of water again at 20°C. Viscodilatometers were filled by applying suction to the capillary containing the porous plug, dipping the other (open) end under the surface of the liquid to be observed, and letting it rise slowly to the required level (allowing for thermal expansion) taking care to exclude all air bubbles from the plug. The ends of the instrument were then joined *via* polythene connections, with glass tubing. Rubber

tubing was originally used for the connections, but although no trouble due to inhibition of polymerisation by sulphur extracted from the rubber was ever noted, it was thought better to abandon its use. The viscodilatometer unit was then clamped to the circular brass disc on top of a glass scale engraved in 1/3mm., as shown in Fig.1. The brass disc, which was mounted on a vertical column rising from a heavy base block, could be rotated through any angle required via a chain drive from a knob at the top of the vertical column. When in use, the whole apparatus except the knob was totally immersed in a thermostatically controlled water bath. On the completion of the series of polymerisation experiments to be described here, a design for a slightly modified instrument was prepared on the basis of the experience gained. The apparatus developed for marketing by Townson and Mercer Ltd. based on this design is shown in Fig.2 together with the original instrument used in this work.

The rate of flow of a column of liquid through the plug was proportional to the sine of the angle of inclination of the viscodilatometer to the horizontal both in theory and in practice (Appendix Table 1). A considerable range of viscosities could therefore be covered with one visco-dilatometer by adjusting the angular setting. A comparison of viscosities measured with a plug viscometer and those using an Ostwald viscometer was made with solutions of polymethyl methacrylate in methyl methacrylate monomer

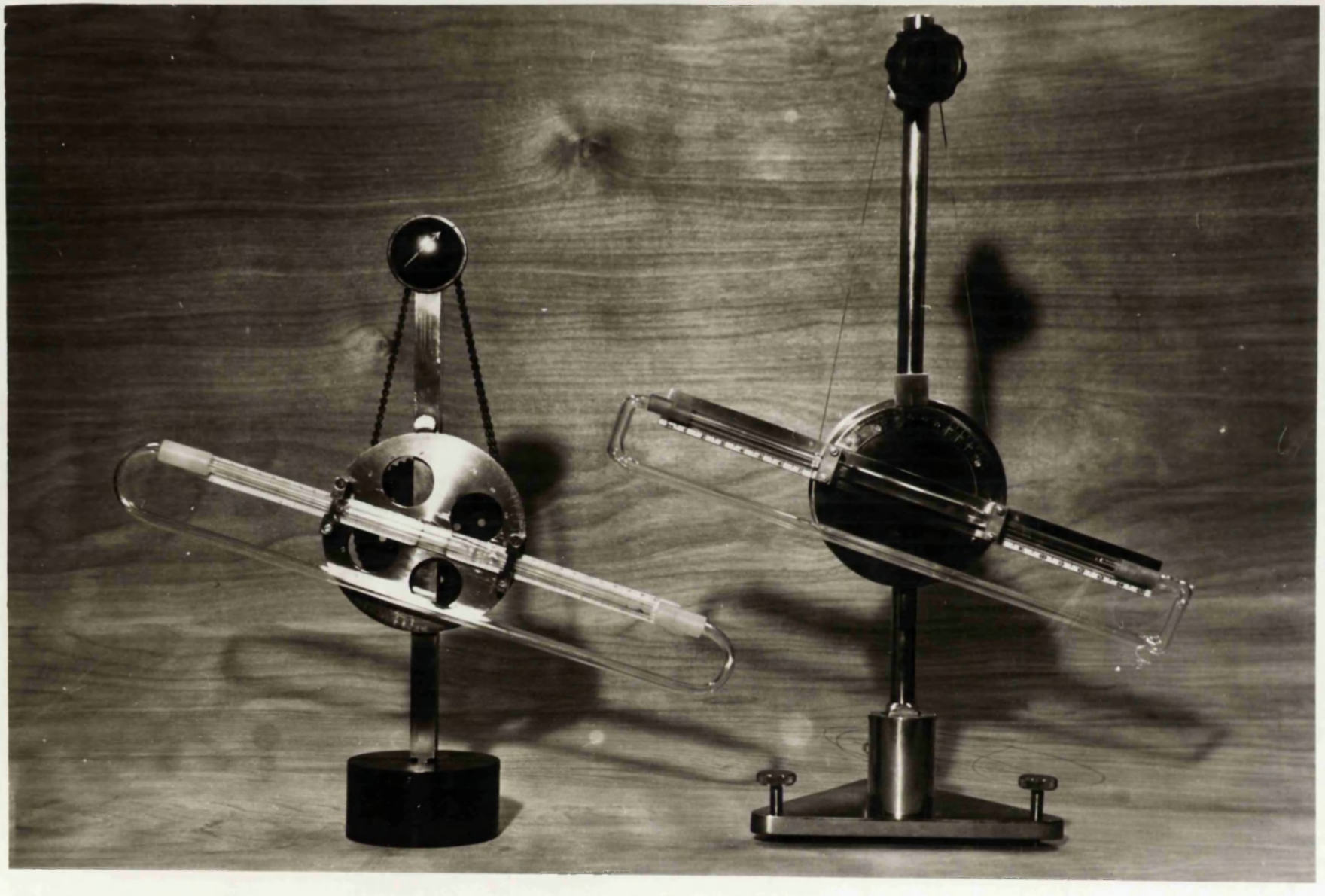

Figure 2.

containing 1% hydroquinone as inhibitor. Good agreement between the two methods was obtained over a viscosity range of three decades as shown in Fig.3.

Fig.4 shows the type of result obtained when using a viscodilatometer to follow the course of a polyethylene fumarate/methyl methacrylate polymerisation. An equimolar mixture of the comonomers together with 2% methyl ethyl ketone peroxide (MEK) as initiator was polymerised at 62°C in a viscodilatometer inclined at an angle of 20° to the horizontal. Readings of the positions of the two resin menisci on the glass scale were taken at intervals, and are here shown plotted against reaction time. The upper curve shows the progress of the meniscus in the plug end of the viscodilatometer. This movement is practically independent of the shrinkage occuring in the resin due to polymerisation, and the reciprocal of the slope of this upper curve is proportional to the viscosity of the resin which can thus be measured at any point. At the end of experiment the viscosity rapidly reaches infinity due to gelling of the resin. The middle curve of Fig. 4 records the readings for the displacement of the meniscus in the open (plugless) end of the instrument. This displacement includes almost completely the decrease in the resin volume. The amount of shrinkage is then plotted at the bottom of the figure as the difference of the two curves, and this plot is a measure of the progress of the polymerisation

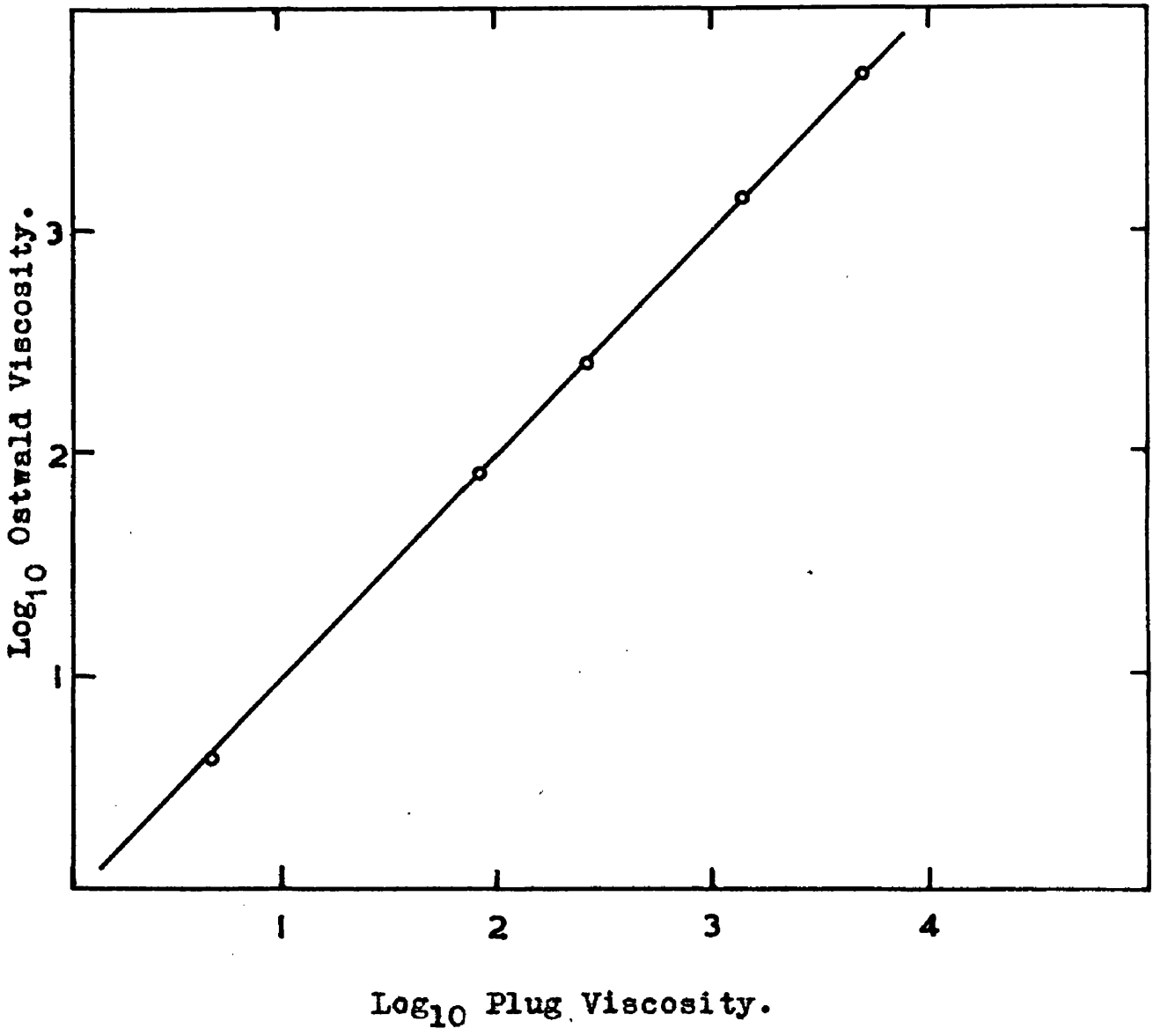

Figure 3 .

Comparison of the viscosities obtained using an Ostwald and a Plug viscometer on solutions of polymethyl methacrylate.

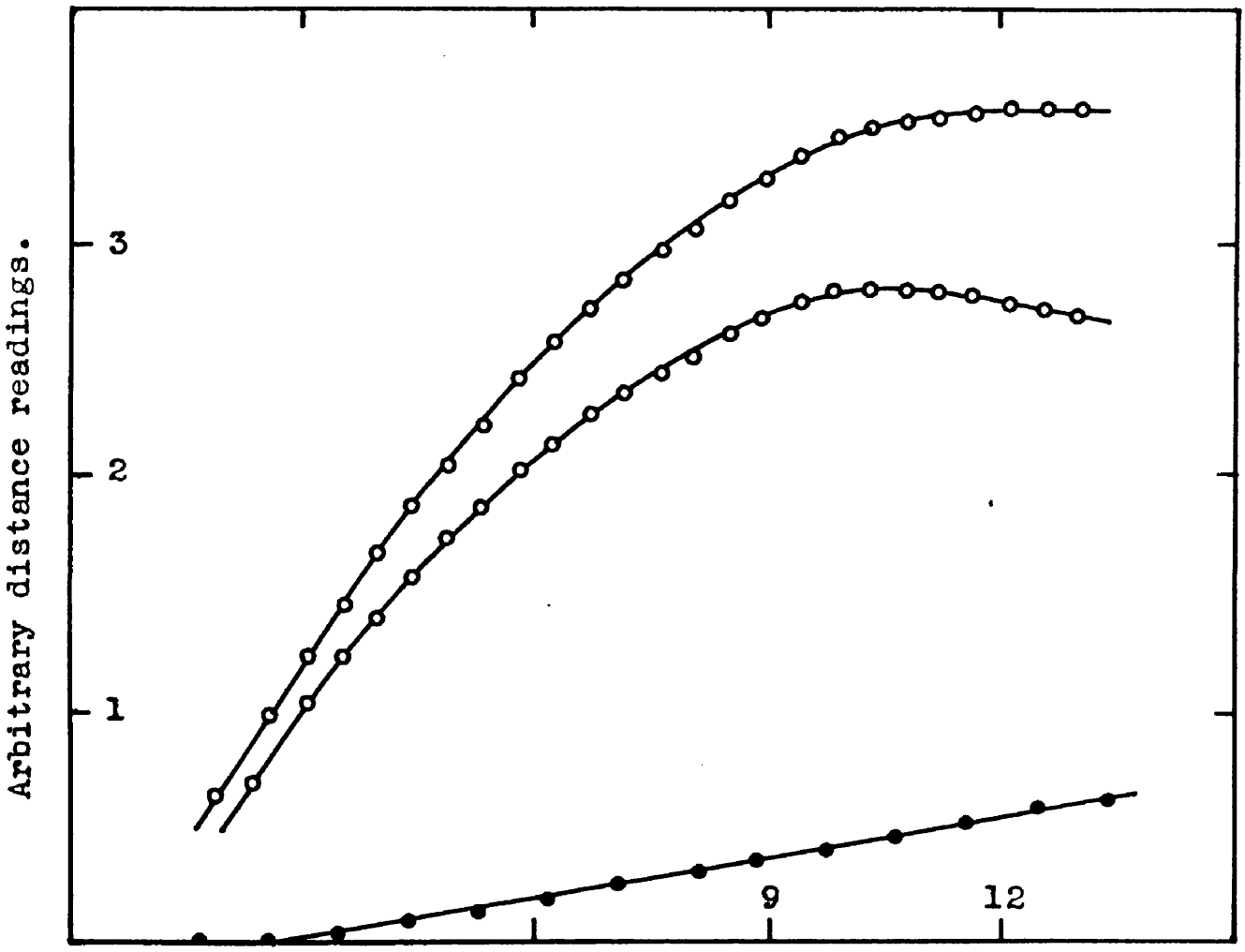

Figure 4 .

Viscodilatometric plot of the results obtained when following a PEF/MMA copolymerisation at 62°C.

o - menisci readings.

• - shrinkage plot,

reaction which is seen to be linear with time after a short induction period.

The meniscus at the plug end is prevented by surface tension from passing through the plug. This conveniently prevents the resin from running out of the instrument. Incidentally, the use of a porous plug in this way instead of the usual tap, to define the volume of liquid in a dilatometer, suggests itself as a general method (ease of filling, absence of leakage and contamination). If the meniscus approaches the plug before the gel point, the instrument can, of course, be rotated from the angle θ to $-\theta$, and the resin thus run back and forward repeatedly if necessary. In a typical run illustrated in Fig.5, it was necessary to invert the viscodilatometer nine times during the run, and at the last inversion, the angle was changed from 10° to 60° in order to make the location of the gel point more accurate (i.e. by increasing the rate of flow by sin 60°/sin 10°).

A further justification of the validity of the visco-dilatometric technique has been furnished since this work was completed. The method was used[35] to evaluate the constant K in the Mark-Houwink equation in the form :-

$$[\eta] = KM_n^{0.8} \qquad (2)$$

A mean value of $K = 5.28 \times 10^{-5}$ was obtained which compares favourably with the independent determination by Bamford and Dewar[36] who quote $K = 5.05 \times 10^{-5}$.

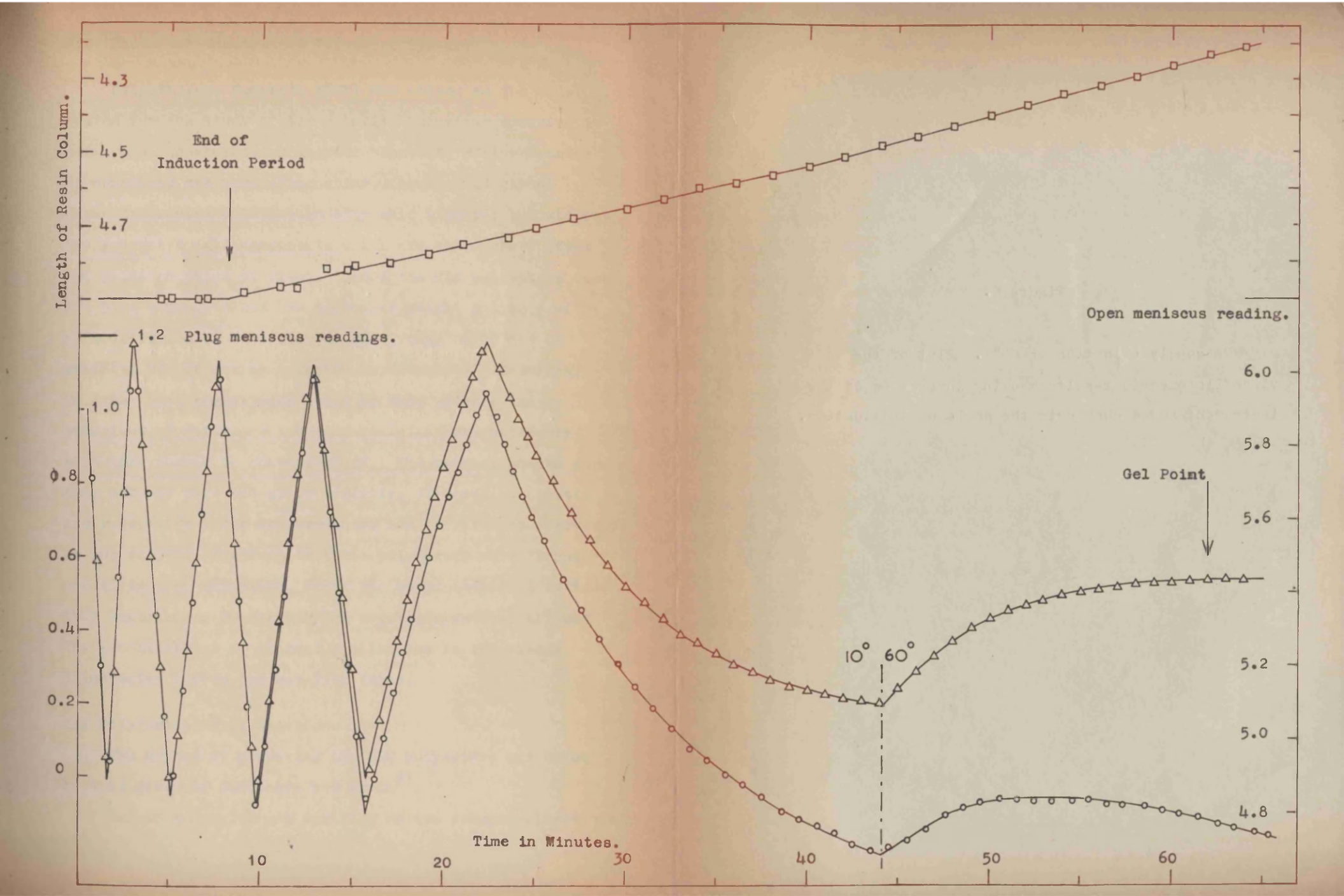
Length of Resin Column.
4.3
4.5
4.7
End of
Induction Period
Open meniscus reading.
1.2
Plug meniscus readings.
1.0
0.8
0.6
0.4
0.2
0
6.0
5.8
Gel Point
5.6
10°
60°
5.2
5.0
4.8
Time in Minutes.
10
20
30
40
50
60

Figure 5.

PEF/MMA copolymerisation at 62°C. Plot of the viscodilatometric results showing inversions of the instrument and a change in the angle of inclination.

2.2 The Model Unsaturated Polyester System.

Polyethylene fumarate (PEF) was chosen as the model system for the study of the gelation behaviour occuring in commercial unsaturated polyester "contact" resins because it contained the same alternating dibasic acid/glycol structure having unsaturated ethylenic linkages but without the saturated acid components which are unnecessary (from the gelation point of view). Since the PEF polyesters were not pure compounds but low molecular weight polymers with a distribution of molecular weights, they could not be purified before use in gelation experiments. Therefore, in order that comparisons could be made between the behaviour of various batches of resin, it was necessary that they should be characterised. The methods chosen for this purpose were end-group analysis, cryoscopic, density and refractive index measurements, and infrared spectroscopy. In one respect, the fact that the polyesters were "impure" was in fact an advantage, since the short induction periods thus experienced in the PEF/MMA copolymerisations allowed the establishment of thermal equilibrium in the visco-dilatometer before the reaction began.

The Polycondensation Reaction.

The method of preparing the PEF polyesters was based on that given by Carothers and Arvin[37].

Maleic anhydride was purified by two recrystallisations

from chloroform, and ethylene glycol was distilled in a current of carbon dioxide at 20mm. Hg. pressure. The anhydride and glycol were mixed in the molar ratio 1:1·05 and were heated to and maintained at 195°C (±5°). A stream of carbon dioxide was bubbled through the stirred melt throughout the reaction, and the aqueous distillate was condensed and led away. Samples were withdrawn from the reaction mixture when the required molecular weights were reached, and these polymers were stored under carbon dioxide in dark bottles at 5°C. Under these storage conditions, it was found that over a period of six months, no measurable change in the degree of polymerisation had occurred.

The glass clear, almost colourless resins ranged from a syrupy consistency (Molecular Weight = 450) to a pitch-like consistency (Mol. Wt. = 1300). They were best handled in the glassy state by cooling with solid carbon dioxide after which they could be chipped and powdered.

Characterisation.

End-group molecular weights were determined by titrating an ice cold solution of about 0·2g. resin in 10 ml. A.R. grade dioxan with decinormal sodium hydroxide solution using phenolphthalein indicator. The end point was judged to have been reached when the addition of one drop of alkali gave a red colouration lasting for at least five

seconds. This end point was reproducible to ± 1·5%, and all values quoted for the end-group number average degree of polymerisation DP_{ne} are averages of three titrations. The refluxing of the dioxan solution before titration to expel any dissolved carbon dioxide did not alter the end point.

The cryoscopic molecular weight determinations were made using A.R. dioxan as a solvent in a standard Beckmann freezing point apparatus. The freezing point depression constant k for the dioxan was determined using benzoic acid (k found = 4.565°C.l.mol^{-1}) and p-toluidine (k found = 4.670°C.l.mol^{-1}). Both reference substances had been purified by repeated recrystallisations and the mean value k = 4.617°C.l.mol^{-1} (± 1.5%) was accepted. All cryoscopic degrees of polymerisation quoted (DP_n) are averages of three determinations.

The resin samples for density determinations were degassed under 15mm. Hg pressure at 100°C. Since the very high viscosity made complete filling difficult, only sufficient resin to fill the pyknometer about three-quarters full was used together with distilled water as confining liquid. The densities were measured at 300°K.

Refractive indices were measured with an Abbé refractometer thermostated at 300°K, small samples of degassed resin being smeared on the prism with a warm spatula.

The condensation times, molecular weights, and physical properties of all resins used are given in the Appendix (Table 2).

For comparison with polyesters produced from maleic anhydride, an isomeric (trans) polyester was prepared from ethyl fumarate and ethylene glycol. The two redistilled liquids were condensed in the mole ratio 1:1·05 in a carbon dioxide atmosphere at 195°C until the required degree of polymerisation had been reached.

The molecular weight of the ethyl fumarate polyester was determined cryoscopically using dioxan as the solvent. It was found that polyesterification took place at less than half the rate observed in the maleic anhydride reaction:

a) ethyl fumarate + glycol, 5 hours 20 mins. condensation time, resultant molecular weight (weight average) 424.

b) maleic anhydride + glycol, 5 hours 15 mins condensation, resultant weight average molecular weight - 967.

The ethyl fumarate resin was much less soluble in methyl methacrylate monomer than the maleic anhydride resins. An attempted copolymerisation at 62°C could not be completed because after a short time, particles of precipitated polyester blocked the viscodilatometer plug. Following polymerisations were therefore carried out at 82°C to ensure that the polyester remained completely in solution.

2.3 Infrared Examination of the Model Polyester System.

The infrared spectra were taken on the double beam recording spectrophotometer described by Brownlie[38]. Spectra of the solid resins were taken on thin films produced by squeezing a warmed sample of resin between two rock salt plates. The spectra of the resin solutions and of the liquids examined were obtained using a rock salt cell which gave a film thickness of 0·0098 cm. The resin solutions in A.R. acetone were accurately made up to give 0·5 mole of resin, with respect to the double bond content, in 1000g. of solvent in order to have an equal concentration of unsaturation in each solution.
(i.e. 0.5 x Molecular Weight/DPg. per 1000g. solvent.)

The spectrum of ethylene glycol was examined to ensure that residual glycol in the polycondensate was not the cause of the absorption band at 975 $cm.^{-1}$ which was chosen as characteristic of the polyesters. The acetone used for the resin solutions was also examined for, and found to be free from, interfering bands in the spectral region under examination.

The spectrum of a typical PEF resin in the region of the 975 $cm.^{-1}$ band is shown in Fig.6, together with the spectra of ethylene glycol and acetone in the same region.

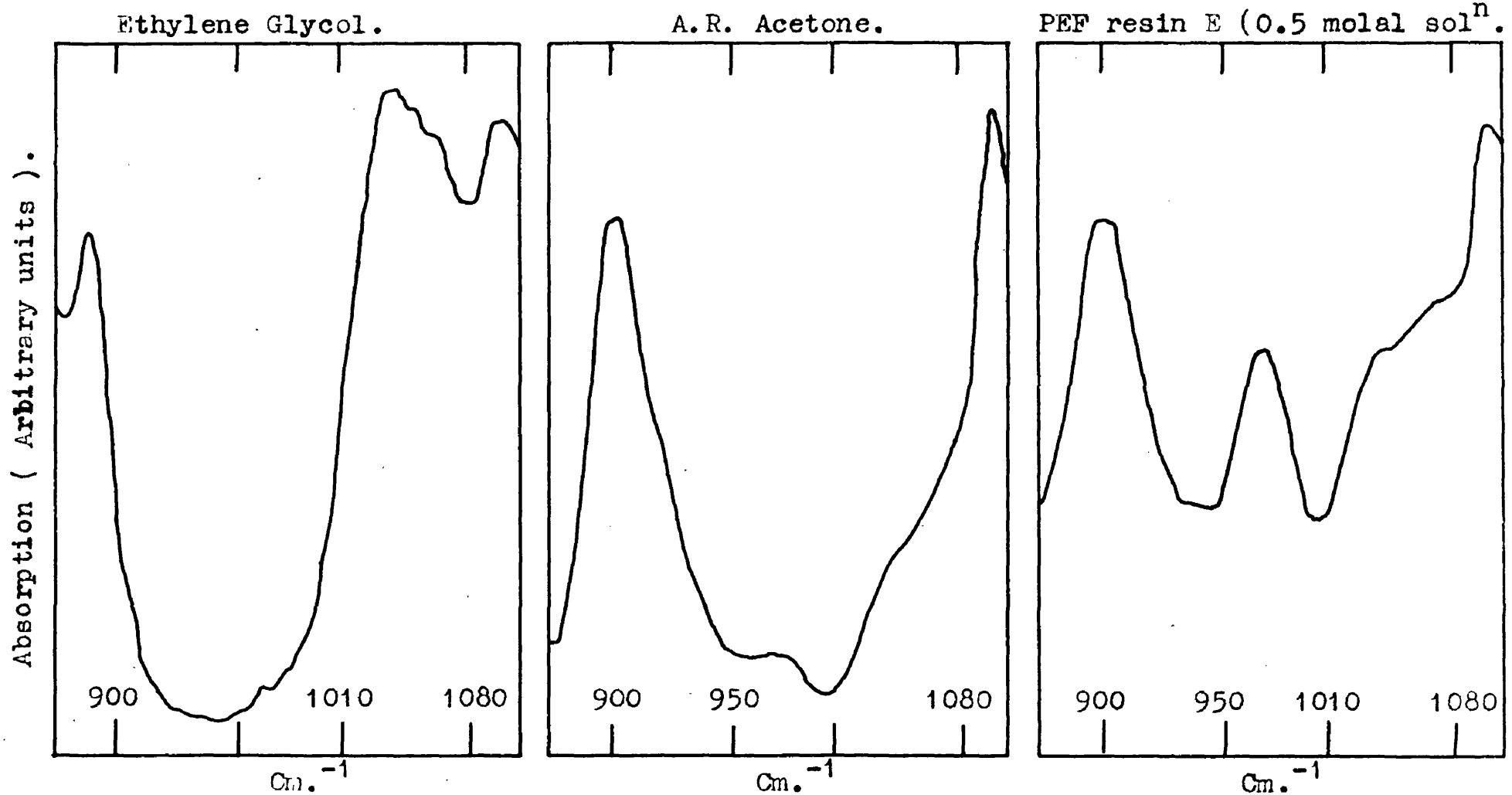

Figure 6. Infra-red spectra.

Both the ethylene glycol and the acetone are free from bands in the 975 cm^{-1} region.

2.4 Preparation of Polyester/Methacrylate Mixtures.

The methyl methacrylate monomer (MMA) (Imperial Chemical Industries - Kallodoc Liquid) was twice extracted with dilute caustic soda solution in order to remove the phenolic inhibitors present. It was then washed with distilled water, dried with calcium chloride, and twice distilled in a carbon dioxide atmosphere at 30mm. Hg pressure. The monomer was stored at 5°C in a dark bottle. This purification was insufficient to free the monomer from all traces of catalysts and inhibitors, but more rigorous procedures were not justified because the PEF resins to be mixed with the MMA could not in any case be highly purified. Moreover, as already noted, the short induction periods experienced when copolymerising the imperfectly purified system were a benefit in that they allowed the establishment of thermal equilibrium before the reaction began.

PEF resin was weighed into weighing bottle and the amount of MMA required to give the desired feed ratio R :-

$$R = \frac{\text{Moles PEF unsaturation}}{\text{Moles MMA unsaturation}} \qquad (3)$$

was calculated and weighed into the bottle which was then tightly stoppered and warmed to 60°C to allow the PEF to dissolve in the MMA. The resin solution was filled in approximately 2·5g. portions into ampoules which were then cooled in solid carbon dioxide, sealed, and stored in

a refrigerator until required.

To ensure that storage under these conditions did not affect the gelling times or rates of reaction of the resins, a freshly prepared mixture was divided into two parts. One part was polymerised immediately and the other was stored for 42 days before it was polymerised under exactly the same conditions as the first. The results were as follows:-

Table 1.

Effect of storage on prepared resin mixtures.
Polymerisation temperature 62°C; Feed Ratio R = 1·00;
Initiator: Methyl Ethyl Ketone Peroxide.

	% Initiator. B	G_o minutes.	t_c minutes.	Reaction Rate x $B^{\frac{1}{2}}$.
Fresh mixture.	1.35	24.25	21.75	2.47
Stored 42 days.	1.56	24.00	22.00	2.54

(G_o = Overall gelling time from immersion of mixture in the thermostat to the gel point.

t_c = Actual gelling time. i.e. (G_o - induction period).

The units of the reaction rate are $10^{-4}.mol.l^{-1}.sec^{-1}$.)

It is seen that the two runs gave the same result to within experimental error, and it was therefore assumed that the much shorter storage times use in practice (maximum 4 days) had no effect on the gelling properties.

2.5 Gelation Experiments.

The viscodilatometric technique described in Section 2.1 was used to follow the gelation reactions. The required amount of initiator was added to the resin mixture which was then filled into a calibrated viscodilatometer. The mounted viscodilatometer was immersed in a thermostat at the reaction temperature and readings of the positions of the two menisci on the scale were taken together with the corresponding times. Figures 4 and 5 are typical plots of PEF/MMA gelation experiments and the set of experimental readings from which Fig.4 was plotted is given in the Appendix (Table 4). The difference plots, which are in fact graphs of the shrinkage of the polymerising system, were used in conjunction with the viscodilatometer calibration to calculate the actual volumes of reactant as the polymerisation proceeded. The calculations for the run shown in Fig.4 are given in the Appendix (page 127). The difference plots were always linear up to the time of gelation and were therefore a linear measure of the degree of polymerisation computed thus:-

$$\text{Fractional Volume Shrinkage} = (0.2188 + 0.000467.T^{\circ}C)\beta \qquad (4)$$

where β is the fraction of all the double bonds present (fumarate plus methacrylate) which have polymerised. This relationship is valid for pure MMA[39] and

must be an excellent approximation in the presence of PEF since it has been found that the polymerisation in the mixture is largely concentrated in the MMA component. Moreover, the shrinkage due to the complete polymerisation of one double bond mole of PEF is estimated from data given by Nichols and Flowers[40] to be almost the same as that for pure MMA. (MMA - 22.8% at 20°C, PEF - 19.9% at 20°C. The calculation is given in the Appendix, page 124).

The gel time t_c for a polymerisation was determined from the end of the induction period i.e. the first kink in the difference plot, to the point at which the plug flow curve attained a horizontal position. This point, where flow ceased owing to the attainment of infinite viscosity, could be located with accuracy because of the sharpness of gelation. Data exemplifying the reproducibility of t_c and of the rates of polymerisation, determined as described above, are given in Table 2. The standard deviations of both gel times and rates lie generally close to 5%.

Table 2.

Reproducibility of Gel Times and Polymerisation Rates. PEF resin G; initiator - 2% MEK; reaction temperature 62°C.

Feed ratio R	Induction period (minutes)	Gel time. t_c mins.	Reaction Rate 10^{-4}.mol.l^{-1}.sec^{-1}.
0.5	2	31.5	3.01
0.5	4	29.0	3.17
0.67	4	30.5	3.19
0.67	2	28.3	2.92
1.0	4	16.5	3.56
1.0	2	15.0	3.25

2.6 Analysis of Initiators.

Several of the peroxide and hydroperoxide initiators used in the gelation investigations were not pure compounds but solutions or pastes of the active component as marketed for the hardening of commercial polyester resins. The concentration of initiator in these mixtures was therefore estimated using a method based on that given by Skellon and Wills[41] for the analysis of organic peroxides.

About 0.2g. of the initiator were weighed from a weight burette into a 500ml. bottle. 25ml. of glacial acetic acid were added followed by 2g. A.R. sodium bicarbonate and the bottle was tightly stoppered. After standing

in darkness for 10 minutes, 2ml. saturated potassium iodide solution were added and the bottle was again tightly sealed and stood in darkness for a further 15 minutes. The reacted mixture was then diluted with 100ml. distilled water and the liberated iodine was titrated with normal sodium thiosulphate solution using sodium starch glycollate[42] as indicator. Some of the peroxides were too stable to be reacted completely within the 15 minutes normally allowed, and for these, longer reaction times and in some cases heating had to be used. The results may be summarised as follows :-

Methyl ethyl ketone peroxide (MEK), 1-hydroxy-cyclohexylhydroperoxide-1 (HCH), and benzoyl peroxide (BZP), all gave reproducible estimations under the standard conditions.

tert.-Butyl Hydroperoxide.

TBHP required an hour for reaction with the potassium iodide under otherwise standard conditions.

Di-tert.-butyl Peroxide.

Even on prolonged boiling under reflux in a carbon dioxide atmosphere, DTBP liberated only a very small amount of iodine and could therefore not be estimated by this method.

tert.-Butyl Perbenzoate (TBPB), and Lauroyl Peroxide (LP).

After standing for five hours at room temperature, TBPB and LP liberated only very small amounts of iodine.

It was found that after two minutes boiling under reflux in a CO_2 atmosphere, the iodine was apparently completely liberated. For the analysis of these two initiators therefore, the addition of the potassium iodide was followed by four minutes boiling, and the solution was then allowed to cool for fifteen minutes before being titrated in the standard way.

α, α'- azobis<u>iso</u>butyronitrile,

The AZBN used was supplied by Kodak Ltd. as a pure chemical and was therefore not subjected to analysis since the low level of purity of the PEF/MMA resin mixtures did not warrant it.

2.7 Viscometric Molecular Weight Determinations.

Several polymerisations of methyl methacrylate monomer alone were carried out for comparison with PEF/MMA copolymerisations performed under the same conditions of temperature and initiator concentration. The molecular weights of the polymers formed in these reactions were measured for use in the calculations of the ratio k_t/k_p^2 which is involved in the proposed kinetic scheme.

Samples of MMA monomer were polymerised to low conversion, isolated by precipitation with methanol from solutions in chloroform, and then dissolved once more in

chloroform for determination of the number average degree of polymerisation DP_n by viscometry. The specific viscosity was determined in an Oswald viscometer in the usual way and the extrapolation to infinite dilution is exemplified for one run in Fig.7. The calculation of DP_n was based on Baysal and Tobolsky's equation for the intrinsic viscosity[43];

$$[\eta] = 2.52 \times 10^{-3} DP_n^{0.8} \qquad (5)$$

For three polymerisations at 62°C with 2% MEK initiator calculated on the MMA monomer, a mean DP_n of 2545 was found together with a mean reaction rate of 0.000363 $mol.l^{-1}.sec^{-1}$. determined viscodilatometrically. From the mean rate and DP_n, the ratio k_t/k_p^2 can be computed from the equation

$$\text{Rate} \times DP_n = k_p^2.M^2/k_t \qquad (6)$$

and is found to be 88. This compares favourably with the value of 67 calculable at 62°C from data by Matheson and co-workers[44], and other similar values in the literature. (The concentration M of MMA was taken as 9 $mol.l^{-1}$ - see Appendix page 124).

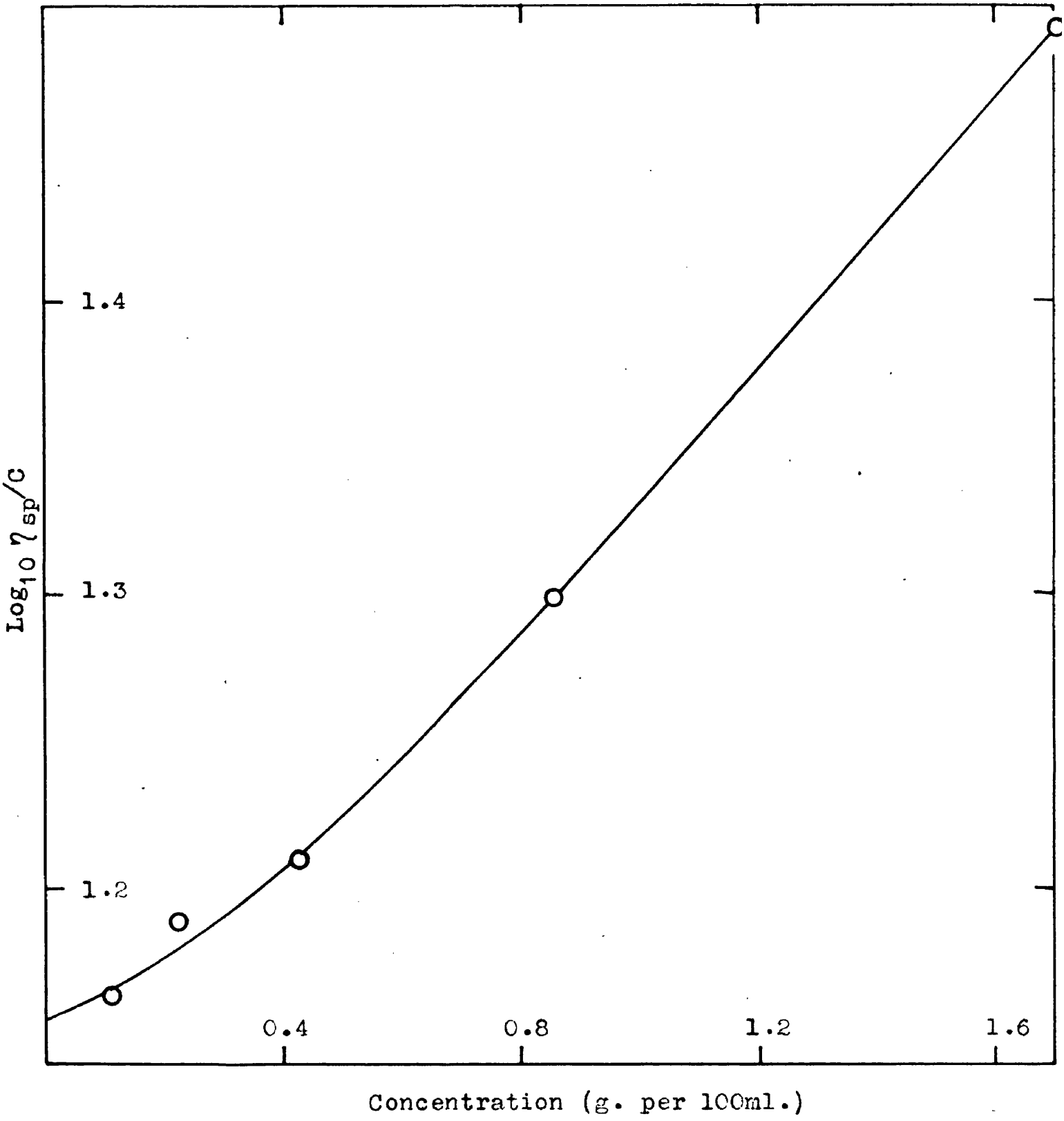

Figure 7 .

Extrapolation of specific viscosity to infinite dilution for the determination of molecular weight. MMA polymerised for 1 hour at 62°C, 2% MEK catalyst. Mol. Wt. of polymer 210,000

3. Results.

3.1 Characterisation of Model Polyester Resins.

The polyethylene fumarate component, which in the model system used in this work, formally takes the place of one of the two comonomers in simpler difunctional copolymerisations, is itself a low molecular weight polymer. It is not a pure compound but hetero-disperse and may contain some ring compounds as well as linear molecules. It contains condensation chain molecules with multiple unsaturation functionalities, the reaction of any one of which suffices to attach it to the cross-copolymer (Fig.18).

The method of preparing polyethylene fumarate goes back before the interest this product has presented as a crosslinker in copolymerisations, particularly to the work of Carothers and Arvin[37]. It was not realised that the isomerisation of maleic to fumaric unsaturation may occur during the polycondensation of maleic anhydride with ethylene glycol, until Batzer and Mohr[45] proved it and evolved a laboratory method for avoiding the isomerisation. The condensation polymer was prepared for this work, from nearly equimolar proportions of glycol and anhydride under substantially the same conditions as those employed by Carothers and Arvin, and it was shown (Section 3.2), by means of infrared spectroscopy, that the isomerisation was substantially complete well before the number average

degree of polymerisation reaches three (the lowest DP_n examined). During the progress of this work, the paper by Feuer et al.[46] became available, which reaches the same conclusion by polarographic and other means. As the polarographic analysis has to be preceeded by hydrolysis of the polyester, there is considerable risk of geometric inversion occurring, while the infrared spectral evidence is free from this objection.

Apart from the question of geometrical isomerism, the characterisation of the condensation polymer centres on the correct weight average number DP_w of fumarate double bonds per polyethylene fumarate molecule. If the resin is prepared from an equimolar mixture of glycol and maleic anhydride, and consists of linear molecules only, as would be expected to be approximately true, the distribution of chain lengths could safely be taken to follow Flory's statistical equation[47]

$$w_x = x\,(1 - p)^2\,p^{x-1} \qquad (7)$$

where p is the fraction of carboxyls esterified and w_x the weight fraction of x-mer. The weight average DP_w and the number average DP_n are given by :

$$DP_w = (1 + p)/(1 - p) = 2\,DP_n - 1 \qquad (8)$$

for this distribution.

Three complicating factors which are causes of possible

deviations of the structure of the polymer from the state defined in equation (7) have been investigated in this laboratory[48]. These were, departures from strictly equimolar composition, the presence of cyclic species in the resin (cf. Jacobson and Stockmayer[49]), and the presence of crosslinked molecules arising from the latent functionalities, viz. the fumarate unsaturation, in the condensation polymer. The experimental evidence showed that none of these factors was, in fact, important.

Equimolarity.

It was shown[48] that the ratio of acid to glycol in the resins used in this work was probably 1:0.955. A theory derived by Flory[50] then suggests that the end-group determinations of the DP will be only about 10% too high even for the highest molecular weight resin prepared, so the assumption of equimolarity is adequate for the purpose of this work.

Rings and Crosslinks.

Jacobson and Stockmayer have shown by viscosity measurements that ring formation can occur when decamethylene glycol condenses with a saturated dicarboxylic acid. Moreover, crosslinking and even gelation are known to present difficulties in condensing glycol with unsaturated dicarboxylic acids on an industrial scale. The cryoscopic and end-group degrees of polymerisation (DP_n and DP_{ne}) of

the resins used in this work were compared by McMillan[48] who found that the close agreement between DP_n and DP_{ne}, and the results of calculations of the amount of cyclic species present, justify the treatment of the resins as purely linear polymers with a weight average degree of polymerisation (DP_w) derivable from end-group analysis with the aid of equation (8).

3.2 Cis-Trans Isomerisation in Polyester Resins.

Batzer and Mohr[45] detected the presence of the isomeric polyethylene fumarate in the condensation polymer formed from ethylene glycol and maleic anhydride. An infrared spectroscopic examination of a typical resin used in this work showed the presence of a strong absorption band at about 975cm^{-1} (Fig.8) which is known[50] to be associated with trans-type ethylenic unsaturation. Infrared examination of ethyl maleate showed no absorption in the 975cm^{-1} region (Fig.9). It was therefore decided to attempt to follow the development of the 975cm^{-1} band as a function of increasing reaction time to obtain an indication of the rate of isomerisation of the cis maleate unsaturation to the trans fumarate form.

Solutions of maleic resins having condensation times of from 1½ hours to 5½ hours were examined (Fig.10) and it

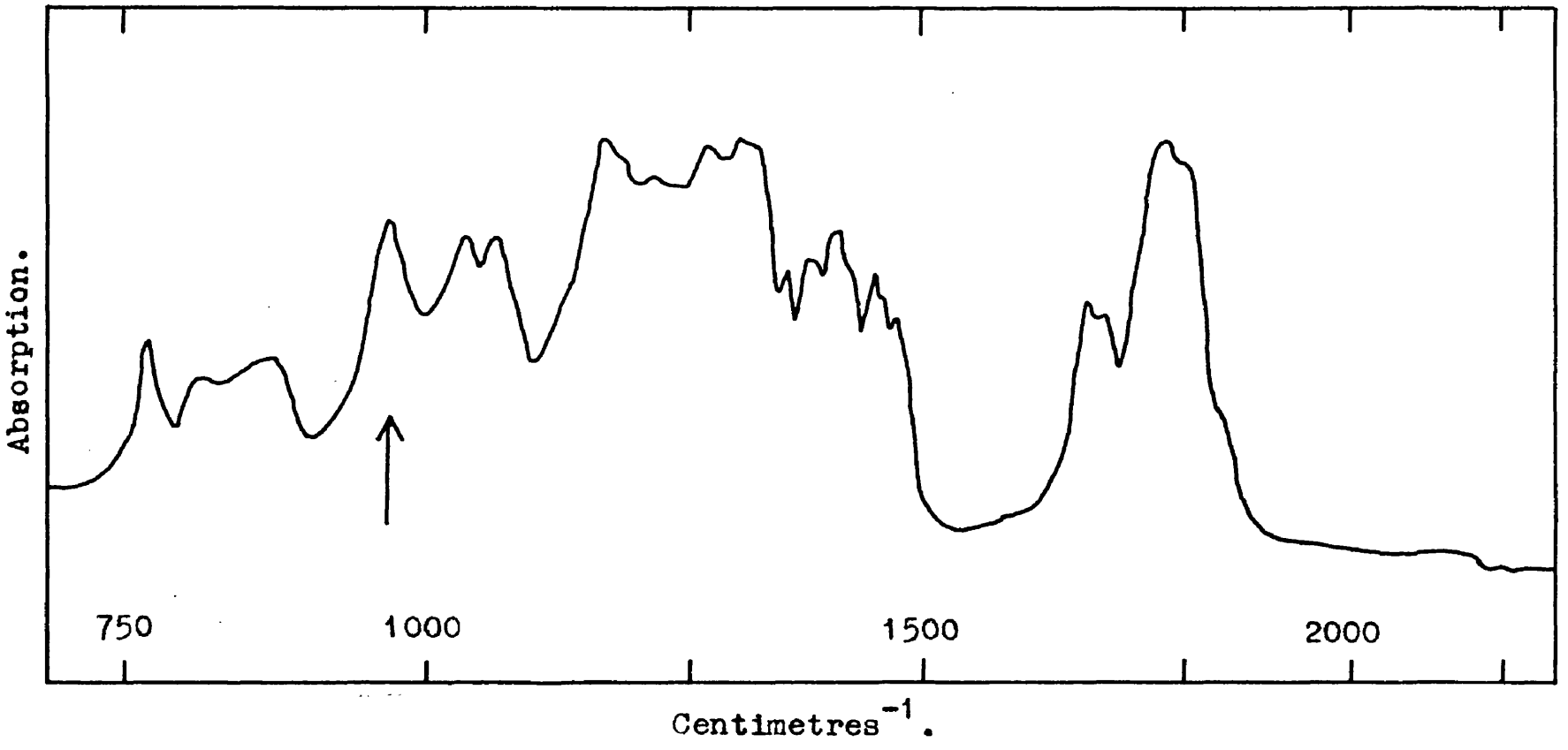

Figure 8.

Infra-red spectrum of polyethylene fumarate resin F (solid). The arrow indicates the 975 cm^{-1}. band assigned to the trans double bonds in the fumarate units.

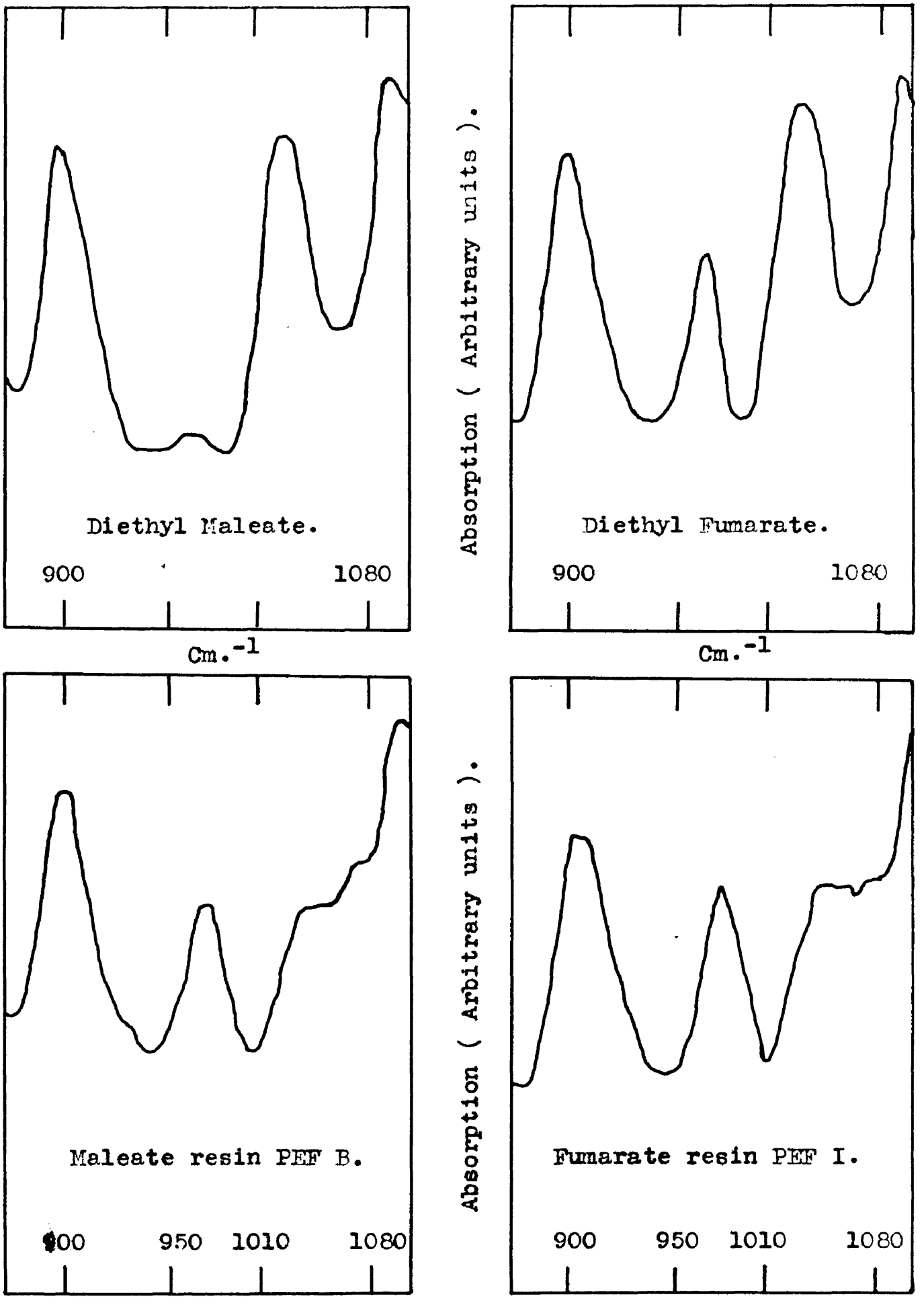

Figure 9 . Infra-red spectra of 0.5 molal solutions in Acetone.

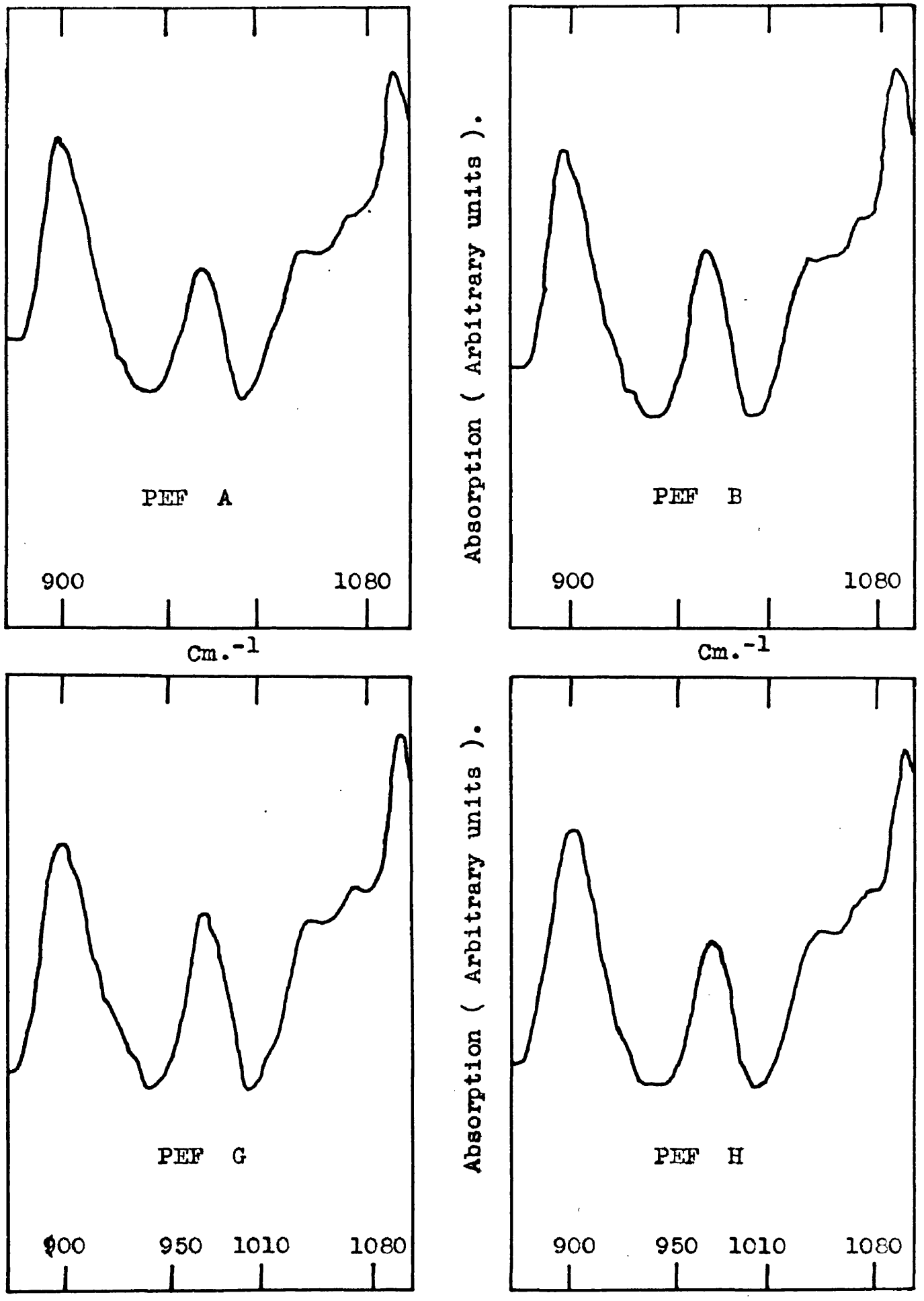

Figure 10. Infra-red spectra of 0.5 molal solutions in acetone.

was found that even in the lowest molecular weight resin (i.e. the least reacted), the 975cm^{-1} peak was fully developed when compared to the specifically 100% trans peak given by a resin prepared from ethylene glycol and ethyl fumarate (Fig.9). This evidence indicated that complete isomerisation of the maleate double bonds occurred very quickly during the polycondensation reaction and was complete before the first resin samples were taken.

The near completeness of the isomerisation has since been confirmed by Feuer et al.[46] using polarographic analysis of the saponification products of a styrene/ethylene "maleate" copolyester and a styrene/fumaric ester copolyester.

The Gelation Properties of "Maleate" and Fumarate Resins.

Since the infrared evidence had indicated that "maleate" polyesters in fact contained a very large proportion of trans (fumarate) ethylenic unsaturation, it was thought necessary to compare the gelation behaviour of a "maleate" resin with a resin known to contain only fumarate double bonds. Exactly similar gelation experiments were carried out with a resin of each type both of which had a similar molecular weight, and the results of these runs together with those of a run on methyl methacrylate alone, are tabulated below.

Table 3.

Comparison of the Gelation Properties of "Maleate" and "Fumarate" Resins.

Polymerisation temperature 82°C. Initiator - MEK.
Feed ratio R of resin mixtures 0.33.

Resin.	Resin DP_n	Gel Time t_c mins.	Conversion at t_c.	Reaction Rate.	Rate x $B^{-\frac{1}{2}}$
"Maleate".	2.86	21	25.4%	18.12	12.70
Fumarate.	2.90	24	28.6%	19.32	15.88
MMA only.	--	--	--	11.43	9.14

(The values quoted for reaction rates are in $mol.l^{-1}.sec^{-1}.10^{-3}$).

As is shown in the table, the gel times, conversions at the gel point, and reaction rates of the two resins are very similar, and the similarity is further demonstrated by the graphs of the relative viscosity of the resin mixtures versus reaction time shown in Fig.11.

The infrared evidence and the supporting gelation behaviour show that the resins prepared from maleic anhydride are in fact largely composed of polyethylene fumarate (PEF) and therefore throughout this thesis they are so designated.

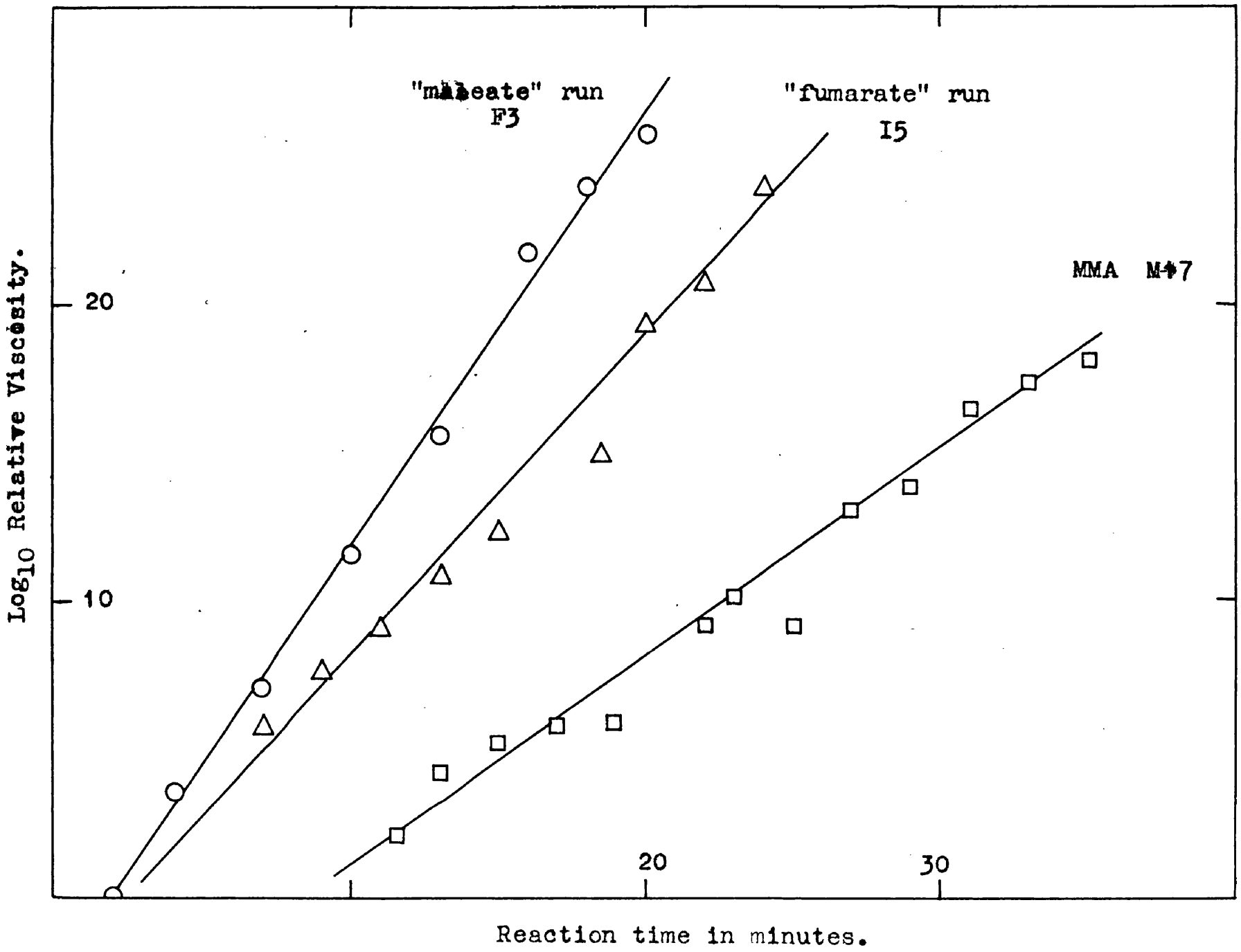

Figure II . Comparison of viscosity change in maleate, fumarate and MMA polymerisation.

3.3 Polymerisation Initiators.

Investigations were made into the effects of ten different initiators on the rate and gel time of the MMA/PEF copolymerisation. Several of the initiators had to be discarded because of incompatibility with the resin system or lack of catalytic activity at the polymerisation temperatures used.

Methyl Ethyl Ketone Peroxide. (MEK)

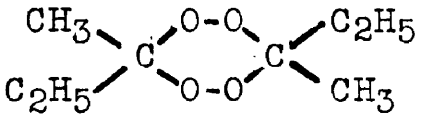

This initiator was obtained from Bakelite Ltd. as a 60% solution in dimethyl phthalate as marketed for the hardening of commercial unsaturated polyester resins. It gave reproducible gel times and rates, the standard deviation of both of these quantities being about 5% (see Table 2, page 25).

Iodimetric estimations over a period of eighteen months showed that the concentration of MEK in the dimethyl phthalate solution fell from 60.2% when fresh to 47.9% at the end of the period. After allowing for this fall in concentration, it was found that the rate of polymerisation of the PEF resins was very little affected by the presence of the decomposition products in the old solution (Table 4).

Table 4.

Effect of Initiator Storage on PEF/MMA Gelation.

PEF resin N, Feed ratio R = 0.49, Polymerisation temperature 62°C, MEK initiator.

Initiator. B%	Gel time. t_c mins.	Conversion at t_c.	Reaction rate.	Rate x $B^{-\frac{1}{2}}$
fresh, 0.68	59.5	11.0%	3.716	4.38
stored 18 months, 0.72	57.5	10.8%	3.475	4.22

(Units of reaction rate:- $mol.l^{-1}.sec^{-1}.10^{-4}$.)

1-Hydroxycyclohexylhydroperoxide-1. (HCH)

This commercially used initiator was obtained from Novadel Ltd. as a 50% paste with dimethyl phthalate, and MEK gave satisfactory reproducible gelation behaviour.

Benzoyl Peroxide (BZP).

This was dried and twice recrystallised from chloroform by adding methanol, and dried under vacuum to constant weight. At the temperature normally used for the polymerisations (62°C), BZP caused very short gelling times which could not be accurately measured. e.g. PEF resin J, feed ratio 1.0, had a gel time t_c of 4.1 minutes at 62°C. The use of BZP as an initiator was therefore abandoned.

tert-Butyl Perbenzoate (TBPB).

The TBPB was obtained from Laporte Chemicals Ltd. as a 90% solution. The results of six gelation experiments using this initiator are shown below.

Table 5.

Effect of Variation in TBPB Initiator Concentration.

PEF resin J, Temperature 62°C, Feed ratio R = 0.91.

Initiator B%	G_o mins.	t_c mins.	Conversion at t_c	Rate	Rate.$B^{-\frac{1}{2}}$
0.18	28.0	9.0	0.68%	1.39	3.32
0.38	17.5	8.8	0.43	0.92	1.05
1.00	13.3	9.5	0.45	0.89	0.89
1.65	12.0	8.3	0.30	0.67	0.52
2.64	15.7	8.5	0.58	1.27	0.78
3.60	9.8	7.8	0.45	1.06	0.56

It is seen that over a twenty-fold concentration range of TBPB the gel time t_c was practically constant and the rate of reaction varied only by a factor of two. A polymer of almost constant DP was being produced. It seems that although the TBPB concentration had the effect of reducing the induction period (G_o - t_c) (see Fig.12), it played no part in the polymerisation reaction which was therefore a trace-catalysed or thermal reaction taking place after the TBPB had removed the inhibitors present.

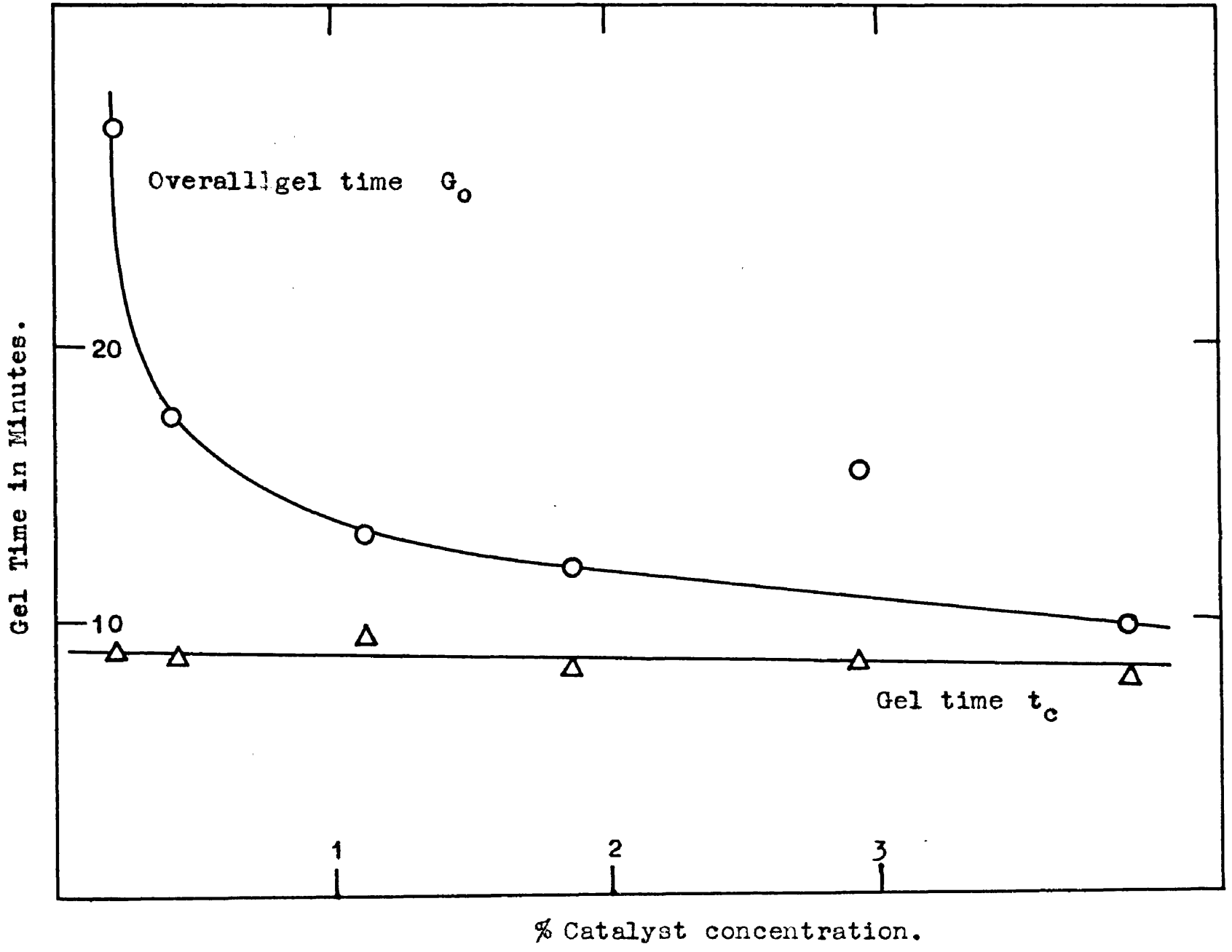

Figure 12. Variation of gel times with t-butyl perbenzoate catalyst concentration.

α,α'-azobisisobutyronitrile (AZBN).

Table 6.

Effect of AZBN concentration on PEF/MMA gelation.

PEF resin N : Temperature 62°C : Feed ratio R = 0.8.

Initiator B%	G_o mins.	t_c mins.	Conversion at t_c	Rate.	Rate.$B^{-\frac{1}{2}}$
0.96	14.0	12	5.13%	6.40	6.53
0.069	17.5	11	0.77	1.05	4.00

Although the gel time t_c was constant over the fourteen-fold change in AZBN concentration, there was a considerable change in the value of the Rate.$B^{-\frac{1}{2}}$ factor which, on the basis of the gelation theory put forward in Section 4.3, ought to have been constant. The deviation from the theory is however not large since the values of Rate.$B^{-\frac{1}{2}}$ only differ by a factor of 1.6 over the fourteen-fold range in initiator concentration.

The polymerisation of a further portion of the same resin mixture as that used in the runs in Table 6, this time with 0.90% MEK as initiator, gave the following results:- G_o= 29 mins., t_c = 26 mins., conversion = 5.17% at the gel point, reaction rate = 2.98 $mol.l^{-1}.sec^{-1}.10^{-4}$, and the rate times $B^{\frac{1}{2}}$ factor = 3.16 $mol.l^{-1}.sec^{-1}.10^{-4}.(\text{initiator conc}^{n}.)^{\frac{1}{2}}$. In view of the totally different nature of the initiating systems, the agreement to within a factor of 2.5 between the AZBN and MEK results is probably satisfactory.

Cobalt Naphthenate (CN).

It is a common industrial practice to add accelerators to the "contact resin" + initiator mixture when cold setting (i.e. at ambient temperature) is required. Amine accelerators are used with benzoyl peroxide[51], and CN is used in conjunction with MEK. Since the gelation behaviour of the PEF resins with MEK alone conformed very well to the theoretical predictions of the kinetic scheme, it was decided to investigate the effect of the addition of an accelerator to the system.

Table 7.

Effect of CN accelerator on an MEK initiated gelation.

PEF resin N, Feed ratio R = 0.8, Temperature = 62°C.

Initiator. B%	Accelerator,	G_o mins.	t_c mins.	Conversion at t_c	Rate
0.89%MEK	---	29	26	5.2%	2.98
0.88% "	0.007%	50	46.5	19.7%	6.36

The presence of 0.007% of CN doubled the reaction rate and also delayed gelation by a factor of two. It seems that the increase in reaction rate was doubly compensated by the reduction of the chain length of the polymer being produced. This cannot be explained on the basis of the reaction mechanism assumed in Section 4.3 and this anomalous behaviour requires further investigation.

3.4 Observations on the Reaction Rate after the Gel Point.

Although the viscosity reached infinity at the gel point, dilatometric readings on the PEF/MMA resin can be taken for a short while after this point. The jelly is still very deformable and the continuing shrinkage is taken up presumably by slippage at the dilatometer walls. Finally, this flow deforms the menisci too far for accurate volume readings to be taken (cf. Mackay and Melville[52]).

Figure 13 presents the shrinkage plot for a visco-dilatometer run with the rate measurements carried beyond the gel point. The rate curve consists of two straight portions meeting at a kink which coincides closely with the gel point observed viscosimetrically (cessation of flow).

To increase the range of the post-gelation rate plot, a simple dilatometer with a stem emerging from the thermostat is preferable. In this case the resin in the colder stem remains liquid after the gel point of the resin in the bulb. When using this method, the gel point was located by including in the dilatometer bulb a glass covered steel wire which could be raised magnetically and allowed to fall under gravity. The gel point was taken as the time at which the probe failed to fall to the bottom. Figure 14, based on an experimental run by McMillan in this laboratory illustrates results obtained by this technique. The extended post-gelation rate plot still conforms to a straight line.

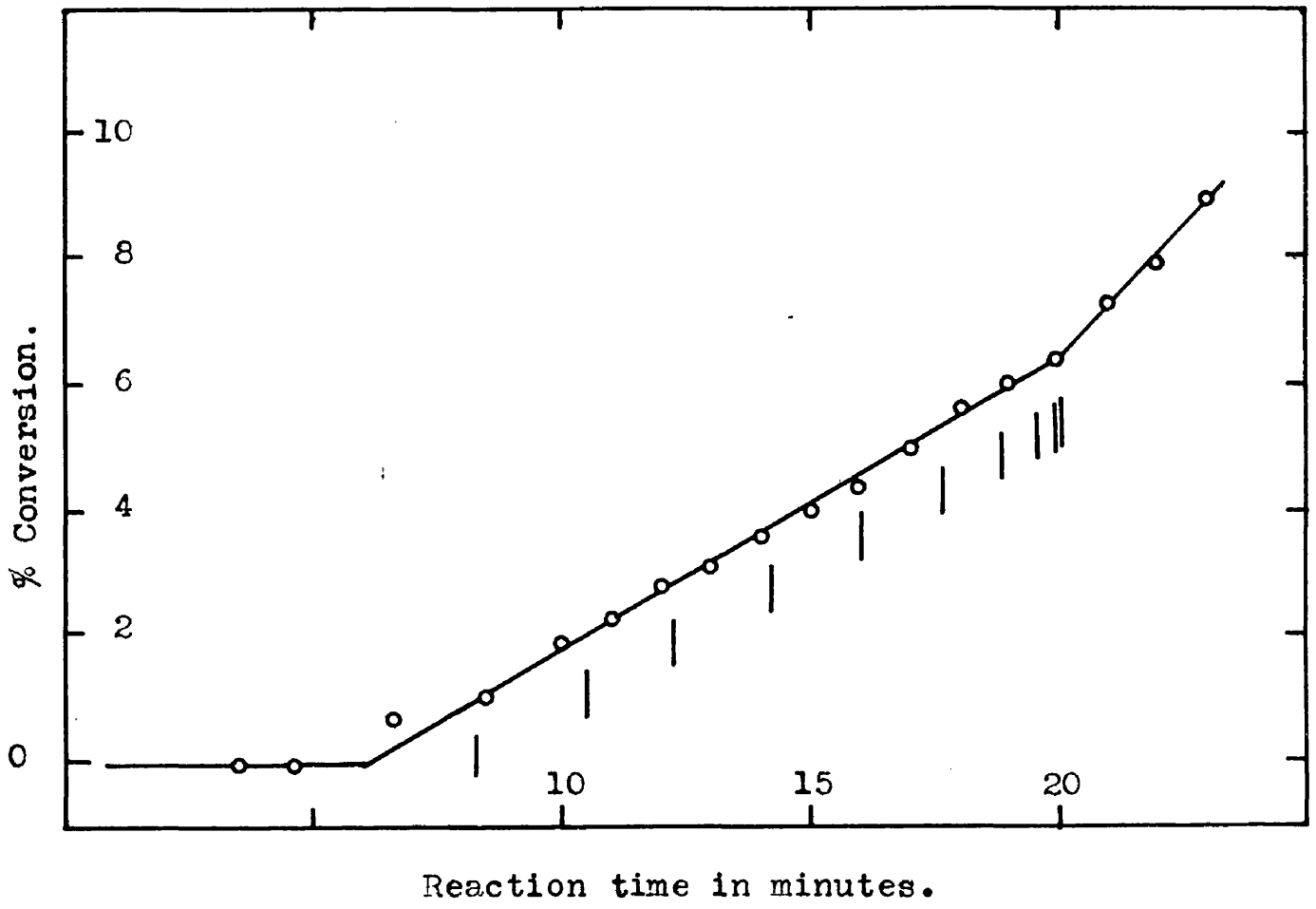

Figure 13.

Rate of reaction for a PEF/MMA copolymerisation. 1.03% MEK catalyst; Feed ratio R = 1.0; Temp. 62°C. Each vertical line denotes a two-fold increase in the measured viscosity.

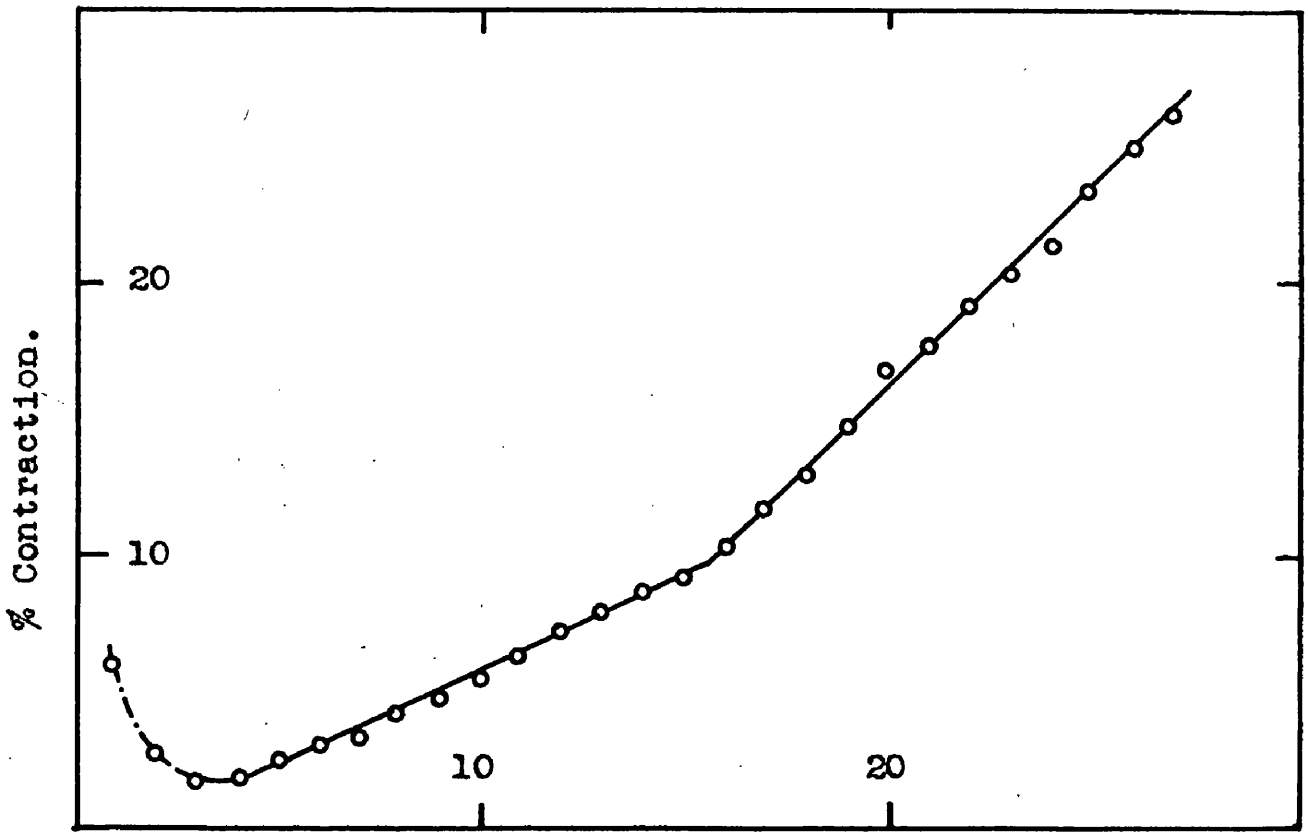

Figure 14.

Rate of contraction in PEF/MMA copolymerisation. After the initial thermal expansion, the rate is linear up to the gel point . It then increases sharply. Feed ratio R = 1.0; 70°C; 1% MEK catalyst.

For comparison with the results just presented, a plot of the polymerisation of pure methyl methacrylate in the absence of PEF crosslinking agent is included (Fig.15). Along this curve, 19 vertical lines indicate the succesive doublings of the viscosity measured. To cover this 2^{18} fold (= 2×10^5 fold) range of viscosity, two runs were combined, one employing a plug viscodilatometer and the other covering the later part of the reaction in the highly viscous state using a viscodilatometer from which the plug had been omitted.

Minor corrections could be applied to the results of the later part. First, the shortening of the resin column in the dilatometer stem caused a decrease in the effective hydrodynamic resistance which in this case no longer resides in the plug. Second, the same shortening caused a decrease in the effective pressure head controlling the flow rate. This decrease occurs in the absence or presence of a plug but was much more serious in this case because of the higher total conversion covered. These two corrections have been ignored because they oppose each other and do not falsify the viscosity by as much as a factor of two.

The shape of the rate curve plot I, Fig.15 is quite general for methyl methacrylate as seen for instance by comparison with plot II reproduced from Mackay and Melville[52] for a photo-initiated polymerisation at 30°C.

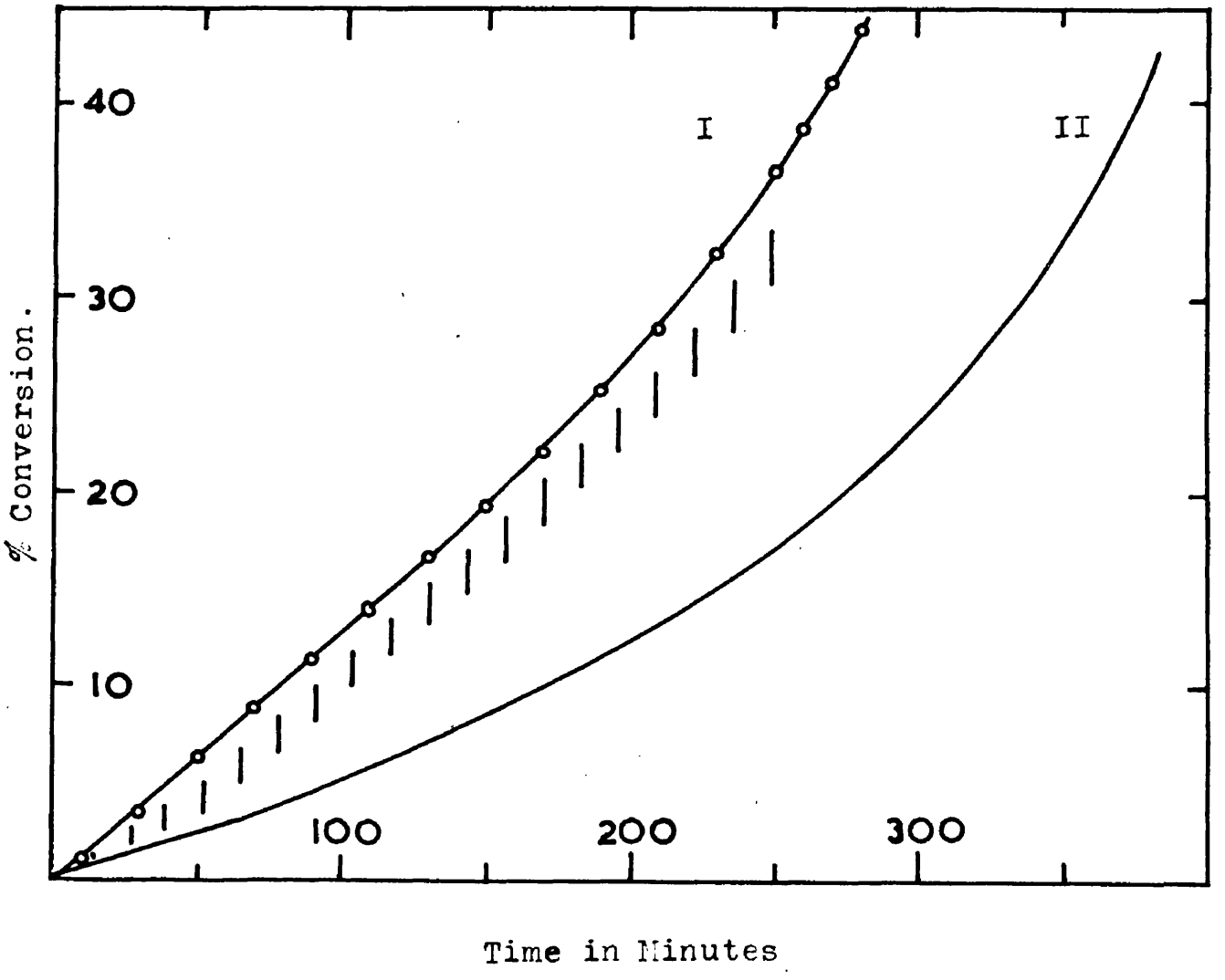

Figure 15.

Methyl methacrylate polymerisation.

I 1% methyl ethyl ketone peroxide as initiator at 62°C.

II Photo-initiation at 30°C.

Each vertical line denotes a two-fold viscosity increase.

When conversion of a PEF/MMA resin had been carried a little, but not too far beyond the gel point, i.e. after measurable flow under the prevailing pressure head of 0.002 atmosphere had stopped, it was still possible to induce flow by applying pressure. For instance, as vacuum was gradually applied to one end of the viscodilatometer, the flow was observed to set in sharply in the region of one atmosphere pressure difference. The plug could thus be freed from the jelly filling it and air, solvent, and finally fuming nitric acid could be sucked into the instrument which could eventually be recovered clean for further use. It is well known that polymer solutions can be degraded with a permanent lowering of viscosity, by flow through capillaries at high shear rates and pressures. In Section 4.1, the observation on the reversibility of gelling by the moderate pressure of about one atmosphere is attributed to the same cause.

3.5 The Gelation of Diallyl Compounds.

The gelation of four diallyl monomers was studied in order to compare results with those obtained by Simpson and Holt[53] who claimed that they were incompatible with the network theory of gelation presented in this work.

The four monomers used, diallyl phthalate (DAP), diallyl isophthalate (DAI), diallyl terephthalate (DAT), and diallyl oxalate (DAO), were those prepared by Simpson. Each monomer was catalysed with 1% by weight of dry recrystallised benzoyl peroxide, and the polymerisation at 80°C was followed using the standard viscodilatometric technique. For all four monomers, a straight line relationship between time of reaction and volume of reaction mixture was observed (e.g. Fig. 16). In Fig. 17 the change in $\log_{10}$ relative viscosity vs reaction time is plotted for the four systems.

Because of the high vapour pressure of DAO at 80°C it was found difficult to follow the reaction in a viscodilatometer after about 200 minutes when bubbles of vapour began to form in the plug of the instrument. The DAO polymerisation rate used in the calculations was therefore based on the results of the first 10% of the total reaction (i.e. up to half way to the gel point). Since the rate is linear with time, the extrapolation is justified. Also since the normal method could not be used to locate the

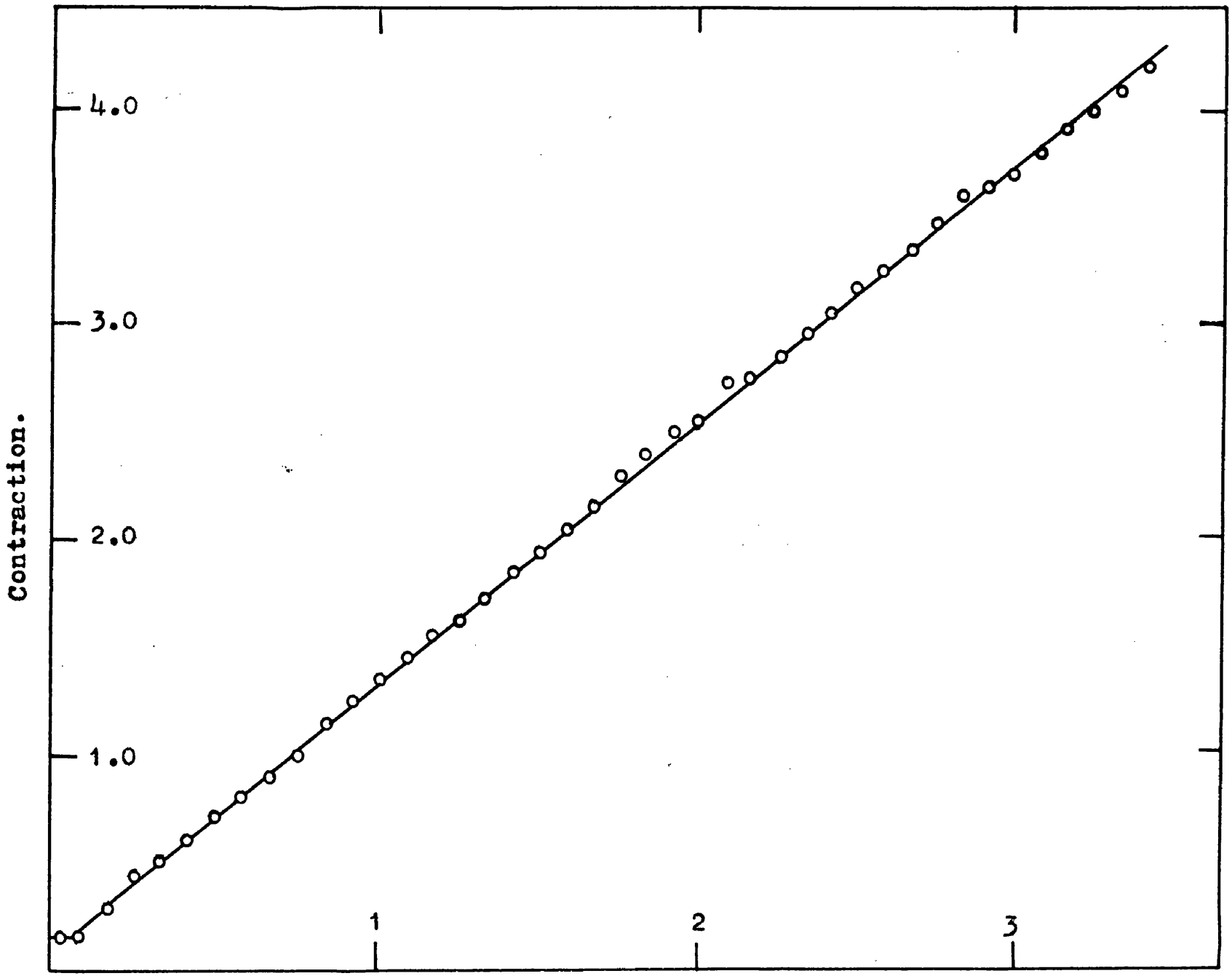

Figure 16. Contraction in a diallyl isophthalate polymerisation (Run DAI 3).

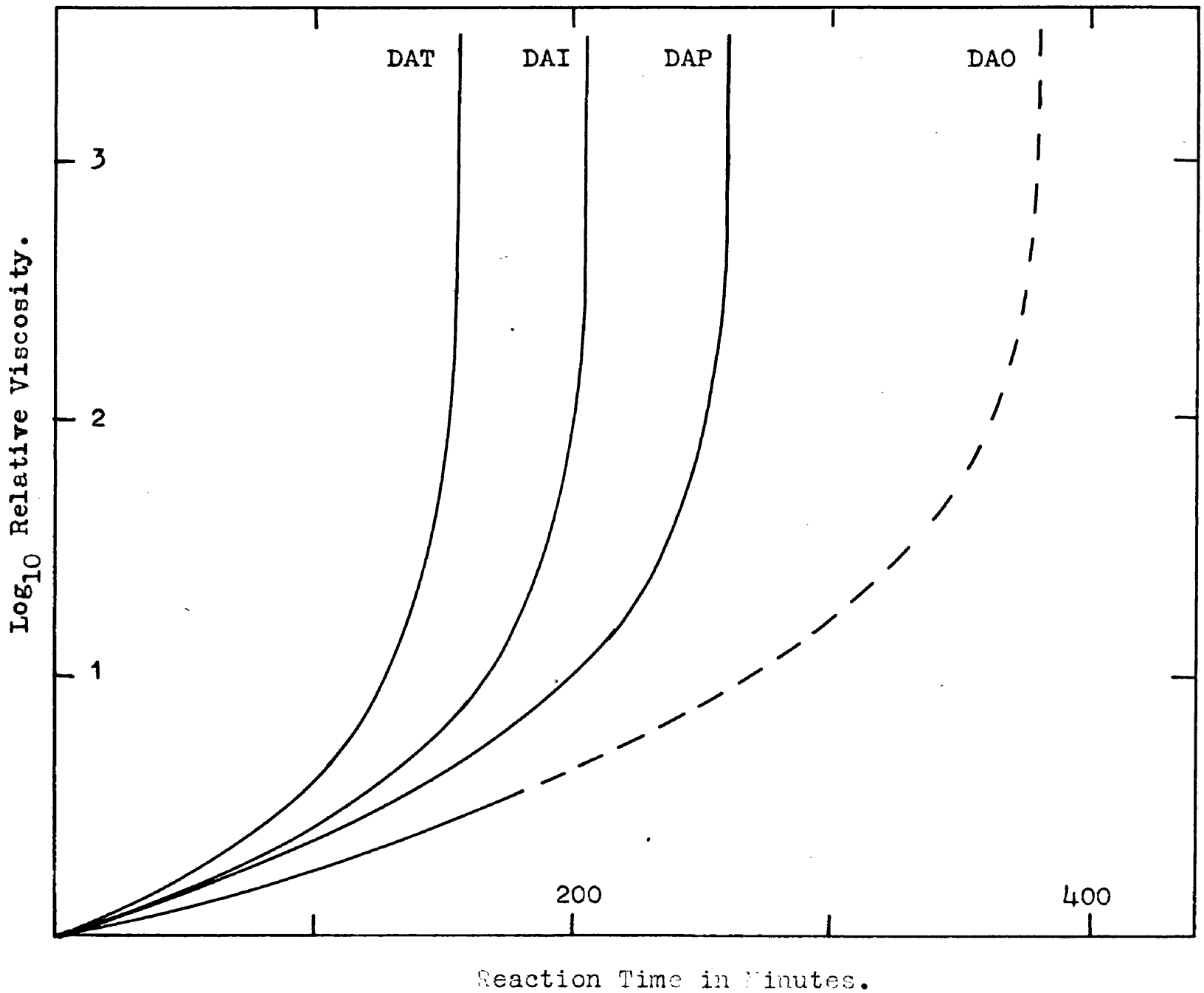

Figure 17. Viscosity changes in diallyl polymerisations.

gel point, this was obtained by measuring the time of bubble rise in a sealed ampoule of catalysed DAO which was polymerised at 80°C.

The results of the gelation experiments are given below. In each case, the value quoted is the mean obtained from duplicate runs.

Table 8.

Polymerisation of diallyl monomers.

Polymerisation temperature 80°C, Initiator 1% benzoyl peroxide.

Monomer.	Gel time t_c	Volume shrinkage at t_c	Density at 80°C. (monomer).
DAO	380 mins.	5.76%	1.021
DAP	285	3.85	1.068
DAI	205	3.09	1.070
DAT	156	2.60	1.078

Nichols and Flowers[40] have measured the relationship between the amount of polymerisation and the corresponding volume shrinkage of the reactant for eighteen mono-olefinic compounds. From a regression line calculated from their results, the following relationship is obtained:-

$$P = 2180/V_m \qquad (9)$$

where P is the percentage volume shrinkage per mole of polymerised double bonds, and V_m is the molar volume of the monomer. Using this relationship, the amount of double bond conversion at the diallyl gel points were calculated.

Table 9.

Conversion of diallyl monomers.

Monomer	Volume shrinkage at t_c.	$P = 2180/V_m$	Double bond conversion at t_c
DAO	5.76%	26.20	22.0%
DAP	3.85	18.90	20.2
DAI	3.09	18.95	16.3
DAT	2.60	19.10	13.6

The conversion of DAP at its gel point has been accurately determined by several methods which give a value of 18.5% double bond conversion[53]. The critical conversion of DAP calculated from the regression line is therefore too high by a factor of 20.2/18.5. Assuming that this correction may be applied also to the other diallyl monomers, the values have been recalculated and are tabulated below.

Table 10.

Corrected experimental results for diallyl gelations.

Monomer	Gel time t_c.	Double bond conversion at t_c
DAO	380 mins.	20.2%
DAP	285	18.5
DAI	205	14.9
DAT	156	12.5

In Section 4.6, these results are compared with those obtained by Simpson and Holt[53] and are discussed in the light of the network theory of gelation.

4. Discussion.

4.1 Irreversible Breakdown and the Sharpness of the Gel Point.

It is necessary to explain why the resin, when polymerised somewhat beyond the kink in the rate curve, can be caused to flow through the sintered glass plug under a pressure of only one atmosphere despite its nominally infinite viscosity. The explanation cannot be that the gel point had not been reached. This is contradicted, on inspection of Fig. 13, by any reasonable extrapolation of the measured viscosities to infinity, by the suddenness of the onset of flow when pressure was applied, and indeed by the jelly-like appearance of the resin. It is necessary to invoke mechanical degradation effects. A semi-quantitative discussion of the relevant theory suffices to show that this assumption is reasonable despite the very moderate pressure employed, and incidentally also emphasises the importance of systems near their gel point for any mechanical degradation studies because degradation is critically dependent on the width of the molecular size distribution present.

The sharpness of the gel point in polyfunctional systems has often been stressed. Gelling has theoretically been compared to liquefaction from this viewpoint (Stockmayer[54]). The reason for the sharpness is that the rate at which a

molecule acquires new links is proportional to the size (number of functionalities) it has already attained. However, since testing for the gel point inevitably involves the application of a shear, the sharpness of the gel point will in principle always be counteracted to some extent by the well-known degradation of the polymer molecules induced by flow. The irreversible decrease in viscosity which attends degradation thus counteracts the "explosive" increase in viscosity due to polymerisation.

Consideration of the balance of these effects brings out three circumstances.

a) At constant rate of shear no gel point can be expected to be reached at all.

b) Under normal experimental conditions, where the rate of shear rapidly falls to zero, there is no theoretical difficulty in admitting the existence of a relatively sharp gel point.

c) Just after this gel point, a minute shear may reverse the system to finite viscosity.

These circumstances arise because mechanical degradation is concentrated even more powerfully in the big molecules present than the growth rate which it counteracts. Morris and Schnurmann[55] have shown that the force causing degradation increases as the square of the size of a linear molecule. At constant rate of shear, this force and the rate of degradation of molecules of any shape will vary as a

power higher than unity of the molecular size, while the rate of bond formation varies only as the first power of the size. Thus, in accordance with a) above, a balance should be struck before infinite networks are formed. To explain b), it suffices to state that, according to the theory of Poiseuille flow, the rate of shear in a visco-dilatometer falls to zero as $(\text{viscosity})^{-1}$. To explain c), it is noted that as the gel point is approached, even a minute rate of polymerisation causes a rapidly divergent rate of viscosity increase. A few bonds formed between giant molecules send the viscosity to infinity. Conversely, when the gel point has just been passed, a minute rate of bond breakage, concentrated as it is in the giant molecules, must suffice to reverse the viscosity to a finite value. Although shear rates of 10^5 sec^{-1}. are normally required[55] to observe degradation of polymer solutions of linear molecules exhibiting normal size distributions, there is no difficulty in attributing the observations of the reversibility of the gel point under very moderate pressure to the effect of molecular degradation.

4.2 The Gel Effect.

It is seen from Fig.15 that the initial rate of polymerisation of pure methyl methacrylate is linear. After the original viscosity has increased by a factor of about 2^{10}, there is a progressive rate increase. This gel effect which was first observed by Trommsdorf[56] and Smith and Norrish[57], is generally attributed to the acceleration of monomer consumption at high viscosity due to the gradual onset of diffusion control in the termination rate of the reaction. Only a two-fold increase is observed in the part of the reaction covered by the graph shown. If allowance is made for the roughly two-fold decrease in the rate actually to be expected from the law of mass action because of the decrease in monomer concentration, the gel effect may be said to cause an approximate four-fold rate increase. As the viscosity is further increased, the propagation and initiation rates in turn become diffusion controlled in addition to the termination step.

The incorporation of polyethylene fumarate as a crosslinking agent into methyl methacrylate is a means of attaining infinite viscosity without essentially altering the mechanism of the reaction in other respects, as it has been shown in this laboratory[58] that the fumarate unsaturation plays only a minor part in this polymerisation. This follows from the measured monomer reactivity ratios:-

(MMA r_m = 10 - 25, PEF r_f = 0 - 0.7). In support of this essential identity of mechanism, it is noted that the initial rate of reaction is little different from that of pure methacrylate under comparable conditions.

Table 11.

Comparison of MMA and PEF/MMA initial reaction rates.

Temperature 62°C.

Resin.	Initiator. B%	Feed Ratio. R	Reaction Rate.	Rate. $B^{-\frac{1}{2}}$.
PEF G	MEK 1.56	1.00	3.91	3.13
MMA	MEK 1.56	--	3.92	3.15
PEF J	BZP 1.90	1.00	9.92	7.20
MMA	BZP 1.90	--	9.64	7.00
PEF N	MEK 0.89	0.80	3.68	3.90
MMA	MEK 0.83	--	3.54	3.88
PEF N	HCH 1.95	0.96	2.29	1.64
MMA	HCH 2.00	--	2.72	1.93

As would be expected, the initial rates of increase of viscosity with time are also practically identical for the two systems. As the reaction in the resin mixture proceeds, the primary polymerisation chains soon become crosslinked via the polyfunctional polyester, and the times required for doubling the viscosity become shorter. The reaction rate plot remains linear over the first ten powers of two in the viscosity just as in the pure MMA polymerisation,

because over this range the termination rate is unaffected by viscosity. However, after this 2^{10}-fold increase in viscosity, the resin reaches the gel point almost at once, and the viscosity is infinite thereafter. This causes the compression of the long drawn out gel effect in the curved part of Fig. 15 into a sharp kink as shown in Fig.13. Once the viscosity has reached infinity, the rate has attained a new steady level reflecting the circumstances of the newly favoured rate control. Effects due to the fall in monomer concentration are in this case small because of the low degrees of conversion concerned.

Note. Comparison of the two curves shown in Fig.15 indicates that the gel effect appears to cause the greater rate increase in the photo-initiated reaction. Conditions there may be more favourable for the effect e.g. because of the absence of catalyst radicals.

4.3 Proposed Kinetic Scheme for the PEF/MMA Gelation.

The mechanism of the polyester "contact resin" hardening reaction has for some time been assumed to be a conventional addition copolymerisation between the two types of ethylenic unsaturation present. This reasonable assumption is used here as the basis for the development of a kinetic scheme for the gelation reaction.

A copolymerisation reaction of the model system PEF/MMA will lead to a molecular structure of the type illustrated in Fig.18; polymerisation chains of methyl methacrylate into which, at intervals depending on the monomer reactivity ratios of the two species, PEF chains are incorporated *via* one of the fumarate double bonds. The resultant macromolecule may then become crosslinked *via* one of the pendent fumarate double bonds into the MMA polymerisation chain of another similar molecule.

The classical theory of gelation[32,33] leads to the following equation for the critical conversion ϕ_c (at the gel point)

$$\phi_c = 1/(f_w - 1) \qquad (1)$$

where f_w is the weight average functionality of the molecules present initially *i.e.* when $\phi = 0$.

For the application of equation (1) to the PEF/MMA system, the following information is required ;-

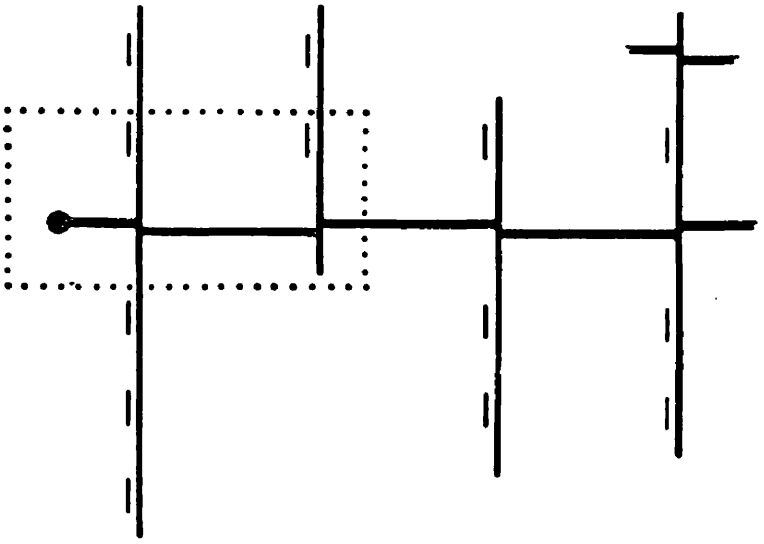

Fig.18a Schematic structure of the cross-copolymer. An enlarged detail of the section within the dotted rectangle is shown in Figure 18b.

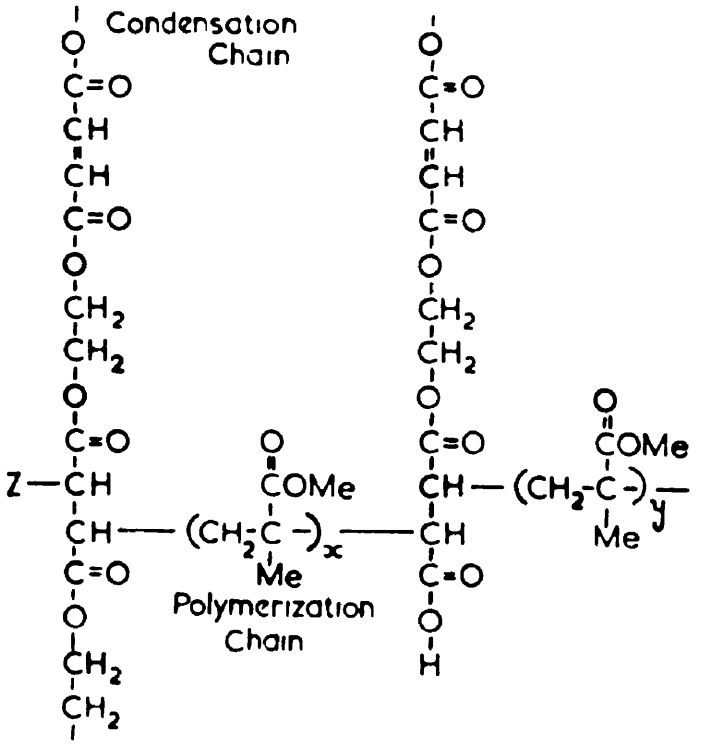

(b) **Fig.18 Detail of cross-copolymer structure.**

he average value of the numbers $x, y, \ldots$, etc. of methacrylate units intervening between the fumarate units is about 18 for an equimolar feed mixture of the two kinds of unsaturation.

DP_{wp} - The weight average number of monomer residues in the polyaddition chain.

DP_{wc} - The weight average number of ethylene fumarate units in the PEF condensation chains.

ρ - The fraction of fumarate units incorporated into the MMA polyaddition chains.

Then a weight average branching unit (MMA chain + PEF branches) will contain one less than DP_{wp} monomer residues of its constituent polyaddition chain. (The missing one is incorporated into the "inward crosslink" required by the network theory of gelation[32b]). Of the $(DP_{wp} - 1)$ monomer units, a fraction ρ are fumarates. Each of the $\rho(DP_{wp} - 1)$ fumarates contributes on average $(DP_{wc} - 1)$ further fumarate units belonging to the same condensation chain and which are therefore available for further crosslinking. (The one unit subtracted from DP_{wc} is that bond which has reacted in attaching the PEF chain to the branching unit). If, of the total of $\rho(DP_{wp} - 1)(DP_{wc} - 1)$ fumarate double bonds originally present, a fraction ϕ have polymerised to form crosslinks, then the critical conversion ϕ_c can be expressed in a form similar to equation (1):-

$$\phi_c = 1/\rho(DP_{wp} - 1)(DP_{wc} - 1) \qquad (10)$$

Of the four variables in (10), only DP_{wc} is easily accessible <u>via</u> the number average, DP_{nc} from end-group titration. Additional relations can be obtained between

the four variables via the kinetic theory of copolymerisation. The main assumptions thus introduced are the copolymerisation equation (16), and a termination reaction involving a pairwise destruction of radical ends, for which evidence independent of the gelling theory will be cited (Section 4.4).

The concentration of fumarate unsaturation remaining unreacted will be denoted by F ($mol.l^{-1}$), that of methacrylate unsaturation by M ($mol.l^{-1}$), and their ratio by

$$R = F/M \qquad (11)$$

Experimentally, the total concentration of unsaturation in the initial monomer mixture is given to an excellent approximation by

$$F_o + M_o = 9 \qquad (12)$$

(see Appendix page **124**), which will be used to simplify the equations. Moreover, where appropriate, F, M, R, dF/dt, dM/dt, and ρ are treated as constants equal to their initial values F_o, etc. and the steady state free radical concentrations F* and M* are also assumed to be constant. This is permissible because the gelling experiments were confined to changes in M of less than 20% while those in F were much smaller. The fractional conversion β of the overall unsaturation is given by:-

$$\beta = 1 - (F + M)/(F_o + M_o) \qquad (13)$$

The constancy of $d\beta/dt$ was checked dilatometrically in every run by the constancy of the rate of shrinkage. Thus the typical rate plots in Figs.4, 5, and 13 are seen to be linear up to the gel point, and therefore:-

$$\beta_c = (d\beta/dt)\, t_c \qquad (14)$$

As noted in Section 3.4, the propagation rate $(d\ /dt)$ increased suddenly at the gel point because of the gel effect, but this is not relevant to the present discussion.

From the definitions already given, it follows that:-

$$\rho = (F_o - F)/(F_o - F + M_o - M) \qquad (15)$$

The copolymerisation equation:-

$$dF/dM = \rho/(1-\rho) = R(Rr_F + 1)/(r_M + R) \qquad (16)$$

introduces the usual monomer reactivity ratios r_F for fumarate and r_M for methacrylate radicals. They are defined in terms of propagation rate constants thus;-

$$r_F = k_{F*F}/k_{F*M}\ , \text{ and } \quad r_M = k_{M*M}/k_{M*F} \qquad (17)$$

Here, k_{F*M} denotes the rate constant for the attack of an F* on an M etc. k_{M*M} is identical with the propagation constant for pure MMA which is denoted simply by k_p in the experimental section. Solving equation (16) yields:-

$$\rho = R(Rr_F + 1)/(r_M + R(Rr_F + 2)) \qquad (18)$$

The fraction β of the total, and the fraction ϕ of fumarate unsaturation reacted are related thus:-

$$\beta = \phi R/\rho(R + 1) \qquad (19)$$

The critical value of the former is found from equations (10), (11), (12) and (18), by substitution in (19):-

$$\beta_c = \frac{M^2(r_M + R(Rr_F + 2))^2}{9(Rr_F + 1)^2(DP_{wp} - 1)(DP_{wc} - 1)} \cdot \frac{1}{F} \qquad (20)$$

As the number average chain length DP_{np} is more readily expressible in terms of the kinetic scheme, the following substitution will be used:-

$$(DP_{wp} - 1) = 1.5\ DP_{np} \qquad (21)$$

This is correct for termination by radical combination, and will rarely be far from the truth in reactions of the type under discussion. While it is not possible to obtain directly an expression for DP_{np} which is free from the unknown radical concentrations F* or M*, or from the initiation rate, the product of DP_{np} and the reaction rate can be obtained. This suggests a transformation from β_c to t_c with the aid of equation (14).

Thus it is assumed that the four propagation steps with rate constants k_{M*M}, k_{M*F}, k_{F*M}, and k_{F*F} make up the total propagation rate, while three termination steps together exhaust the possibilities of chain termination.

These involve the binary radical collisions of the type $M^* + M^*$, $M^* + F^*$, and $F^* + F^*$, with respective rate constants k_t, k_t' and k_t''. If these collisions lead to radical combination, the expression for the product of reaction rate and DP_{np} may be written:-

$$(d\beta/dt)\ DP_{np} = \frac{1}{9} \cdot \frac{(k_{M^*M}M^*M + k_{M^*F}M^*F + k_{F^*M}F^*M + k_{F^*F}F^*F)^2}{k_tM^{*2} + k_t'M^*F^* + k_t''F^{*2}}$$

(Equation 22)

The factor of 1/9 is provided by equation (12).. From (22) the unknown radical concentrations F^* and M^* can be eliminated together, because they occur homogeneously, by means of the stationary state assumption.

$$k_{F^*M}F^* = k_{M^*F}M^*R \qquad (23)$$

In addition, substituting for $(d\beta/dt)$ from (14) and then for β_c from (20), gives the final general form for the gel point condition.

$$t_c = \frac{\frac{k_t}{k_{M^*F}^2} + \frac{k_t'R}{k_{M^*F}k_{F^*M}} + \frac{k_t''R^2}{k_{F^*F}^2}}{1.5\ (Rr_F + 1)^2(DP_{wc} - 1)} \cdot \frac{1}{F} \qquad (24)$$

This form is attractive because the gel time t_c is directly involved without any conversion factors relating to density, volume shrinkage, etc. The gel time is industrially

important as an empirical production control test in polyfunctional polyadditions, for which purpose a special measuring device is available[59].

4.4 Effect of Initiator Concentration and Initiation Mechanism.

According to equation (24), the gel time t_c should be independent of the concentration and even of the nature of the initiator. This is a surprising conclusion in view of the fact that in commercial practice the gelling times of "contact resins" are usually regulated by changing the concentration or nature of the initiator system.

Table 12.

Variation of gel time with initiator concentration in commercial polyesters (Source, reference 60).

Gel times in minutes at 100°C.

Monomer system.	Per cent Benzoyl Peroxide.			
	0.1	0.5	1.0	2.0
Polyester alone	-	-	10.0	4.0
Polyester/DAP (55:45)	13.5	1.5	0.5	-
Polyester/Styrene (67:33)	2.5	0.5	-	-
DAP alone.	-	250	-	39.0

It must be remembered however, that equation (24) applies only under isothermal conditions, while the reaction heat is usually allowed to build up to a considerable degree in commercial practice. Under adiabatic conditions, gelling should be speeded up by an increase in the initiator concentration even on the proposed theory. In any case, it is not claimed that the kinetic scheme fits all resin and initiator systems, but the evidence is overwhelming that it fits the methyl ethyl ketone peroxide initiated copolymerisation of the MMA + PEF mixture. In particular, the constancy of t_c over considerable ranges of initiator concentrations has been verified with three resin condensates at different temperatures, and typical results are shown in Table 15. At the same time it is verified there that the rate of polymerisation varied as the square root of the initiator concentration (B). This provides a confirmation of the kinetic scheme adopted which is independent of the gelation theory. The dependence of the rate on $B^{\frac{1}{2}}$ is, of course, a well-known consequence of the pairwise destruction of radical ends in chain polymerisation.

The constancy of t_c with varying initiator concentration is offered, not only as a proof of classical gelation behaviour, but also as a general confirmation of the chain reaction nature of polymerisation of unsaturated compounds. Thus, apart from any detailed mechanism, the

observed constancy of the gelling time in the face of observed variations of the reaction rate with $B^{\frac{1}{2}}$ demands some compensating factor varying with $B^{-\frac{1}{2}}$. It seems impossible to see what this factor could be if the reaction were not a chain reaction. If it is a chain reaction, then the gel point theory suggests that the compensating factor must be the chain length DP_{wp} and the kinetic scheme leads to precisely the variation of this factor with $B^{-\frac{1}{2}}$.

It would seem desirable to prove the constancy of t_c demanded by equation (24) also in the presence of other initiators or in the complete absence of initiator. It is not surprising that this proves less successful, because the gelling system is critically affected by side reactions falling outside the range of elementary steps admitted in the kinetic scheme. Thus a certain PEF/MMA mixture took 26 minutes to gel in the presence of 0.9% MEK. In the absence of added peroxide, the (trace-initiated) reaction proceeded, after a prolonged induction period, at 0.13 times the rate of that with 0.9%MEK. The gel time was then 45 minutes. Under the conditions of the trace-initiated reaction, e.g. the great chain length, a minute incursion of a new termination step would suffice to explain the delayed gelation.

A fairly successful test for the constancy of t_c with known variations in the nature of the added initiator is presented below.

Table 13.

Comparison of PEF/MMA gelation behaviour with MEK and HCH initiators.

PEF resin N, Feed ratio R = 0.5, Temperature = 62°C.

Initiator B %	Gel time. t_c	Conversion. β_c	Reaction rate.	Rate. $B^{-\frac{1}{2}}$.
MEK 0.29 (Batch 1)	56.0 mins.	7.0 %	1.86	3.45
MEK 0.73 (Batch 1)	59.5	11.9	3.01	3.55
MEK 0.68 (Batch 2)	57.5	10.8	2.81	3.42
HCH 0.32	50.0	3.2	0.95	1.68
HCH 0.42	56.6	4.5	1.44	1.81
HCH 0.62	69.0	6.6	1.43	1.82
HCH 0.96	70.0	8.6	1.84	1.88
HCH 1.11	69.3	9.9	2.14	2.03
HCH 1.66	83.0	13.8	2.50	1.94
HCH 2.33	81.5	14.4	2.66	1.74

It is seen that, like MEK, HCH obeys the square root dependence of rate on initiator concentration and produces an average gel time of 68.4 minutes under the same conditions in which MEK gives a gel time of 57.7 minutes. These two initiators differ appreciably, one being a hydroperoxide and the other a cyclic peroxide, and their initiating activity differs by a factor of two. The agreement between the average gel times is therefore satisfactory.

However while MEK correctly gave constant gel times to within experimental error, there was a significant trend towards higher gel times with increased HCH concentration. Gelation behaved as if the chain length varied approximately as $(HCH)^{0.7}$ instead of $(HCH)^{0.5}$, a minor unexplained deviation.

An entirely different type of initiator, α,α'- azobis-isobutyronitrile (AZBN), also caused very satisfactory constancy of the gel times in the PEF/MMA system over a fourteen-fold range in initiator concentration. The square root dependence of the overall reaction rate on the initiator concentration was not so well obeyed, but the observed deviation was only a factor of 1.6 over the whole fourteen-fold range in the value of B.

Table 14.

Effect of AZBN initiator concentration.

PEF resin N, Feed ratio R = 0.8, Temperature = 62°C.

Initiator. B %	Gel time. t_c	Conversion. β_c	Reaction rate.	Rate.$B^{-\frac{1}{2}}$
0.069	11 minutes	0.07%	1.05	4.00
0.960	12	5.13	6.40	6.53

The observed constancy of the gel times for the PEF/MMA system are offered as a proof of the classical gelation behaviour of the copolymerisation. This conclusion has been further supported by work carried out

simultaneously by McMillan, whose results[48] on the dependence of the gel time on the PEF/MMA feed ratio and the PEF condensation chain length also agree with the predictions of the postulated kinetic scheme.

Table 15.

Influence of MEK initiator concentration on the PEF/MMA gelation.

Temperature - 62°C.

Resin.	Feed ratio R	Initiator B %	G_o	t_c	Reaction rate.	Rate.$B^{-\frac{1}{2}}$
C	0.80	0.38	23 mins	17 mins	2.22	3.60
C	"	1.29	20	16	3.95	3.48
C	"	2.29	19	16	4.85	3.21
D	0.96	0.12	19	10.4	1.44	4.11
D	"	0.42	15	10.0	1.94	3.90
D	"	1.52	13.5	9.5	4.89	3.97
N	0.49	0.29	64	56	1.86	3.45
N	"	0.68	67.5	56.5	2.81	3.42
N	"	0.72	68	59.5	3.01	3.55

4.5 Analysis of Assumptions.

The neglect inherent in equation (24) of two side reactions should be discussed here. Firstly, chain transfer reactions have been totally discounted in the kinetic scheme. Chain transfer to MMA monomer is known to be inappreciable. Chain transfer to the PEF resin may occur to a small extent, but the constancy of the gel time (Table 15) with variations in initiator concentration forms a sensitive test for the absence of such transfer. Secondly, delay of gelation through internal cyclisation reactions[61,62,63]. has been entirely discounted by McMillan's results[48].

The assumption tacitly made, that all fumarate double bonds have equal reactivity constants irrespective of their position in a PEF condensation chain, seems plausible on theoretical grounds. The possibility that terminal bonds only differ in reactivity from all others towards the centre of a PEF chain may be considered. If the terminal double bonds were completely unreactive to addition polymerisation, all the apparent DP_{wc} values used would have to be reduced by two, i.e. the number of terminals per weight average chain. This would not significantly affect the treatment. If conversely, only the terminal double bonds of a PEF chain were reactive, the gel point would be expected to be delayed as the actual chain length DP_{wc} was increased. This was completely ruled out by McMillan's results[48].

4.6 The Gelation of Diallyl Compounds.

The gel point theory advanced by Flory[64], Stockmayer[65], and Walling[66] for polyfunctional reactions, takes no account of the tendency of both vinyl groups to be occasionally incorporated into the same chain in the polymerisation of a divinyl compound ("incestuous"[62] or "unnecessary"[53] polymerisation.) This factor causes a delay in the gel point, and was investigated for the diallyl phthalate (DAP) system by Simpson et al.[61]. Kinetic and statistical derivations by Gordon[62] for the gel point condition in this system showed fairly good agreement with the experimental results on DAP, but further examination of a series of diallyl compounds by Simpson and Holt[53] gave results which they claimed were irreconcilable with the theory. Since the kinetic theory for the gelation of the PEF/MMA system studied in this work was derived in precisely the same way as that applied to the phthalates by Gordon, the claims of Simpson and Holt were regarded as a challenge to the validity of the PEF/MMA theory.

A viscodilatometric reexamination of the gelation of four diallyl monomers was therefore undertaken (Section 3.5). The assumption made by Simpson, that the reaction rate was constant up to the gel point, was proved by the linearity of the shrinkage plots obtained e.g. Fig. 16, but the gel times observed viscodilatometrically were considerably

different from those previously reported.

Table 16.

Comparison of results for diallyl gelations.

Gel times in minutes at 80°C with 1% benzoyl peroxide.

Results.	DAO	DAP	DAI	DAT
Simpson [53]	176 mins.	300	180	260
This work.	380	285	205	153

The viscometric gel times are in agreement with the gelation theory in that the delay in the gel point caused by incestuous reaction of the second double bond within one monomer molecule increases with the increasing proximity of the two unsaturated linkages. Simpson's gel times on the other hand, do not show the same trend. This was probably due to the less refined technique used to locate the critical point (observation of the time at which particles of "gel" could first be seen).

Simpson isolated and measured the amount of polymer formed at the "gel point" and compared it with the quantity predicted by the network theory of gelation. A similar comparison was made viscodilatometrically because of the doubt about Simpson's gel times. The calculation entails a knowledge of the amount of unsaturation present in the polymers, and for this, the values used were those obtained by Simpson using bromide/bromate estimations. (These results were accepted as reliable, having been checked both

by iodine chloride estimations and infrared measurements, and also because the amount of unsaturation in the polymers was independent of the position of the gel point). The amount of polymer formed at the gel point was calculated from equation (25).

$$\text{Polymer at } t_c = 1/(1 - \text{unsaturation}) \times \text{Double bond conversion} \quad (25)$$

In Table 17 below, two theoretical values are quoted for the amount of polymer formed at the gel point. This is because of the uncertainty of the DP_w/DP_n relationship in the polymers which normally lies between the limits

$DP_w = DP_n$ for polymer chains of uniform length, and

$DPw = 2\ DP_n - 1$ for a random distribution of chain lengths.

Table 17.

Comparison of theoretical and experimental values for the amount of polymer formed at the gel point.

Monomer.	Double bond conversion. (this work)	Unsaturation of polymer. (reference 53)	Polymer at t_c (25).	Theoretical polymer	
				Uniform	Random
DAO	0.202	0.39	0.331	0.150	0.077
DAP	0.185	0.26	0.250	0.266	0.140
DAI	0.149	0.42	0.257	0.143	0.073
DAT	0.125	0.42	0.216	0.136	0.069

The agreement between the experimental values for the amount of polymer formed at the gel point and the value predicted

by the theory is no better than that shown by Simpson's results, and it seems that further investigations into the cause of the discrepancies are necessary. It should be noted, however, that there is nowhere a factor of more than two between the experimental values and those predicted for polymers containing uniform chain lengths. When it is remembered that the theory of gelation as applied to polyaddition reactions is critically affected by the presence of side reactions not considered in the kinetic scheme, it seems that the rather poor agreement is reasonably satisfactory especially when factors of 100 have been previously thought to exist[66].

5. Ball Rebound Relaxation Measurements.

5.1 The Ball Rebound Technique.

The diffusion controlled decay of the curing rate in a polymerisation reaction as the system nears its equilibrium is a relaxation process[67]. This led to the choice of a relaxation method for the study of this phase of the hardening reaction in the PEF/MMA polyester resin model system.

A fairly simple method of making dynamic mechanical relaxation measurements, the tripsometer technique, has been used in the rubber industry for several years. It measures the energy absorbed when a polymer specimen, mounted at the end of a pendulum arm, is allowed to rebound from a steel surface. This method involves difficulties in mounting the specimen when investigations are required in temperature regions in which the polymer becomes very soft or melts, and also the specimen is squashed by the heavy impact used. It was therefore decided to modify the method by using an unmounted specimen, in fact a small sphere, which could be dropped on to the steel surface. The energy absorbed could then be obtained from measurements of the height of rebound. This method was never put into practice because of the difficulty of producing small spherical polymer specimens. Pearl polymerisation[68] of the PEF/MMA resins was unsuccessful, the few reasonably

spherical pearls which were produced contained quite large quantities of the inorganic stabilisers used and were thus unsuitable for fundamental investigations.

By reversing the positions of the polymer and the elastic surface, no change was made in the relaxation characteristics of the system, and a much more convenient and widely applicable procedure was established. It was therefore decided to make energy absorption measurements by studying the rebound of a steel ball from a polymer surface.

The following requirements were considered in the design of the ball rebound apparatus:

1) Testing should be rapid in order to facilitate accurate measurements on systems in which curing reactions were proceeding.
2) The temperature of the polymer specimen should be accurately controlled and capable of rapid adjustment.
3) Facility should be provided for testing in vacuo or in an inert atmosphere to eliminate the possiblity of oxidation reactions occuring in the polymer when at elevated temperatures.

Since a simple and reliable instrument for the measurement of "cure" in polymer hardening reactions is needed by industry[69], it was decided to keep this factor in mind by designing an apparatus suitable for adaptation to such uses, which required only small test specimens, and was,

if possible, non-destructive.

With these considerations in mind, the ball rebound apparatus shown in Fig.19 was designed and constructed. A patent application No.31858/56 covering the apparatus has been filed, and the responsibility for its commercial development has been assumed by the National Research and Development Corporation.

A small disc of polymer is mounted on a brass block containing a heating element, and the temperature of the specimen surface near the impact point is measured with a thermocouple and read from the indicator (Fig.19, top right). The mounted specimen is placed inside the glass dome (left hand side) which can be evacuated or filled with an inert gas. The test ball is released electromagnetically from the top of the dome, and after the rebound (which is measured against an illuminated scale at the back of the dome), it is returned by a magnetic lift to the top of the dome in readiness for the next drop. The control box (bottom right) houses the electrical controls for the heating circuit and the magnetic lift. The rate of testing (i.e. the interval between successive ball rebounds) may be adjusted from 10 seconds to 3 seconds per test, and the mounted specimen can be heated from 0° to 300°C at rates of up to 30°C per minute. A detailed description of each part of the apparatus is given below.

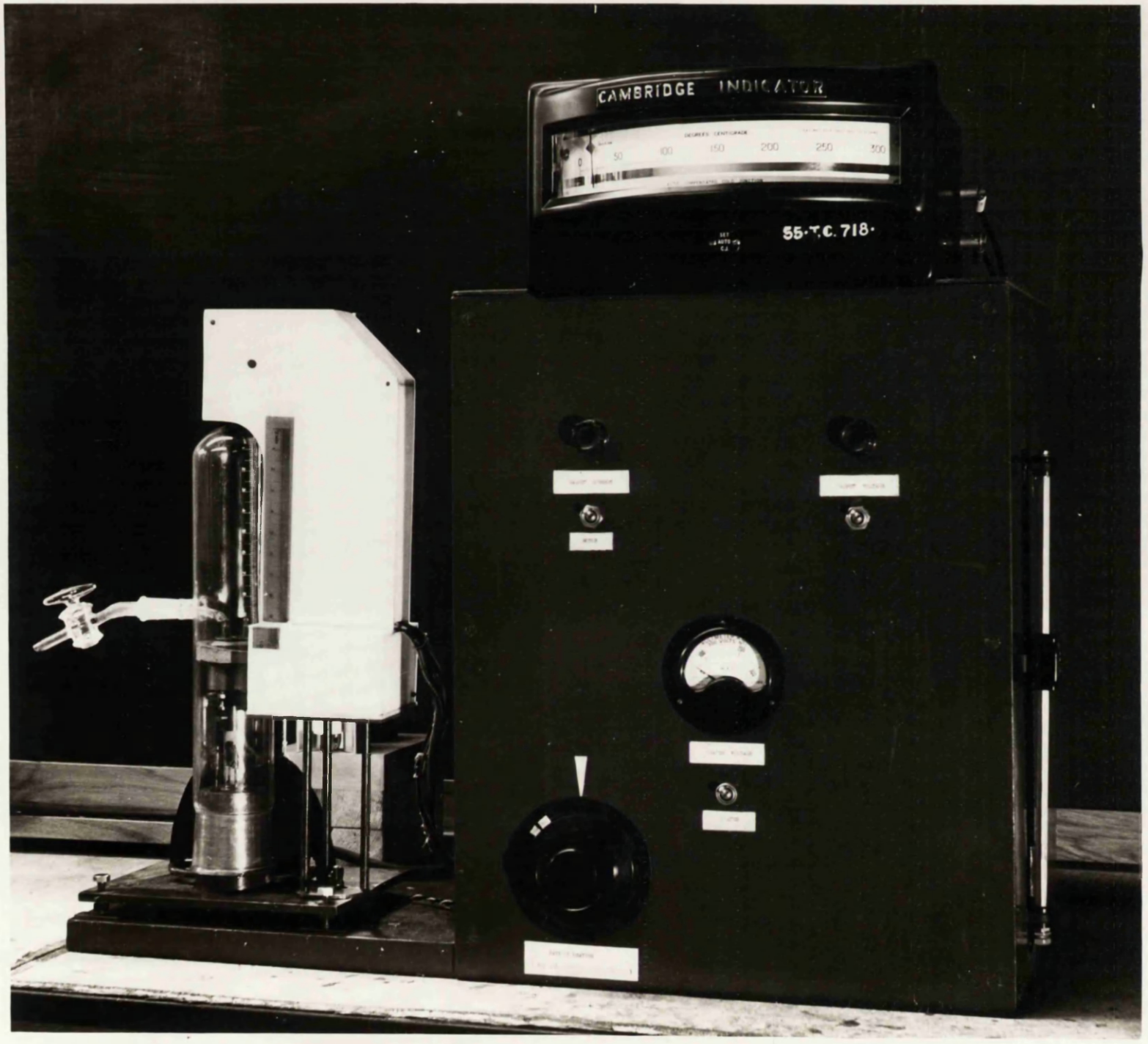
CAMBRIDGE INDICATOR
55-T.C. 718-

After the apparatus had been constructed, it was found that in 1952 Jenkel and Klein[70] had used a simple ball rebound apparatus for the investigation of relationships between ball rebound energy absorption measurements and molecular relaxation phenomena in polymers. The apparatus was however, not adapted for rapid measurements on systems in which curing reactions were taking place, or for following the rate of curing in such systems.

5.2 The Ball Rebound Apparatus.

The Specimen Mounting.

The polymer specimen rested in a $\frac{1}{2}$" diameter circular depression 1/16" deep on the top of the heater block, and was clamped in position by the thin spring-loaded brass disc (K - Fig. 20). The disc had a 3/16" diameter aperture in the centre through which the ball bounced on the specimen. Retaining nuts were fitted to the screws below the clamping disc to prevent the pressure of the springs causing thermoplastic polymers to flow upwards through the aperture when they reached their softening points.

It was found that unless the specimen was perfectly flat on both sides, very irregular bouncing occurred until the specimen began to soften when its temperature was

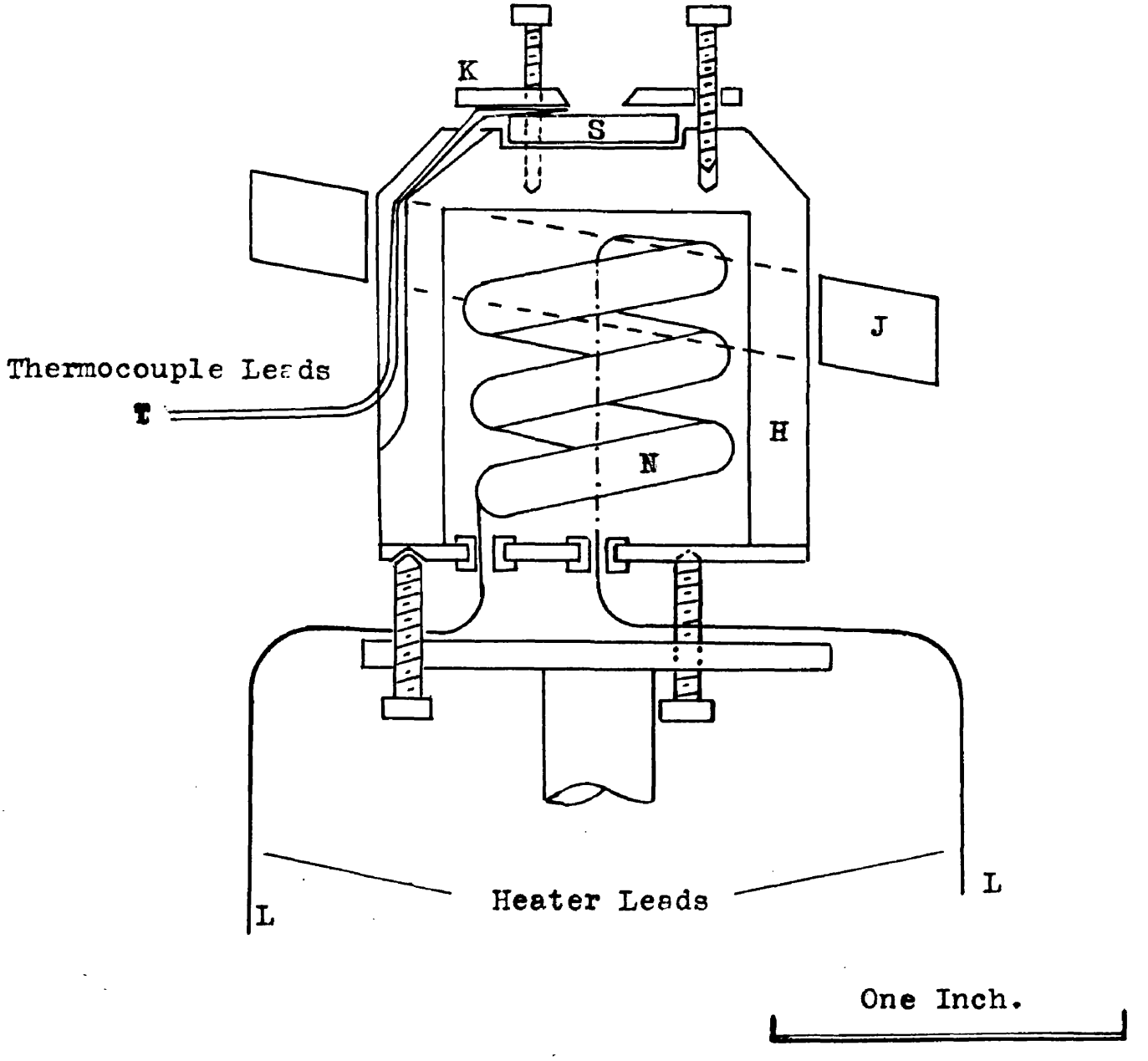

Section of Heater Block. Figure 20.

raised to the softening point and became pressed into good contact with the heater block by the pressure of the springs. It was found that careful filing was a satisfactory method of smoothing the surfaces of rough specimens.

The Heater.

The 300g. brass block (Fig.20) on which the specimen (s) was mounted, was hollow, and into the interior, a 180 ohm nichrome heater coil was fitted. The coiled coil was wound around a steatite former and was insulated from the surrounding brass with mica sheeting. The leads (L) to the heater (H) were passed through the detachable base plate of the heater block via small Pyrex bushes and connected to the extension pieces emerging from the top of the cone (B,Fig.24). The corresponding terminals (R, Fig.24) at the base of the cone were connected to a variable output transformer, the output voltage of which was indicated by a voltmeter mounted in the control box. The diagram of the heating circuit is given in Fig.21 together with the alternative circuit used when thermostatic control of the specimen temperature was required (during isothermal curing experiments - Section 6.4). The curved glass window of the Cambridge temperature indicator was removed when isothermal runs were to be performed, and a Perspex window, having a 1/8" groove running parallel to and 1" from the

Heater circuit diagrams. Figure 21 .

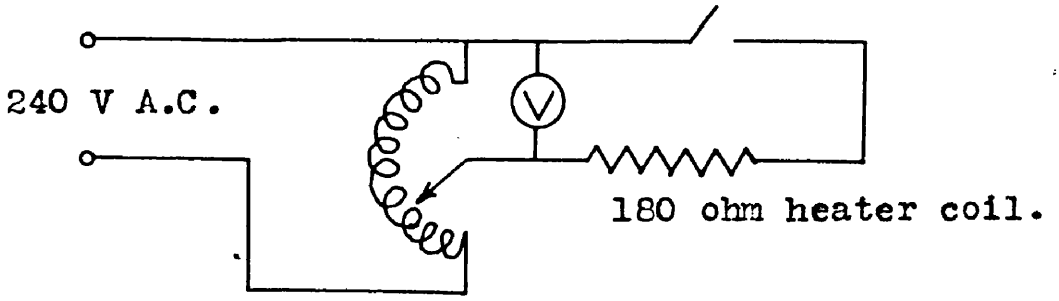

Heater circuit as normally used.

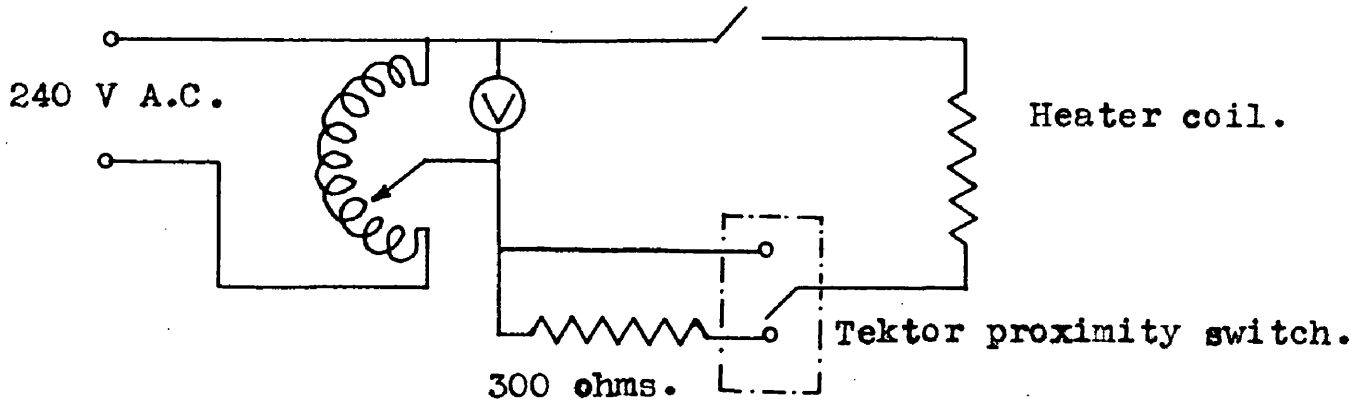

Modified heater circuit incorporating the "Tektor" and series resistance for use in isothermal experiments.

top, was substituted. A sliding brass terminal was fixed in the groove and carried a thin brass plate 1/4" wide which lay parallel to, and within 0.05" of, the track of the diamond shaped head of the indicator pointer. The terminal was connected to a Tektor proximity switch and its position was adjusted so that when the polymer specimen was heated to the desired temperature, the movement of the indicator pointer towards the brass plate increased the capacity of the system causing the Tektor to switch. This action brought an additional 300 ohms resistance into the circuit and thus reduced the heating current to one third of the normal value. The reduced current was insufficient to maintain the specimen temperature which accordingly fell until the falling capacity between the indicator pointer and the Tektor "plate" switched the series resistance out of the circuit to recommence heating the specimen. It was found necessary to earth the indicator pointer to prevent the electrostatic force between the two "plates" of the capacitor system causing the pointer to read incorrectly as it neared the switching position. This method gave temperature control of the specimen to $\pm$ 2°C.

The range of heating rates obtained as measured at the polymer specimen are shown graphically in Fig. 22 for the whole available range of heater input voltages.

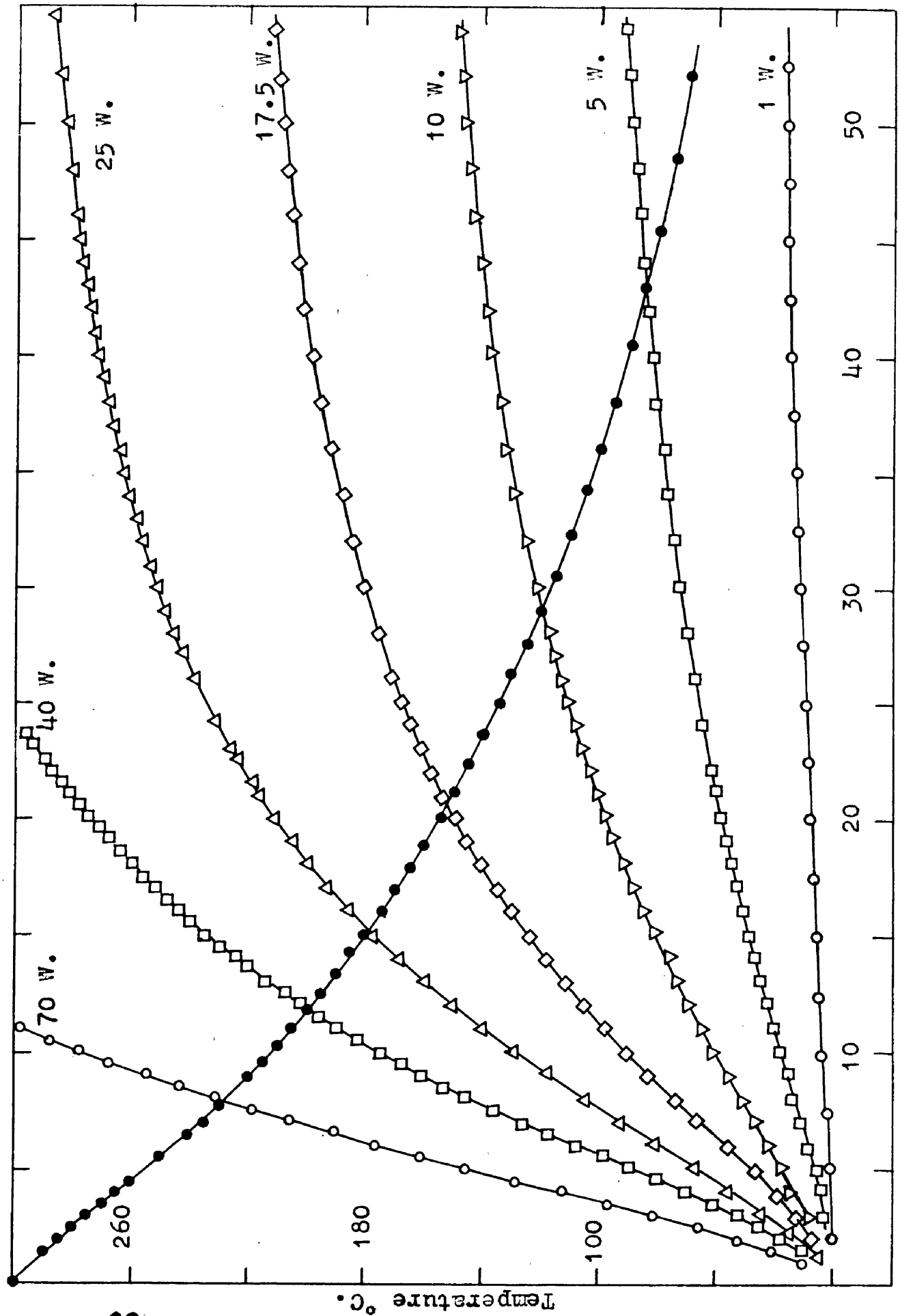

Figure 22. Rate of specimen heating vs. power consumption.
● - Fall in temperature during free cooling.

Temperature Measurement.

The temperature of the specimen under examination was measured using a platinum/platinum-rhodium thermocouple in conjunction with a Cambridge indicator (Fig.19 top right) reading from 0° - 300°C in 2° divisions. It was found possible to estimate the temperature to approximately 0.2° from the antiparallax scale. An automatic compensating cold junction was incorporated in the indicator which was regularly checked for accuracy of calibration against melting ice and boiling water.

The thermocouple head was held between the clamping plate (K, Fig.20) and the specimen (S) within 1/8" of the point of impact of the ball. In order to find whether there was any difference due to time lag between the temperature of the specimen surface and that shown on the indicator, a series of peak curves (see Section 6.1) for Perspex were obtained using widely different heating rates (from 30°C per minute to 3°C per minute). The curves obtained were all (practically) coincident. The results of a different type of lag investigation are plotted in Fig. 23. A fully cured specimen of epoxide resin at 170°C was suddenly cooled through 10° by a blast of cold carbon dioxide gas. Readings of the ball rebound and the temperature recorded on the indicator were noted against time. A cooling curve for the resin was taken over the same temperature range,

Figure 23. Lag Investigation.

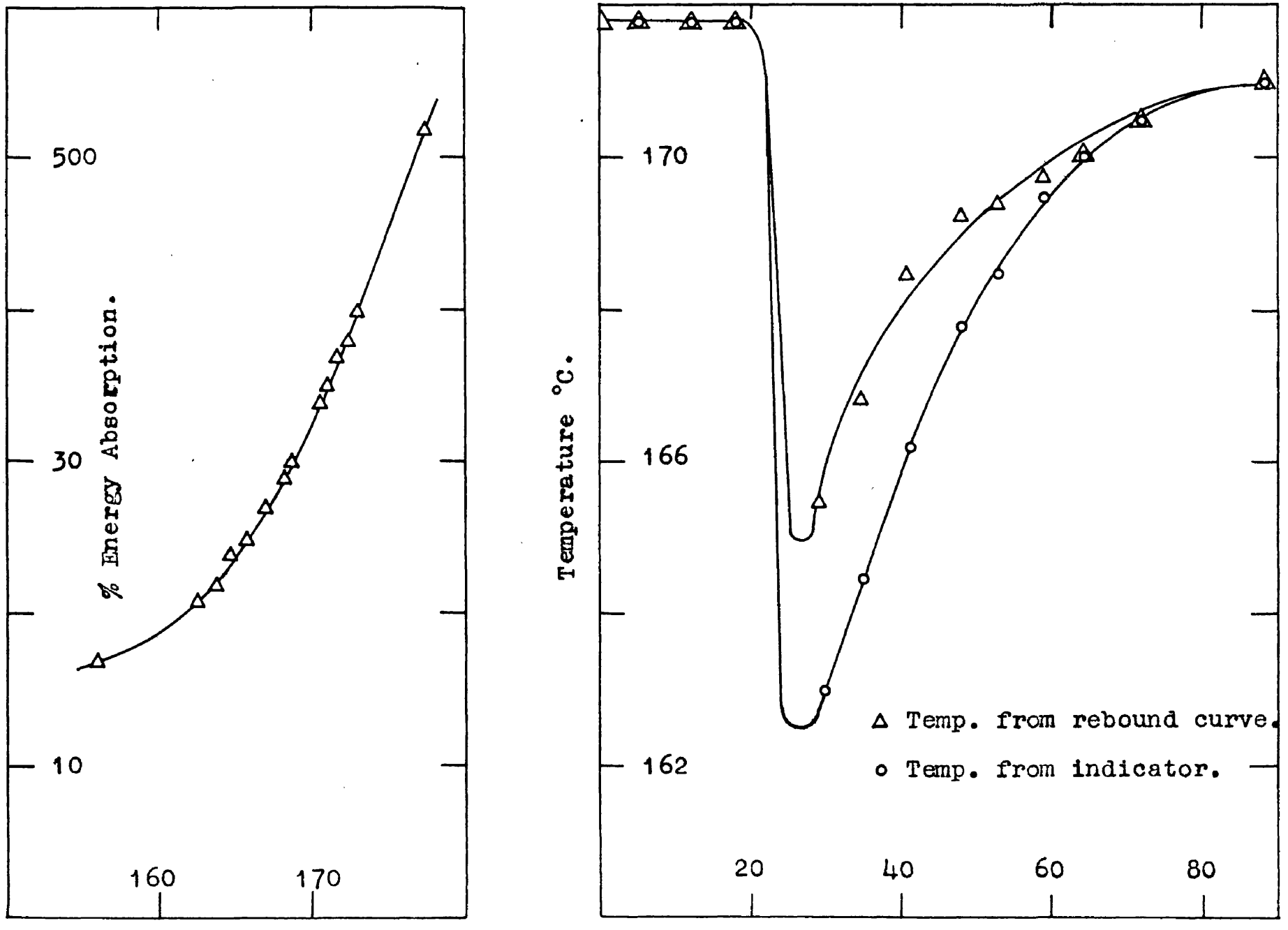

and from it, the temperatures corresponding to the noted ball rebounds in the first experiment were found and plotted against the corresponding times. The indicator temperatures were also plotted against the times, and the two curves thus obtained give a measure of the lag between the indicator reading and the actual impact point temperature caused by the sudden cooling. Fig. 23 shows that within 30 seconds of the cooling, the difference between the two temperatures had disappeared.

The Dome.

The Pyrex dome (A - Fig. 24) 35cm. high was fitted with a B55 standard socket. The tap (F) was used for admitting gases, in particular for directing a stream of cold carbon dioxide upon the specimen surface (with the vacuum pump left running). By this means, the specimen could be cooled through 100°C in a minute.

A scale (G), fixed to the rear of the dome, was used for measuring the height of the ball rebound. The 17.5 cm. scale (= the drop height) was calibrated for energy absorption in ½% divisions. Thus, a 5.8cm. bounce represented a 33% height rebound or a (100 - 33%) 67% energy absorption.

Figure 24 .

Ball rebound apparatus.

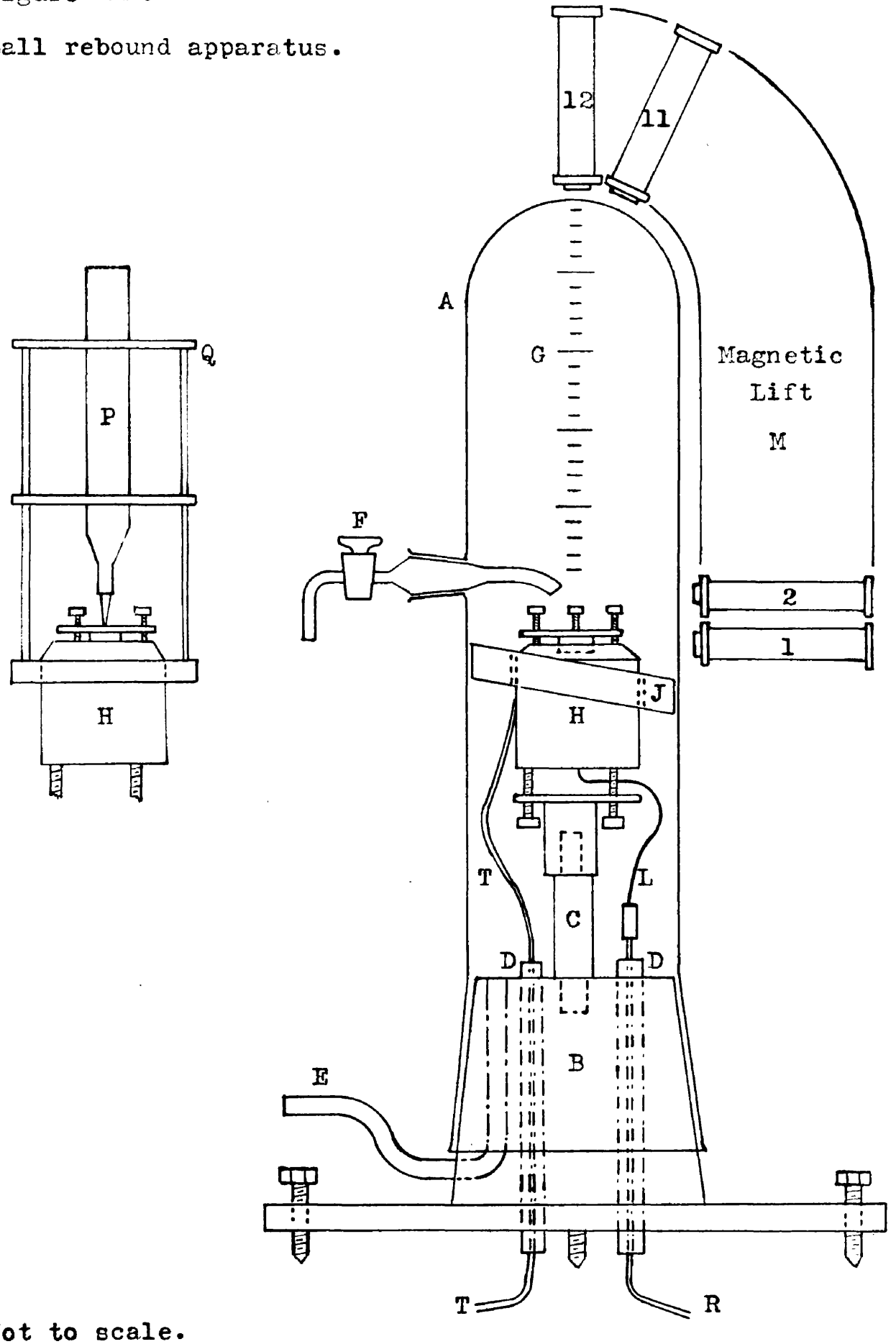

Not to scale.

The rebound measurements were made visually using a subsidiary scale mounted on the magnetic lift housing to avoid parallax. The trace of the ball could also be photographed as shown in Fig. 25A. The measurements obtained in this way were in good agreement with those estimated visually. In Fig. 25A, the recorded energy absorption is 62% and the corresponding visual estimate was 61.5%.

The Cone, Baseplate, and Heater Mounting.

The brass cone (B, Fig.24) which was machined to standard B 55 dimensions, was mounted on a baseplate fitted with levelling screws. The cone was internally water-cooled to prevent thermal expansion causing seizure or cracking of the glass socket on the dome, and carried the vacuum take-off (E, Fig.24). The vacuum take-off and cooling water pipes are shown in the photo of the assembled heater mounting unit (Fig.25B). Three threaded Bakelite sleeves were screwed vertically through the cone. Two of these each carried a lead for the heater current through the centre, and the third was used for the two glass cloth sleeved thermocouple leads. Vacuum-tight seals of both the insulating sleeves into the cone, and the electrical leads into the sleeves, were obtained using Picein wax.

A central Sindanyo (asbestos composition) column (C, Fig.24) was screwed into the top of the cone and

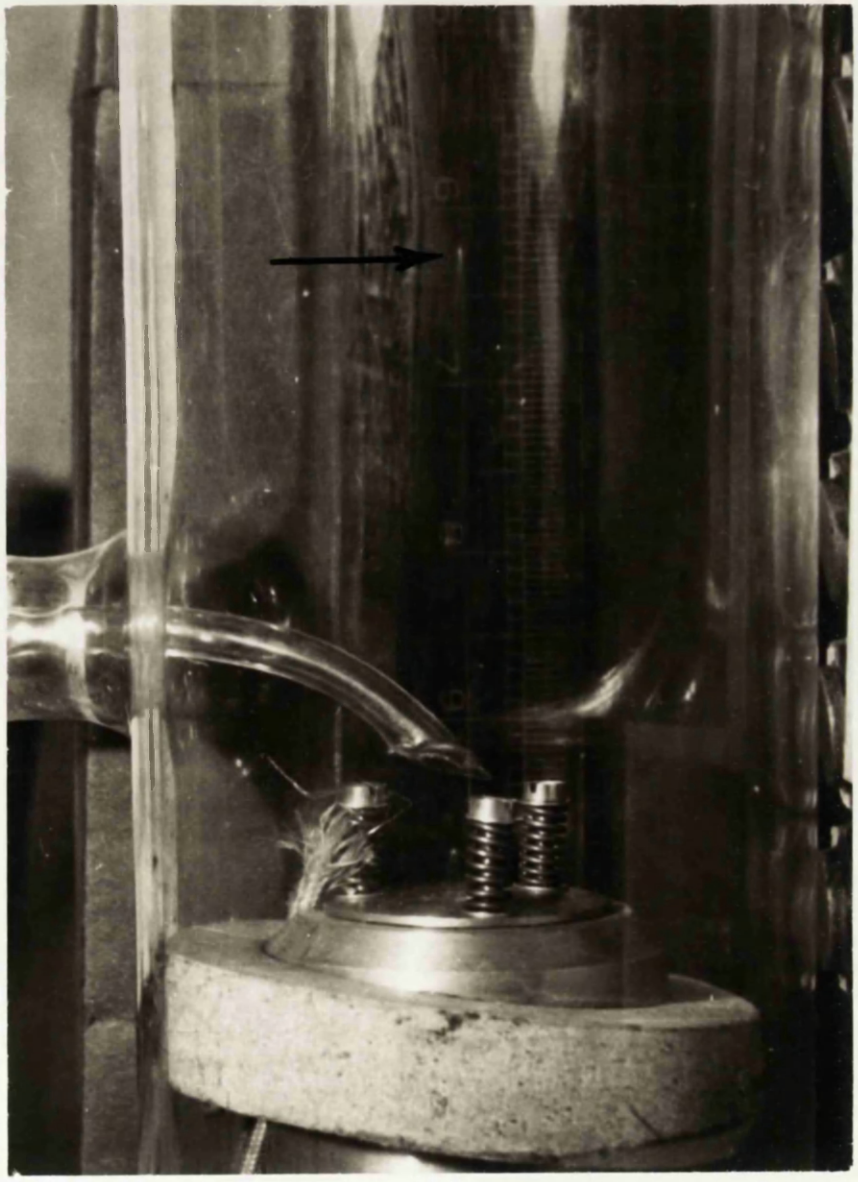

A

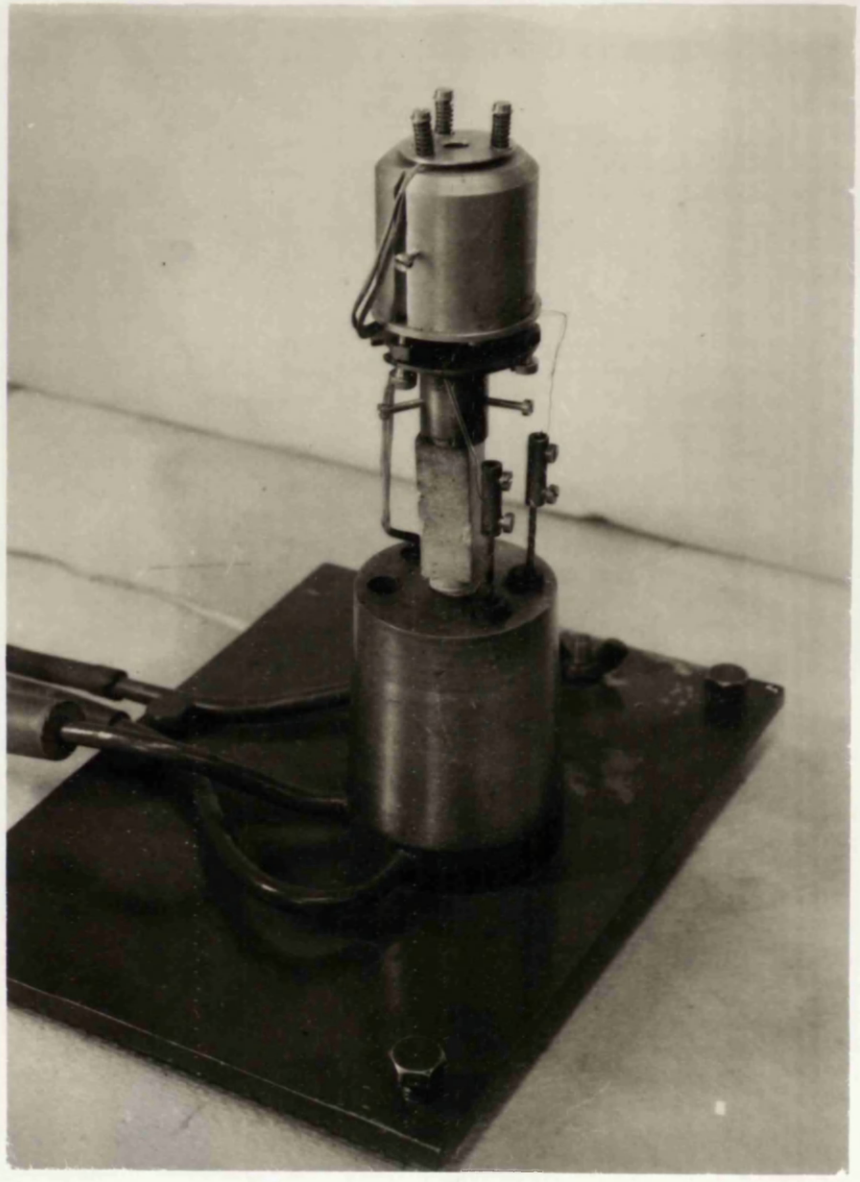

B

Figure 25

supported the heater baseplate on which the heater block was levelled with the aid of the levelling screws shown.

In order to return the ball (after bouncing), to the first magnet in readiness for lifting, an inclined Sindanyo ring (J, Figs. 20 and 24) was fitted round the heater block. This was machined to a sliding fit both over the heater, and also inside the glass dome. Since the internal diameter of the dome was 0.2" greater than the minimum diameter of the B 55 socket, the ring was prepared in two parts and assembled inside the dome. When the dome was placed in position over the cone, the inclined ring slipped over the heater and was held at the correct height by a stop fixed in the side of the heater block (see Fig.25A).

The Magnetic "Lift".

The lift consisted of twelve electromagnets, mounted one above the other, which were switched on in rotation so that the steel ball was lifted stepwise from the level of the test piece to the top of the dome.

Each 150 ohm solenoid was held in two spring clips mounted on a brass strip which was in turn bolted through a slot in a brass guide plate. The slot in the guide plate was cut parallel to the wall of the glass dome so that vertical adjustments of the position of any solenoid could

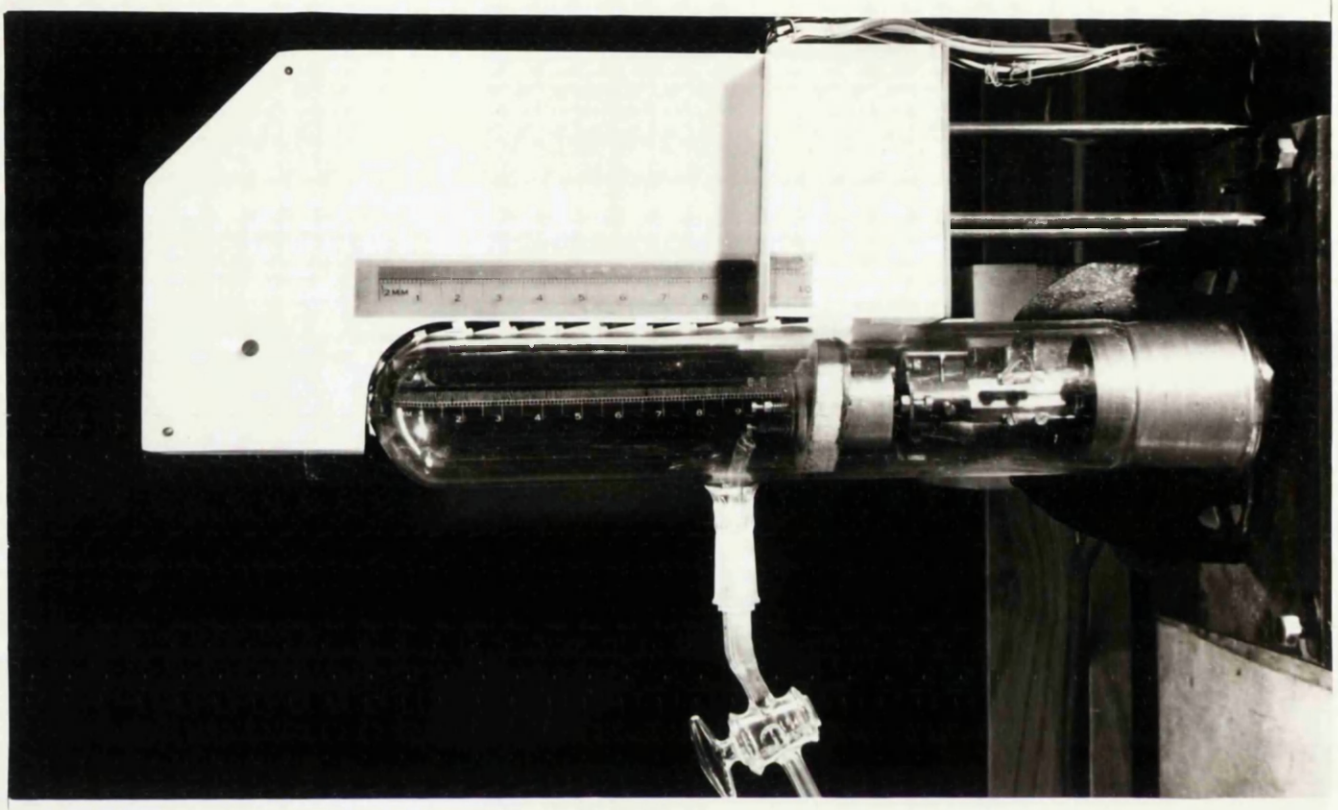

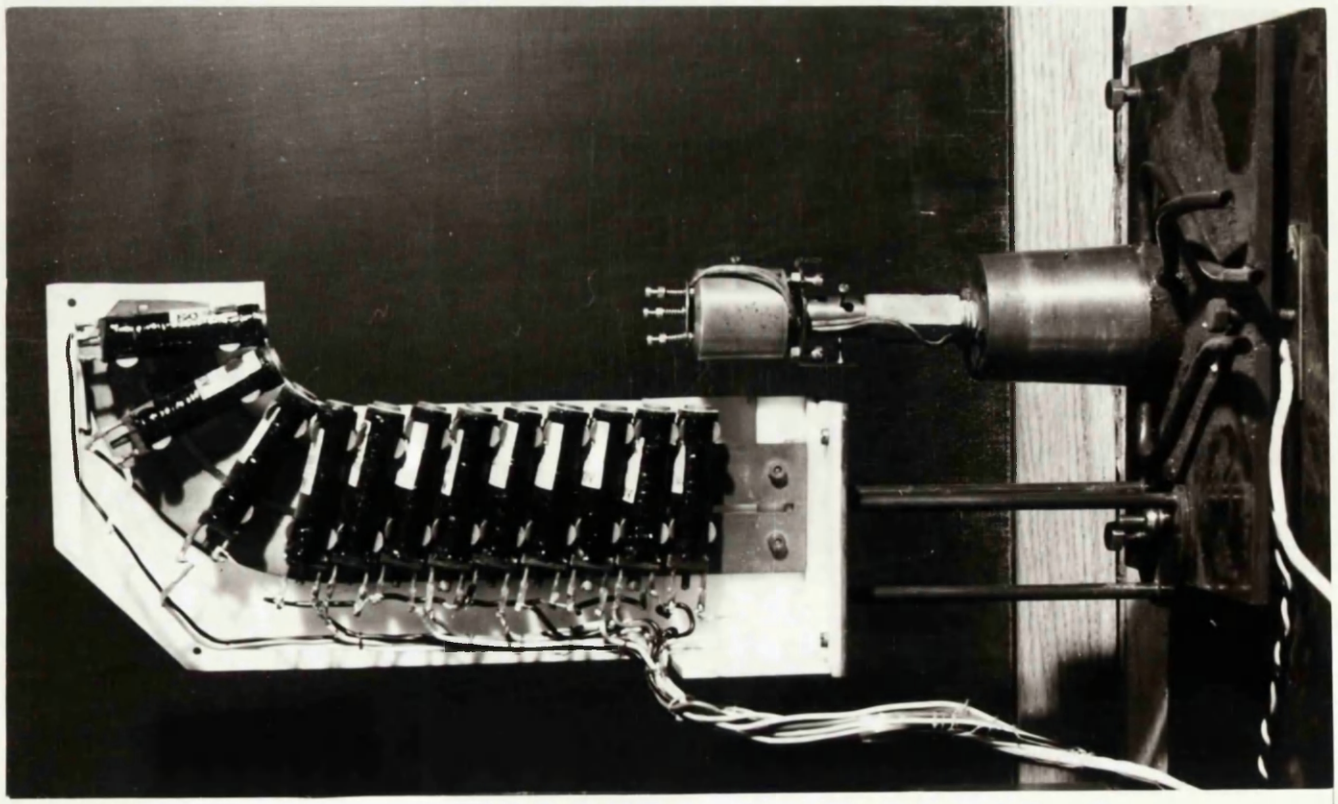

Figure 26.

be made without altering its distance from the dome. The single bolt fixing of the mounting strips ensured that the solenoids could be tilted about a horizontal axis, and they could be moved nearer to, or away from the glass dome by slackening the spring clips. These three adjustments were necessary since the solenoids were only just powerful enough to lift the ball provided that:-

a) They were in contact with the outer wall of the dome.

b) Each was as close as possible to the solenoid below.

c) They were tilted slightly downwards (10° to the horizontal).

The last adjustment concentrated a more powerful portion of the magnetic field in the direction of the ball.

The twelve solenoids clamped on the guide plate as described, were then mounted in a Perspex housing which was supported by a tripod rising from a slotted base plate. The whole magnetic lift was clamped in position against the wall of the glass dome using a screw and wing nut on the dome base plate. In Fig.26, the magnetic lift is shown (a) with the cover removed to show the solenoids, and (b) mounted beside the dome ready for operation. A second screw and wing nut were provided on the baseboard of the control box so that the magnetic lift could be clamped out of the way while the glass dome was removed for specimen mounting or adjusting operations.

The electrical circuit for the magnetic lift is shown in Fig.27. The solenoids were wired so that the lifting poles were alternately North and South, as experiment had shown that an arrangement of all poles having like polarity gave less lifting power. A 0.5 microfarad capacitor and a 500 ohm resistor were connected across the terminals of each solenoid to minimise the effect of the back EMF generated when the current was switched off. The lift was powered by a 110 volt D.C. supply via a six-bank "uniselector" rotary switching device. The switching action in the uniselector was produced by an electric bell type vibrator which gave a minimum speed of one revolution i.e. 50 switching actions, in one second. This was not suitable for the lifting operation and the vibrator mechanism was therefore removed and replaced by a cam driven by a 24 volt electric motor via a 60:1 speed reducing gear train. The power for the motor was obtained from the 110 volt supply through a potentiometer which thus provided a convenient means of varying the speed of the lifting cycle.

Each solenoid (except the first and the last) was energised for only one pulse of the uniselector. An attempt to obtain better lifting efficiency by using a two pulse on-period which overlapped with that of both the previous and the succeding magnets was not successful. A three pulse on-period was used for the bottom magnet

Magnetic Lift Circuit.

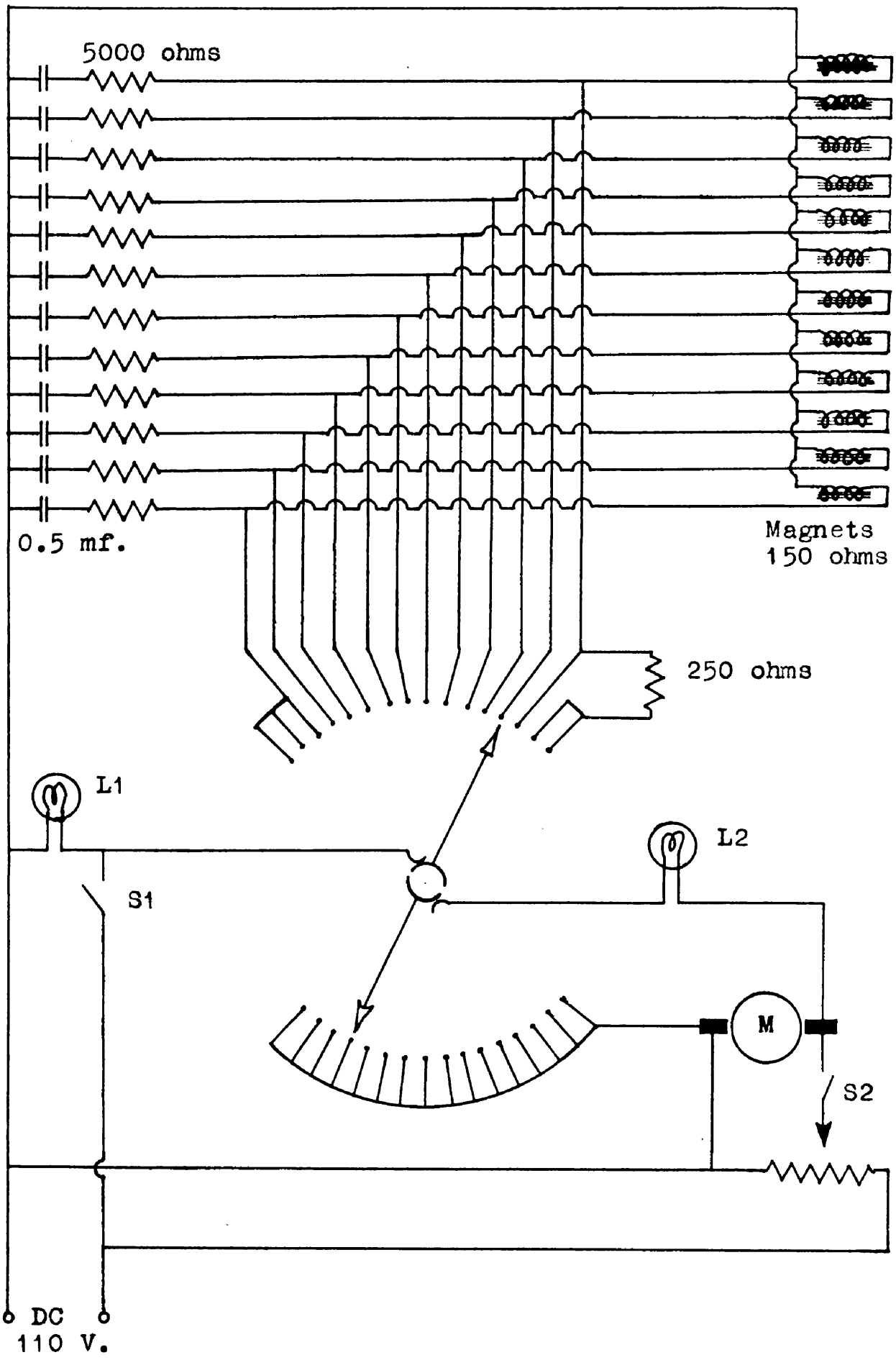

Figure 27 .

(No.1 in Fig.24) in order to give the ball time to reach it. The last magnet (No.12) was also given three pulses to give the ball time to become steady before being dropped, the second and third pulses being at a reduced voltage obtained by incorporating in the circuit a 250 ohm resistor. This was done in order to cut down the considerable heating effect caused by the normal power dissipation of 80 watts. The complete cycle of the magnetic lift was therefore as follows:-

No.1 solenoid	-	Three pulses.
Nos. 2 to 11	-	One pulse each.
No. 12	-	Three pulses.
Off-period	-	Nine operations of the switch. (While the ball was bouncing.)

To operate the magnetic lift, switch S2 (Fig.27) was closed to start the motor M. The motor speed was adjusted, using the potentiometer, to give a suitable cycle period (ussually in the range 4 to 6 seconds), then when the indicator L2 lit showing the commencement of an on-period, switch S1 was closed thus completing the lifting circuit. S1 (together with its indicator light L1) was incorporated so that the heating effect previously mentioned could be avoided if lifting was not required, while the motor was running and the lift was ready for instant use.

One complete cycle of the six-bank uniselector consisted of fifty switching operations; twenty five blank actions

followed by twenty five moves from one contact to the next. To eliminate the blank actions which would have caused too long an off-period between lifts, three contact arms were moved to a position opposite the other three, so that as one on-period ended, the next (on the other bank of three) started. Two rows of contacts from each triple bank were used to switch the magnet current in order to divide the heavy load (one amp at 110 volts) which tended to cause arcing when the contacts were opened. The third row of contacts was used to switch the current for the indicator light L2, and was wired so that L2 lit only while a solenoid was energised.

The Penetrometer.

The penetrometer, which was similar to one described in the literature[71], consisted of a $\frac{1}{2}$" diameter glass tube into one end of which was fitted an I.P. standard penetrometer needle. The tube was filled with sufficient mercury to give the required load on the needle (usually 250g.). The penetrometer was supported in two knife-edged rings mounted on a rigid framework which could be clamped over the heater block (Fig.24). Movement of the penetrometer (P) was measured with a cathetometer. The plot of a typical penetrometer experiment is shown in Fig.28, the second order transition temperature being taken as the point at which movement of the needle first began.

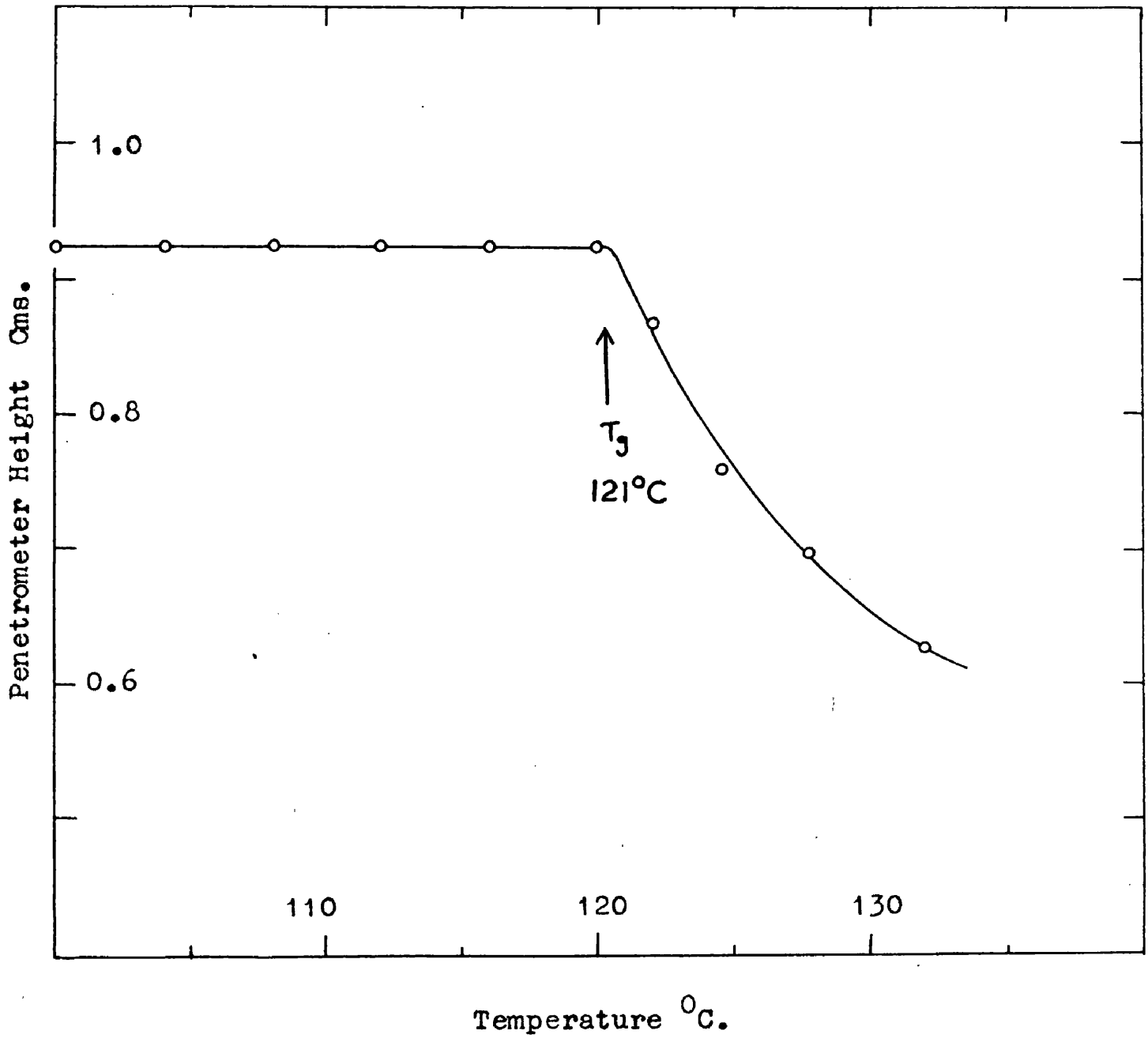

Figure 28.

Penetrometric determination of the second order transition temperature of polymethyl methacrylate (Perspex).
I.P. standard penetrometer needle, 100g. load.
Rate of heating - 10°C per minute.

5.3 The Preparation of Test Specimens.

Polyester "Contact" Resins.

The polyethylene fumarate resin used in the preparation of specimen discs for ball rebound examination was PEF resin N which was copolymerised with methyl methacrylate at 62°C using methyl ethyl ketone peroxide as initiator. The reaction mixtures were prepared exactly as for the gelation experiments (Section 2.5), and discs were cast in aluminium moulds in a carbon dioxide atmosphere. In order to follow the progress of the crosslinking reaction, a duplicate sample of each resin was copolymerised in a dilatometer as previously described. From the point at which density measurements in a dilatometer were no longer feasible because of bubble formation in the polymer, measurements were made on the test discs themselves using a density gradient tube technique[34].

Specimens cut from a commercial polyester resin glass laminate were also examined (Fig.29). This had been prepared from Laminac 4128 resin (polyester + diallyl phthalate). Twelve layers of glass cloth were used, and the 65% glass, 35% resin mixture sheet was cured at 120°C for 30 minutes using 1% tert-butyl perbenzoate as initiator.

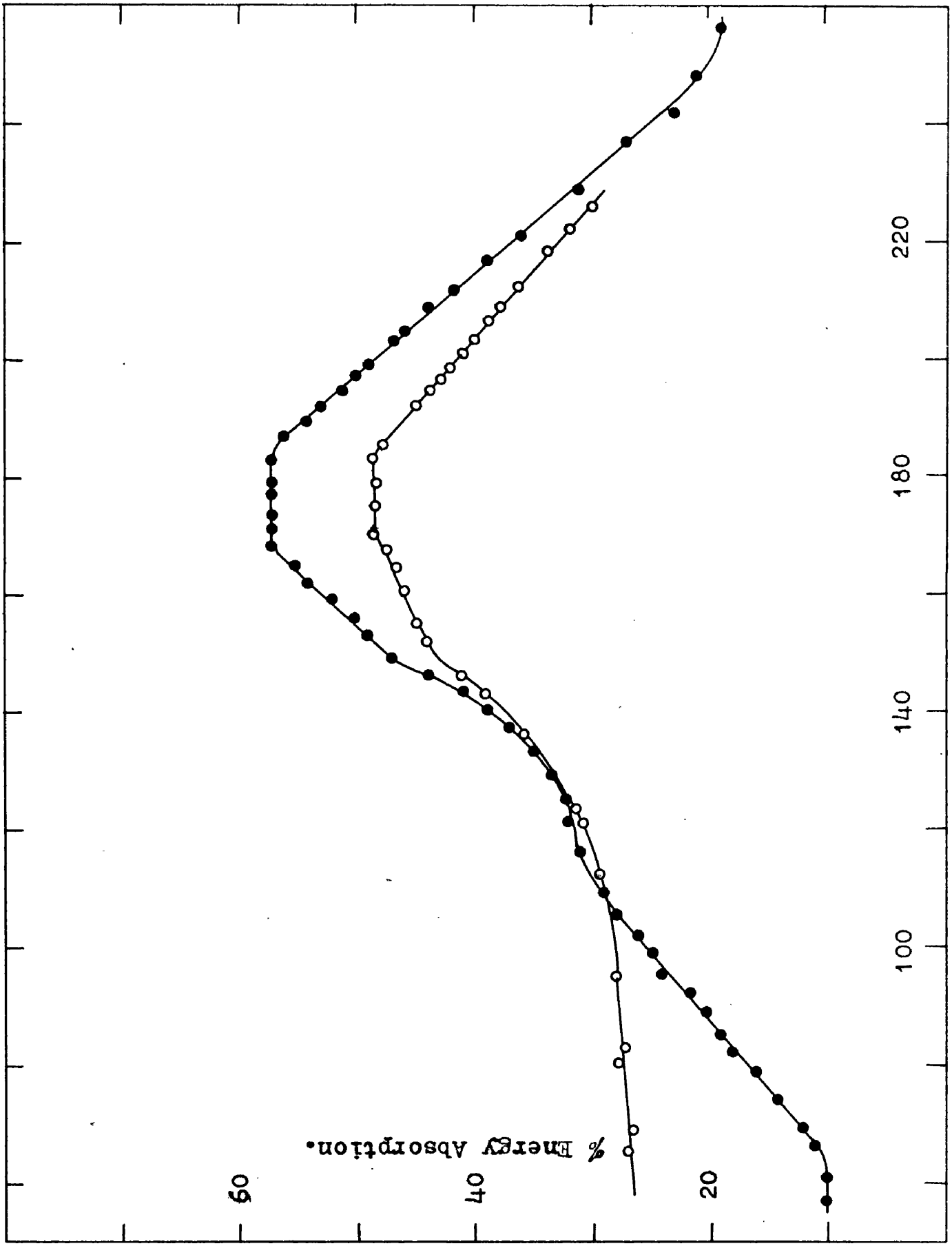

Figure 29 . Energy absorption spectra of a polyester resin (•) showing the flattening effect caused by the inclusion of glass cloth to form a laminate (o).

Epoxide Resins.

The majority of the epoxide resin samples investigated were prepared from Epikote 828 resin syrup (supplied by the Shell Chemical Co.) which was mixed with the curing agent, poured into an aluminium mould, and cured to the required extent at 110°C. The curing agents studied were piperidine, m-phenylene diamine, aniline-formaldehyde resin[72], and a boron trifluoride complex BF_3.400 (marketed by the Shell Chemical Co.). Apart from experiments with varying concentrations of aniline-formaldehyde resin in order to study the effect on the final state of cure, all other specimens were prepared with the known optimum amounts of curing agent (i.e. the amount which gave the highest second order transition temperature in the fully cured polymer). The optimum amounts were:-

aniline-formaldehyde resin (mol.ratio 1:0.85)	33.5%
m-phenylene diamine	12.5%
piperidine	5.0%
boron trifluoride complex BF_3.400	5.0%

Investigations were also made on epoxide discs cut from commercially produced sheets, laminates with glass cloth, and quartz filled samples. These specimens had been prepared from Epikote 828 resin cured with m-phenylene diamine and BF_3.400.

Polyethylene.

All the polyethylene specimens examined were cut from moulded sheets of commercial materials. The polymers studied included: branched polyethylenes Alkathenes 70, 20, 7, and 0.2 (all manufactured by I.C.I. Ltd.), linear polyethylenes Alkathene HD (I.C.I. Ltd.), Marlex 50 (Phillips Petroleum Co.), and Hostalen 1 (Zeigler catalysed material). Mixtures of Alkathene 7 and Marlex 50 produced by milling were also examined. The dilatometric and cooling curve measurements quoted in the discussion of the results on the polyethylenes were performed by Dr.M.H.Dilke of the Distillers Co.Ltd. who supplied all the samples.

Polypropylene.

The polypropylenes studied were prepared from a commercial (Zeigler catalysed) specimen which contained between 70% and 90% of crystalline isotactic material together with an amorphous residue. There seemed to be two types of polymer molecule present, only one of which was crystallisable, since heat treatment and quenching had little effect on the crystallinity of the product. The amorphous material, a sticky rubber, was separated from a 90-100% crystalline material by extraction with diethyl ether. The six blends of different ratios of crystalline to

amorphous material were produced by milling together the two types. The proportion of crystalline isotactic material in each sample was estimated by means of infrared spectroscopic measurements.

Poly(methyl methacrylate).

Penetrometric and energy absorption measurements were made on discs cut from 1/8" thick Perspex sheet and also on discs produced from MMA monomer polymerised at 62°C in aluminium moulds using 1% MEK as initiator.

Polytetrafluoroethylene (PTFE).

Discs were cut from a 0.1" thick specimen of commercial PTFE and their energy absorption characteristics were investigated in the temperature range 0 - 100°C in order to study the marked step in the absorption curve caused by the first order transitionassociated with an increase in chain segment mobility within the crystallites.

Polystyrene.

Specimens were cut from 1/8" thick sheets of commercial polystyrenes of a range of molecular weights.

Poly(vinyl acetate) (PVA).

Rebound spectra were obtained for five different specimens of PVA. The discs were cast from commercial emulsions with the exception of the B.D.H polymer which was moulded from a laboratory grade powder. The properties of the various samples are given below.

Table 18.

Properties of PVA polymer specimens.

Polymer.	Colloid or Emulsifier used in preparation.	Mol.Wt.	% Insoluble in ethyl acetate.
Polimul 498	Sulphonated oil	79,210	1.1
Polimul 595	Poly(vinyl alcohol)	41,490	20.6
Polimul 660	Gum Acacia	16,730	37.9
Vinamul 8800	Not known	41,490	4.2
B.D.H.	Solution polymerised	43,080	0

Resorcinol-formaldehyde resin.

A mixture of 9 ml. formalin and 4g. resorcinol together with 0.1g. sodium hydroxide was heated at 25°C for 20 minutes. The undercured resin disc produced in this way showed a very broad absorption peak with its maximum at approximately 10°C, but attempts to follow its further cure in the rebound apparatus failed because of cracking when a temperature of 70°C was reached.

Aniline-formaldehyde resins.

The aniline-formaldehyde resins used as curing agents for the epoxide resins were themselves studied using the ball rebound technique. The specimens used were obtained from Dr.R.R.Bishop who has described the method of their preparation[72]. Three brittle low molecular weight polymers having aniline:formaldehyde molar ratios of 1: 1, 1:0.9, and 1:0.85 were studied. They were all insufficiently soluble for ebullioscopic molecular weight determination, but the Rast method gave a value of 285 ± 10 for the 1:0.85 resin.

It was found that, at temperatures below their second order transition points, the impact of the normal 1/8" diameter steel ball caused all three resins to shatter. A 3/32" ball (having less than half the mass) was therefore used for the rebound measurements on these polymers. The brittleness also prevented specimens from being firmly clamped on the heater block with the result that considerable scatter appeared in the energy absorption values observed at lower temperatures.

Phenol-formaldehyde resins.

The curing study on the phenol-formaldehyde system was carried out with discs machined from a very undercured sample of a polymer manufactured by Catalin Ltd.

Urea-formaldehyde resin.

Urea-formaldehyde resin syrups were prepared by R-J.Roe of Manchester College of Technology as follows:- A mixture of 34% formaldehyde, 26% methanol and 40% water was brought to pH 4.8 by the addition of small amounts of sodium dihydrogen phosphate and disodium hydrogen phosphate. Urea was then added to give a urea:formaldehyde molar ratio of 3, and the mixture was maintained at 100°C for an hour under reflux. Water and methanol were then allowed to evaporate at 100°C until the volume had decreased to one third of the original.

The resin syrup was cured for two days at 60°C in aluminium moulds to produce glass-clear, rubbery discs.

Poly(triallyl cyanurate) (TAC).

Monomeric TAC was polymerised in vacuo at 100°C with 1% benzoyl peroxide until the gel point was just reached (25 minutes). The gel was then further polymerised at 100° in an aluminium mould until a stiff rubbery disc was obtained. These undercured TAC discs cracked when heated above 130°C, and so absorption peak curves could not be measured. Mechanically stronger specimens obtained by longer curing at 100° were found to have absorption peaks somewhere above the maximum temperature measureable in the ball rebound apparatus (300°C).

6. Ball Rebound Relaxation Spectra.

Ball rebound measurements of the energy absorption in polymers show a marked maximum in the same temperature range in which the second order transitions occur. Typical rebound absorption peaks for three polymers of widely different properties are plotted in Fig.30. These curves demonstrate that, as the name implies, the shape of the second order transition curve is exactly similar to that obtained by differentiating the S-shaped curve of a first order transition (cf. Fig.32).

During the temperature scanning of the energy absorption characteristics of a polymer by ball rebound, the frequency ω of the applied strain during the impact remains almost constant, and the resultant stress relaxes to its equilibrium value with a relaxation time τ. As the polymer is heated through the "glass" to "rubber" transition, thermal motion of the chains continuously accelerates and the value of τ decreases with increasing temperature. The observed impact energy absorption maximum occurs in the region $\omega\tau \sim 1$, and at the same point, the elastic modulus changes from one limiting value to another (i.e. the absorption peak occurs at the temperature at which the average frequency of the segmental movements in the polymer becomes equal to the reciprocal of the experimental impact time). The temperature T_m

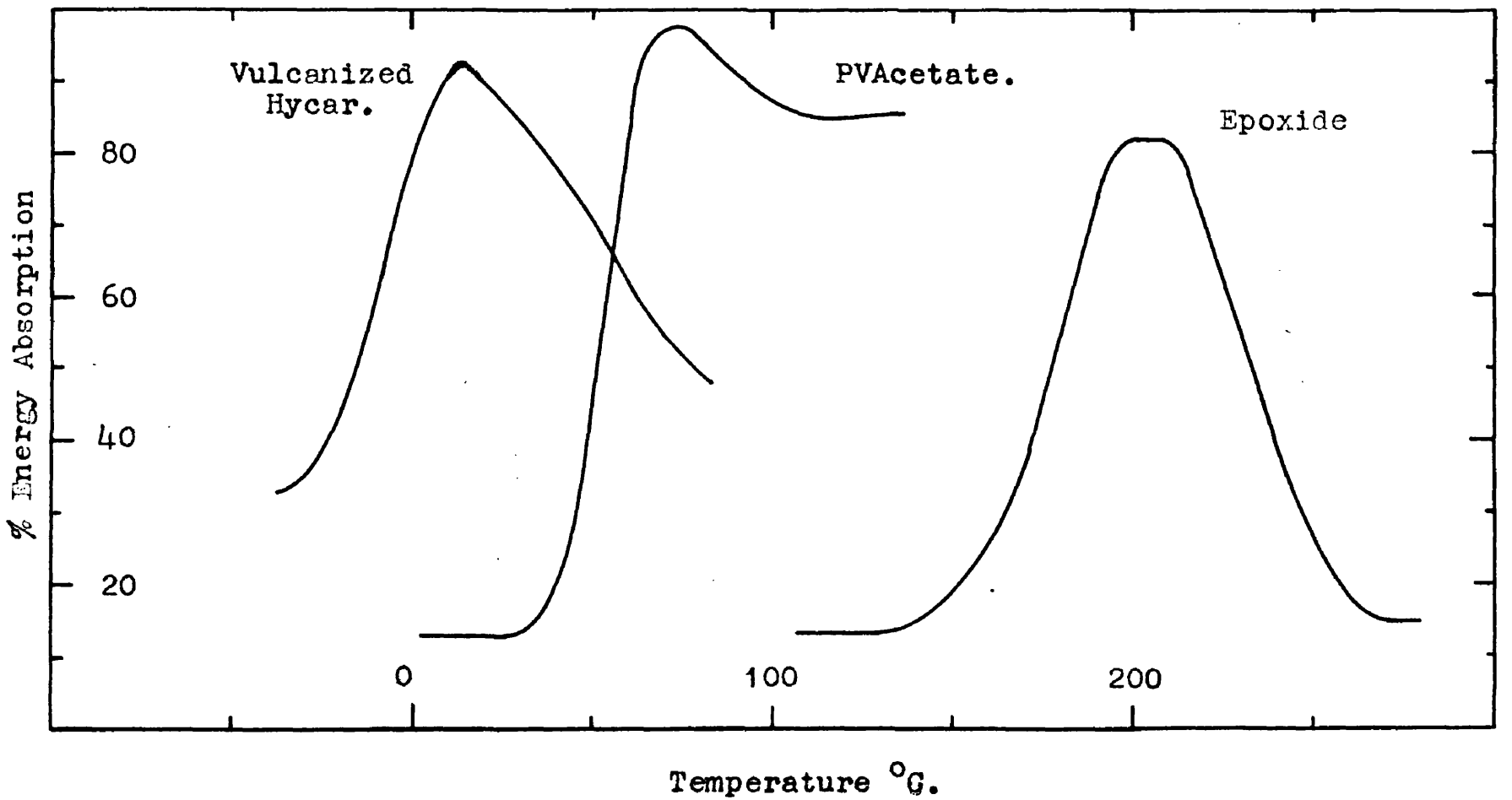

Figure 30.

Ball rebound relaxation spectra.

at which the peak occurs is therefore directly related to the second order transition temperature T_g of the polymer via ω the impact frequency (the reciprocal of the impact contact time), and is characteristic of the polymer provided that ω is kept constant. The use of impact times of a different order of magnitude would obviously give different values of T_m. This time-dependence or "frequency effect" is universally observed in both dynamic mechanical and dielectric measurements of second order transitions. The impact frequency of the 1/8" steel ball used in the work described here was calculated from published data[73] to be of the order of 10^3 sec^{-1}. This frequency gave values of T_m between 20° and 40°C above the static T_g depending on the size distribution of the molecular species present in the polymer. In Fig.31 it is seen that, for the aniline-formaldehyde resin with the A/F molar ratio of 1, there is a very large difference between the penetrometric (static) determination of the transition point and the temperature indicated by the peak of the broad dynamic relaxation spectrum. There is much less difference between the two values for the other polymers which have very narrow distributions of relaxation times. Experimentally, the ball impact frequency was not absolutely constant because of temperature-dependent changes in the elastic moduli of the polymers. The spectra obtained were therefore slightly oblique sections of the temperature-frequency-absorption surface, not solely temperature-absorption plots.

Figure 31 .

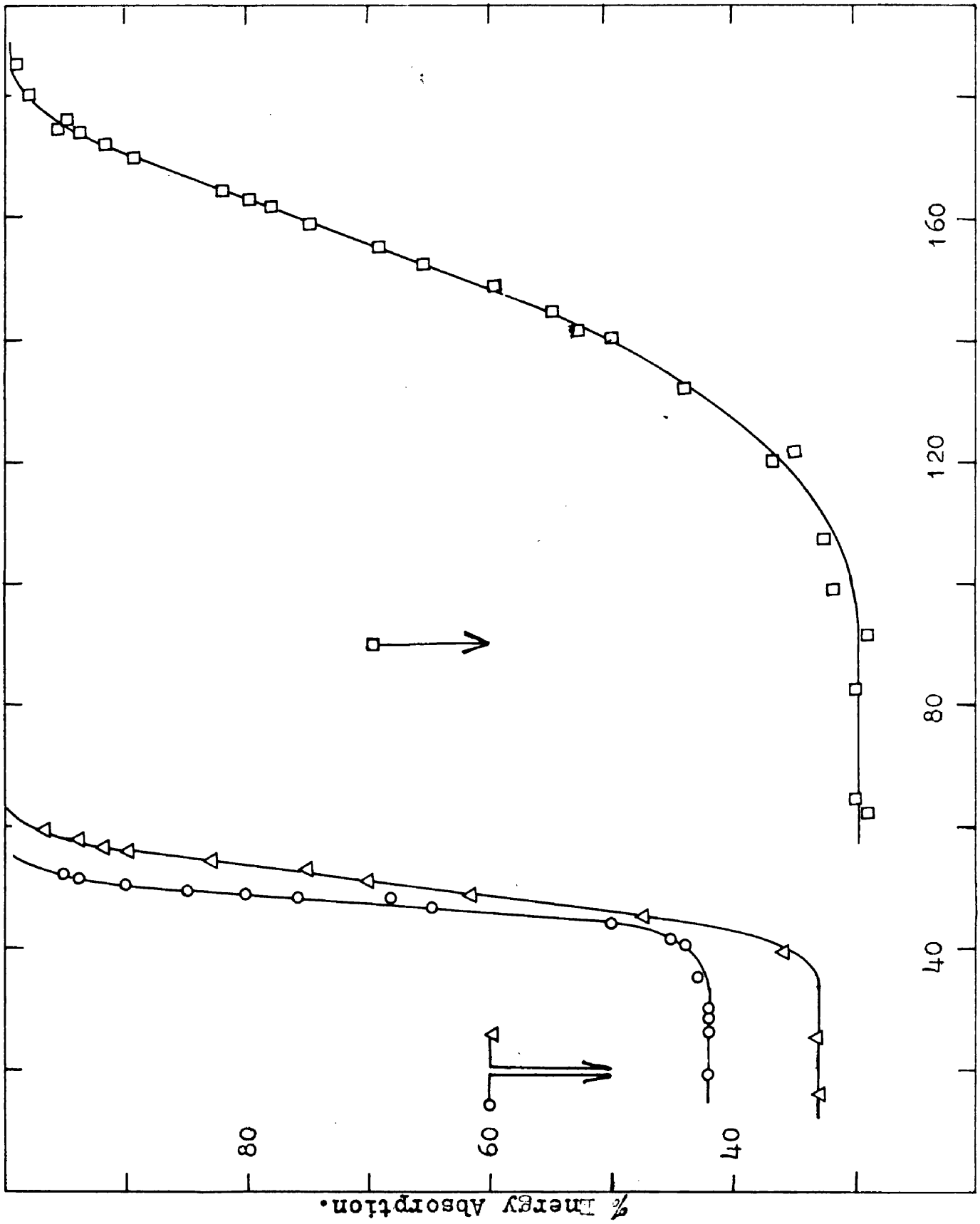

Energy Absorption spectra for three aniline-formaldehyde resins. The arrows indicate the position of the penetrometric SOTT's.

o - Mole ratio 0.85.
Δ - " " 0.90
□ - " " 1.00

6.1 Justification of the Ball Rebound Technique.

The relationship between the energy absorption spectra obtained by ball rebound measurements and changes in the dynamic mechanical properties within the polymer specimen has been investigated by Jenkel and Klein[70] who have given a theoretical interpretation of the energy absorption curves in terms of relaxation spectra.

It should be noted here that the term "energy absorption spectrum" strictly refers to the result of a frequency scan of the absorption-frequency-temperature surface. The ball rebound technique provides a temperature scan of this surface, but for convenience, these are also referred to throughout this thesis as energy absorption spectra.

The response of the ball rebound to the changes caused by known transition phenomena was studied in the course of this work. Fig. 32 shows the step observed in the energy absorption curve for poly(tetrafluoroethylene) in the region of its known first order transition[74] associated with an increase in chain segment mobility within the crystallites. Again, the shoulder observed on the rebound absorption spectrum of poly(methyl methacrylate) (Fig.33) occurs at the same point below the dynamic second order transition temperature as the "β-process" peak obtained by several workers using much more elaborate resonance

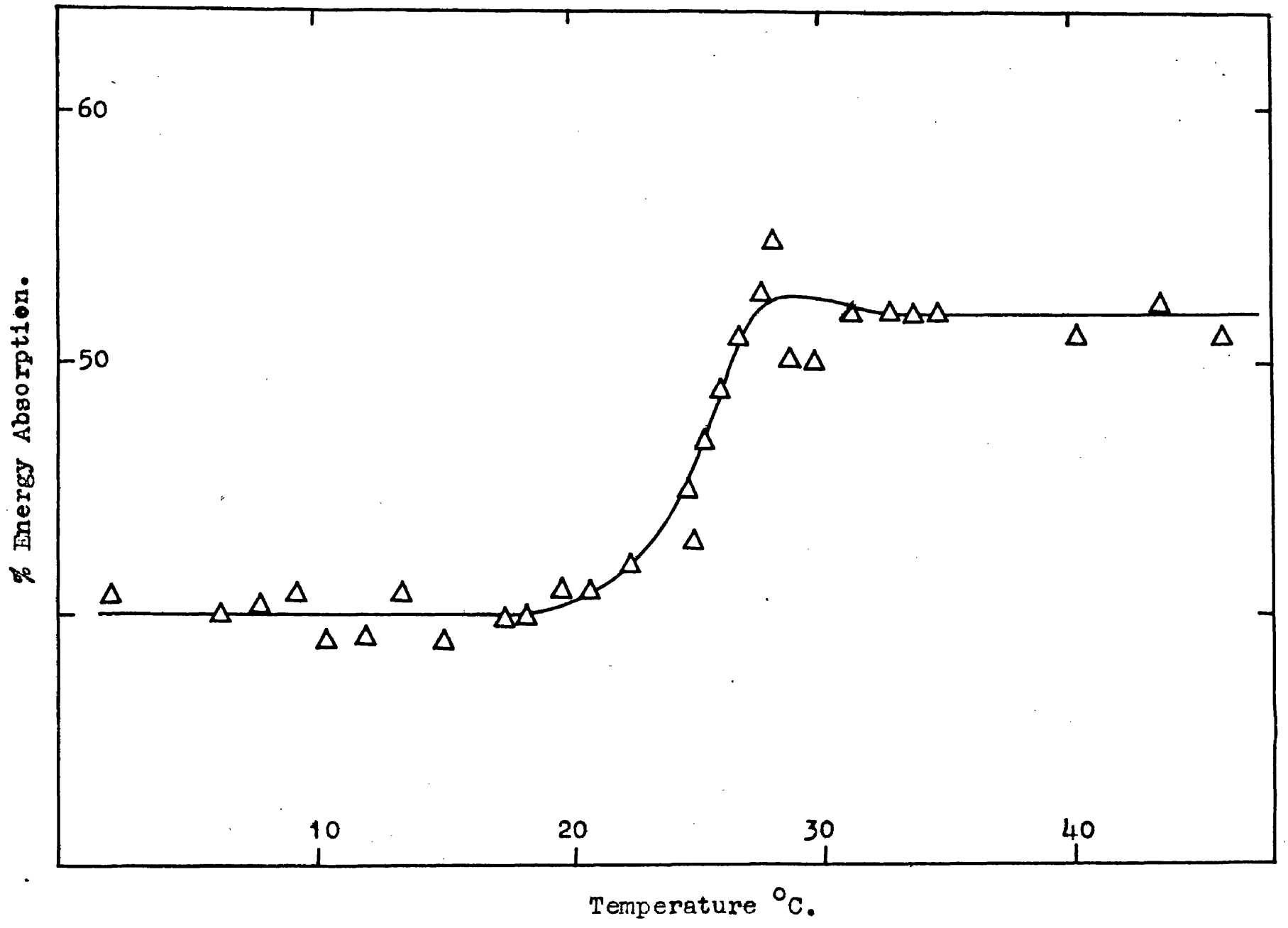

Figure 32. Energy absorption change at the first order transition temperature in polytetrafluoroethylene.

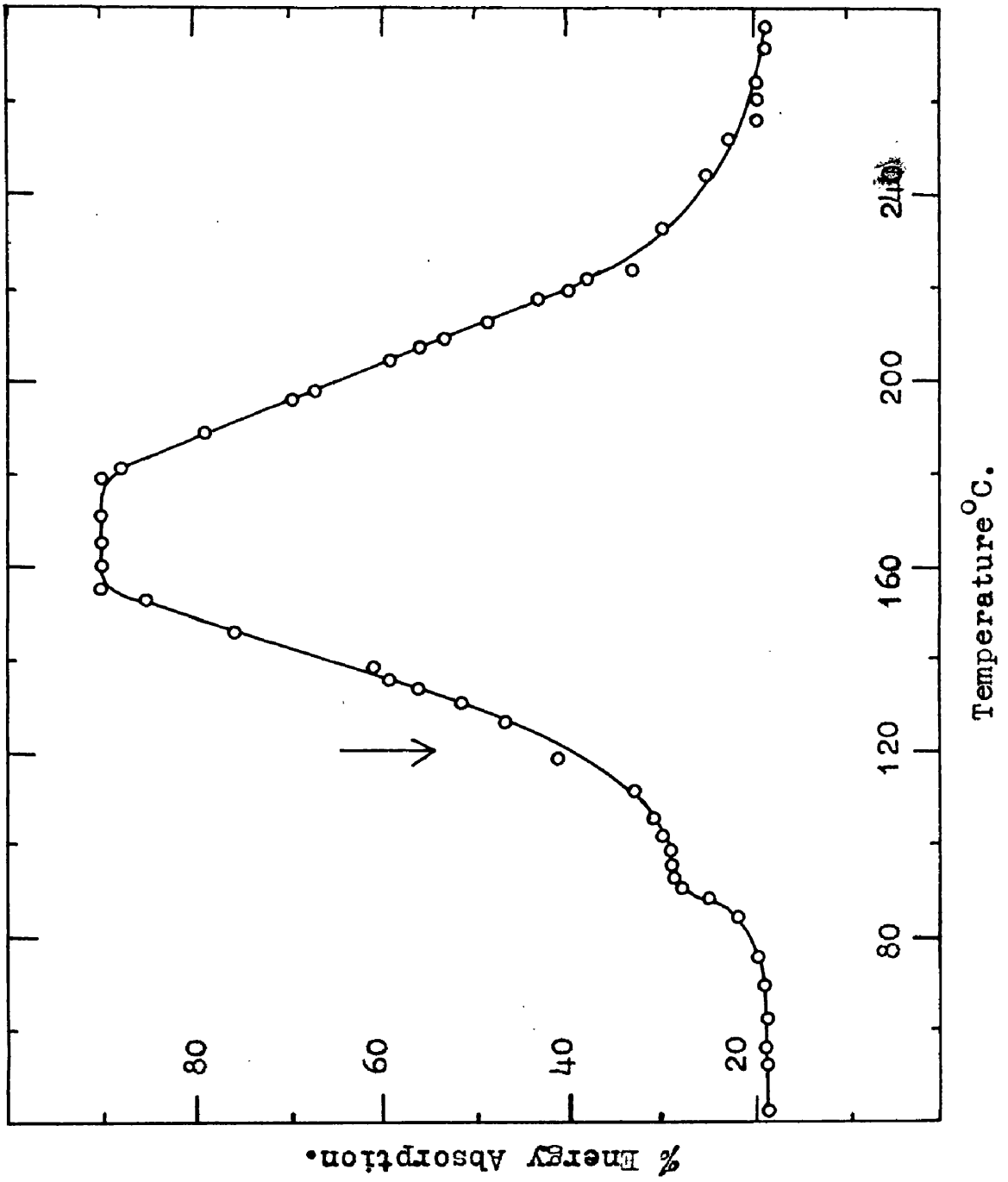

Figure 33 .

Energy absorption spectrum for polymethyl methacrylate. The arrow indicates the second order transition temperature found by penetrometer measurements. This is 42°C. lower than that as measured by ball rebound.

frequency and dielectric methods of studying relaxation (References 75 to 77). Finally, the response of the ball rebound to first and second order transitions and the influence on these transitions of polymer molecular weight, crystallinity, and plasticiser content, are all in line with the theory of these phenomena. This indicates that the use of this technique can give results which are intelligible in the light of molecular theories.

6.2 Relaxation Spectra of First Order Transition Phenomena.

Ball rebound investigation of a polymer over the region in which a first order transition occurs gives an energy absorption plot in which a sharp change in absorption level takes place at the transition temperature. The transition in poly(tetrafluoroethylene) in the region 20° to 30°C due to changes within the crystallites is indicated by a rise in energy absorption level from 40% to 52% (Fig.32). The melting transitions of a series of polyethylenes and polypropylenes are illustrated in Figs. 34 to 37, and the variations in the shape and position of the energy absorption steps may be interpreted in terms of the molecular weight, structure, and degree of crystallinity of the polymers.

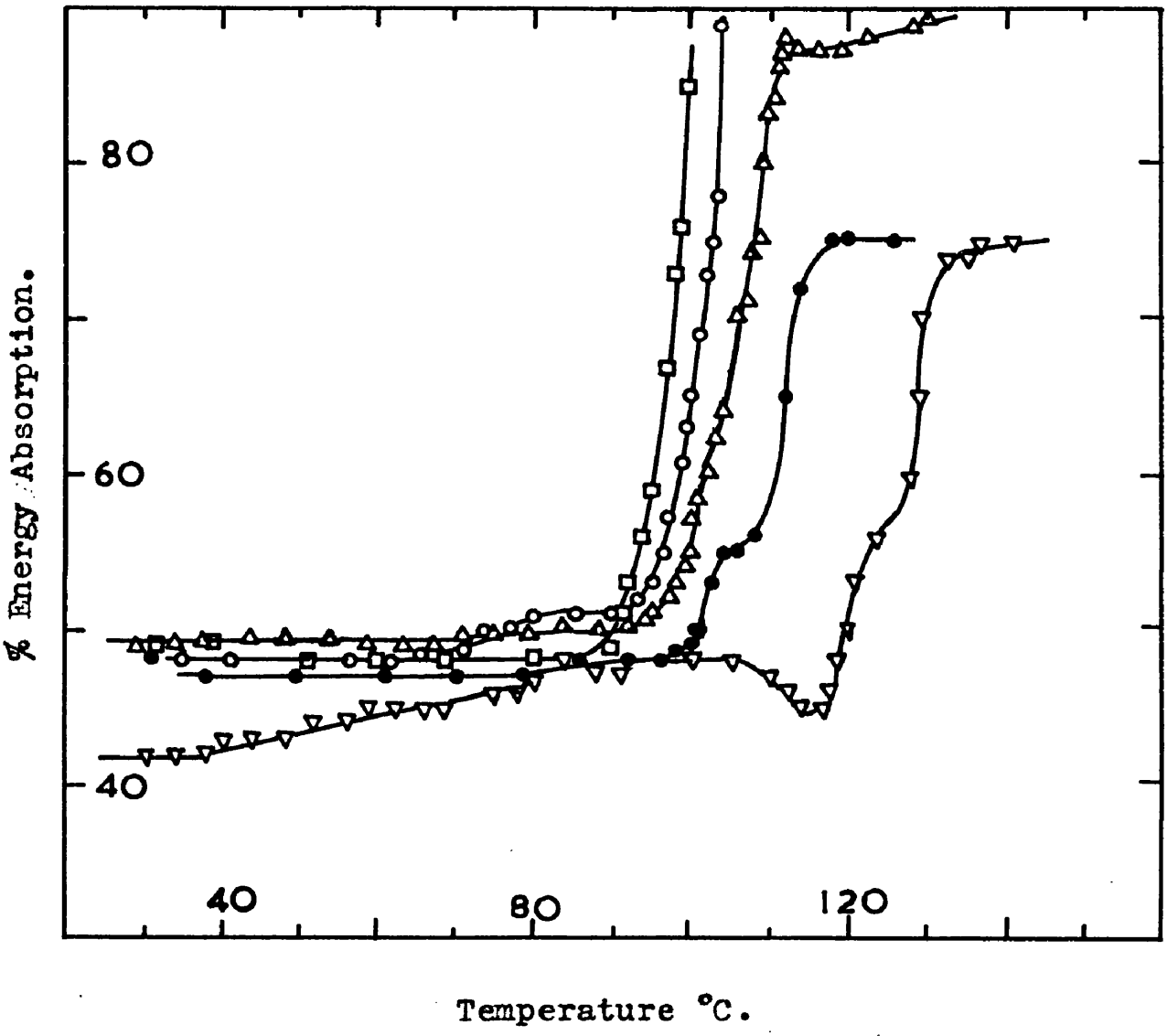

Figure 34.

Energy absorption spectra for a series of polyethylenes in the region of their melting points.

□ - Alkathene 70
○ - Alkathene 20
△ - Alkathene 7
● - Alkathene & 2
▽ - Alkathene HD

In Fig.34, the rebound spectra are shown for a series of polyethylenes of different molecular weights. The temperatures corresponding to the mid point of each transition step together with the "melting points" as determined dilatometrically are tabulated below.

Table 19.

Effect of molecular weight on the softening point of branched polyethylene.

Alkathene Grade.	Molecular Weight.	Transition Temp. (Rebound).	Melting Point[78] (Dilatometric)
70	16,000	98°C	---
20	17,000	102.5	109.0
7	18,000	107.0	109.0
0.2	21,000	111.0	110.5
HD (linear)	300,000	129.0	123.0

Increasing molecular weight caused a rise in the transition temperature. The lower molecular weight polymers softened to form liquids upon which the steel ball could not be bounced, but the higher molecular weight specimens formed melts with better viscoelastic properties. The energy absorption curves for the latter levelled off before reaching the 100% absorption state, and it was found possible to continue readings up to 20°C above the softening temperatures (when formation of bubbles in the polymers began to cause inaccuracy in the measurements).

The linear polyethylene Alkathene HD produced by a low pressure technique, had a much higher softening point than the branched polymers. Rebound measurements on three linear polyethylenes manufactured by different methods, showed differences in the softening temperatures in agreement with the degree of branching deduced from the physical properties and infrared spectra. The most branched polymer softened first. In each case, there was a preliminary step in the absorption curve before the main melting step was reached. This effect is attributed either to an initial softening of the amorphous phase, or possibly to the presence of a secondary crystalline phase such as that detected in the X-ray examination of a Ziegler catalysed polyethylene[79].

Table 20.

Softening temperatures of linear polyethylenes (Fig.35).

Polymer.	Softening Point (Rebound).	Softening Point[78] (Dilatometer)
Marlex 50	138°C	133°C
Hostalen 1	135	130
Alkathene HD	129	123

The effect of mixing a linear polyethylene with a branched polythene is illustrated in Fig.36. Marlex 50 + Alkathene 7 blends produced by milling together the two polymers at 150°C in varying proportions gave products which,

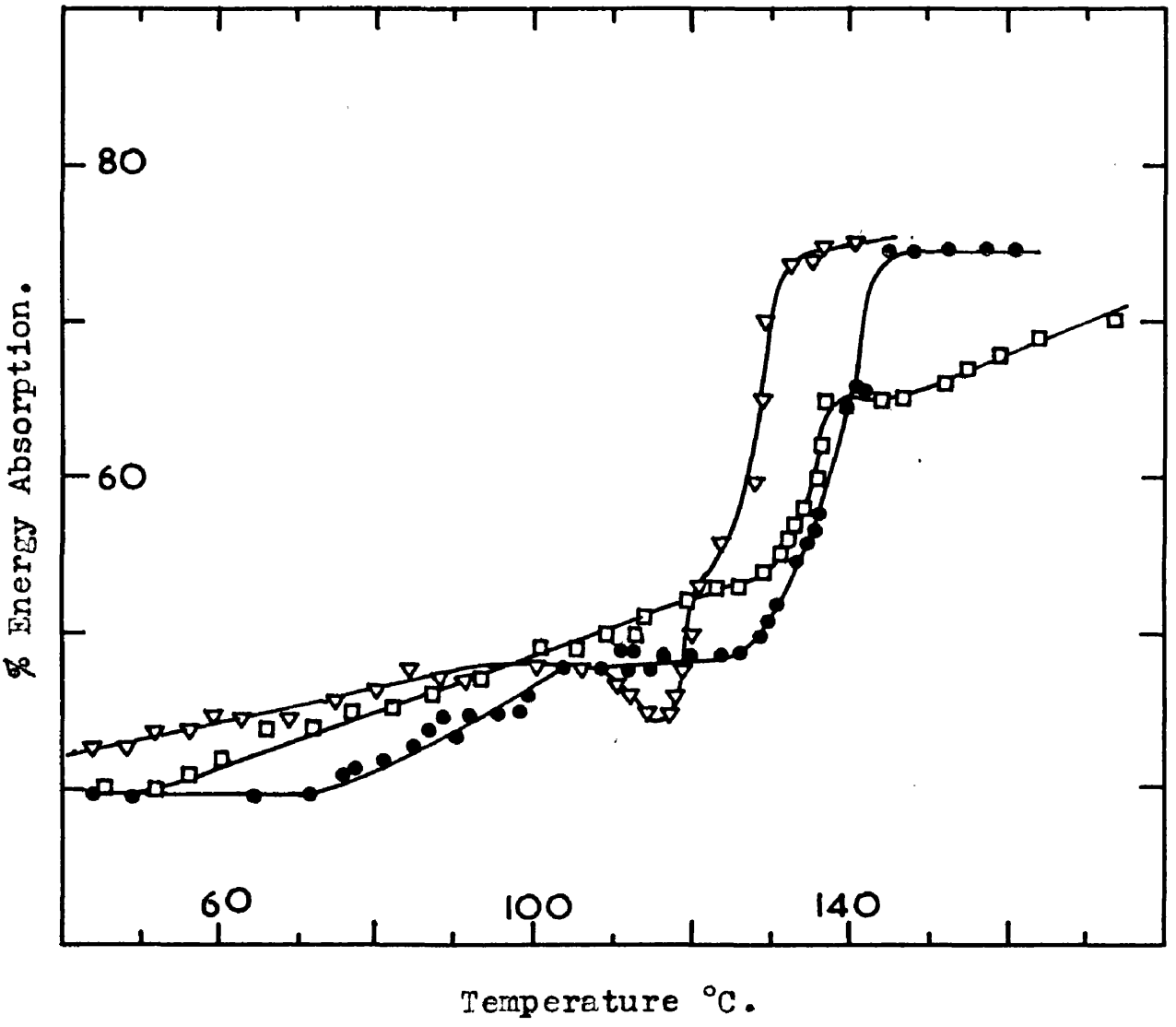

Figure 35 .

Energy absorption spectra of three linear polyethylenes in the region of their melting points,

▽ - Alkathene HD

● - Marlex 50

□ - Hostalen 1

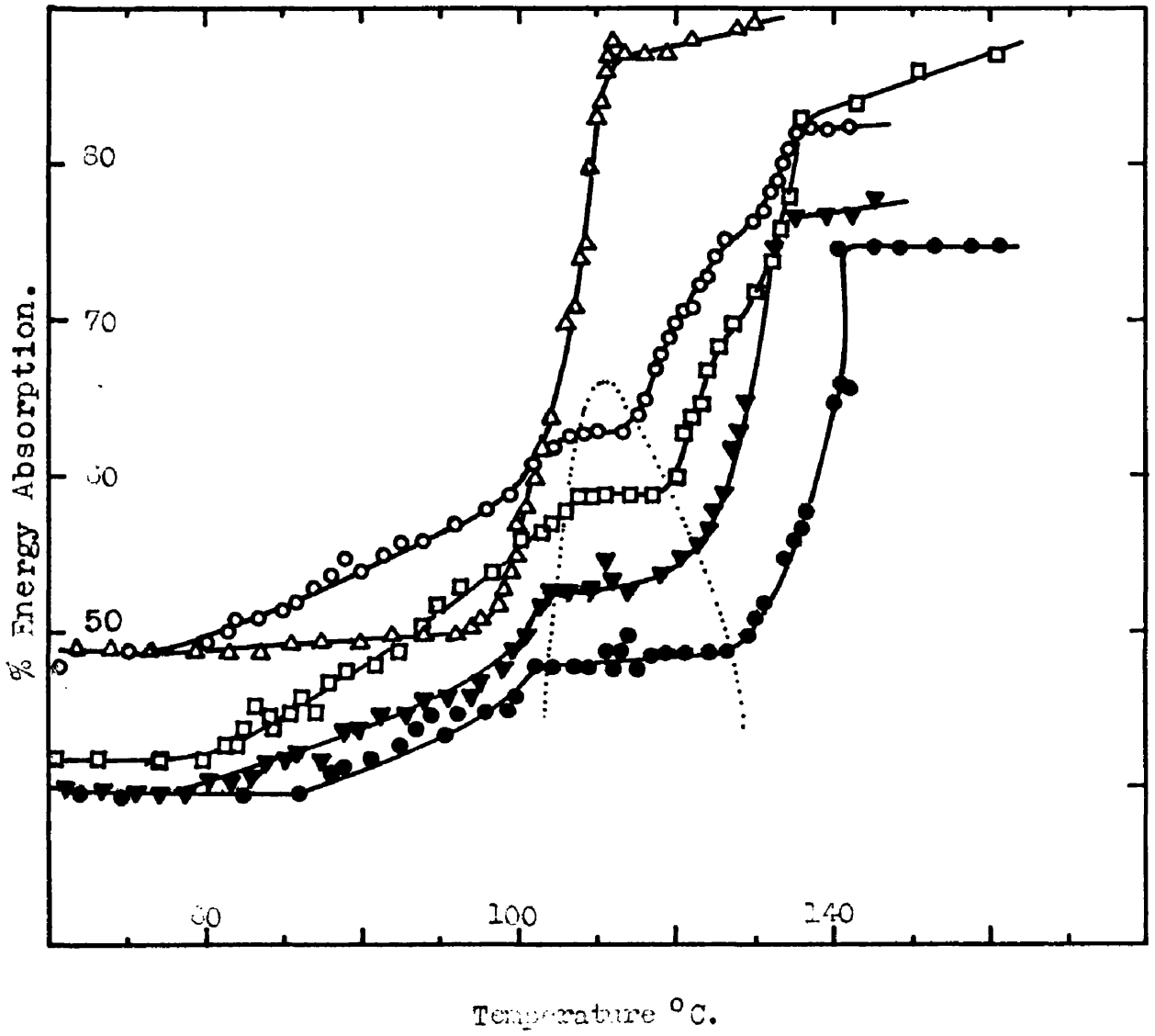

Figure 36.

Energy absorption spectra showing the effects caused by mixing a branched polyethylene (Alkathene 7) with a linear polyethylene (Marlex 50).

△ - 100% Alkathene 7

o - 75% Alkathene 7

□ - 50% Alkathene 7

▼ - 25% Alkathene 7

● - 100% Marlex 50.

although still apparently retaining the high softening point of the linear polymer when examined dilatometrically, were shown by rebound measurements to begin to soften at lower temperatures. The energy absorption spectra showed that although the softening of the blends was not completed until within a few degrees of the pure Marlex 50 softening point, it began at much lower temperatures.

Table 21.

Softening points of mixtures of a linear and a branched polyethylene.

Polymer.	Softening Point (Rebound).	Softening Point[78] (Dilatometer)
Marlex 50	138°C	133°C
75%M:25%A	129	132.5
50%M:50%A	123	131
25%M:75%A	118	130
Alkathene 7	107	109

It is seen from Fig.36 that the preliminary step, which occurs in the absorption curve of the pure linear polymer before the main softening transition is reached, also persists in the spectra of the mixtures. This effect again suggests the presence of two phases in the linear polymer. The region in which the effects of the secondary phase are observable is enclosed by a dotted line in Fig.36.

The presence of crystalline material in a polymer has the effect of raising the softening temperature. This is illustrated in Fig.37 for four samples of Ziegler catalysed polypropylene containing different proportions of crystalline isotactic material.

6.3 Second Order Transition Temperatures.

The energy absorption peaks given by three samples of polystyrene of different molecular weights are illustrated in Fig.38. The levelling out of the absorption curves above the second order transition peak because of the softening of the polymers occurred in the order of the molecular weights, the lowest molecular weight polymer softening first. The two specimens with the higher molecular weights had almost coincident absorption curves below T_m while the curve for the other sample was 12°to 14°C lower. Flory[80] has established a relationship between the molecular weight of pure polystyrene and the transition temperature, and on the basis of this, the values of T_m for the three specimens used here should all have fallen within a 2°C range. The two higher molecular weight polymers gave results agreeing with this prediction, but it seems that the presence of traces of residual monomer in the low

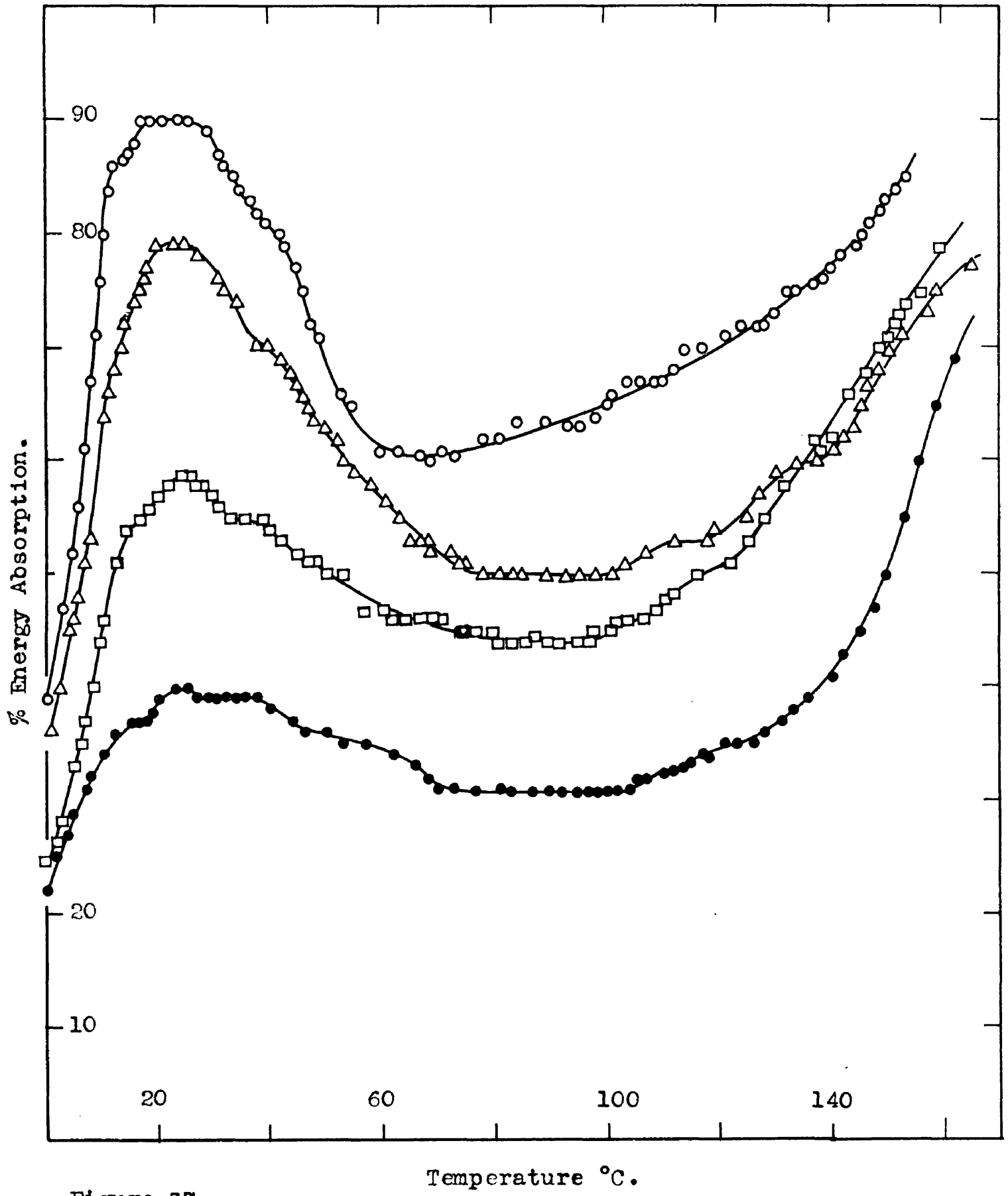

Figure 37 .

Energy absorption spectra for a series of Ziegler catalysed isotactic polypropylenes.

o - 5% crystalline:

□ - 84% crystalline.

Δ - 65% crystalline:

● - 97% crystalline.

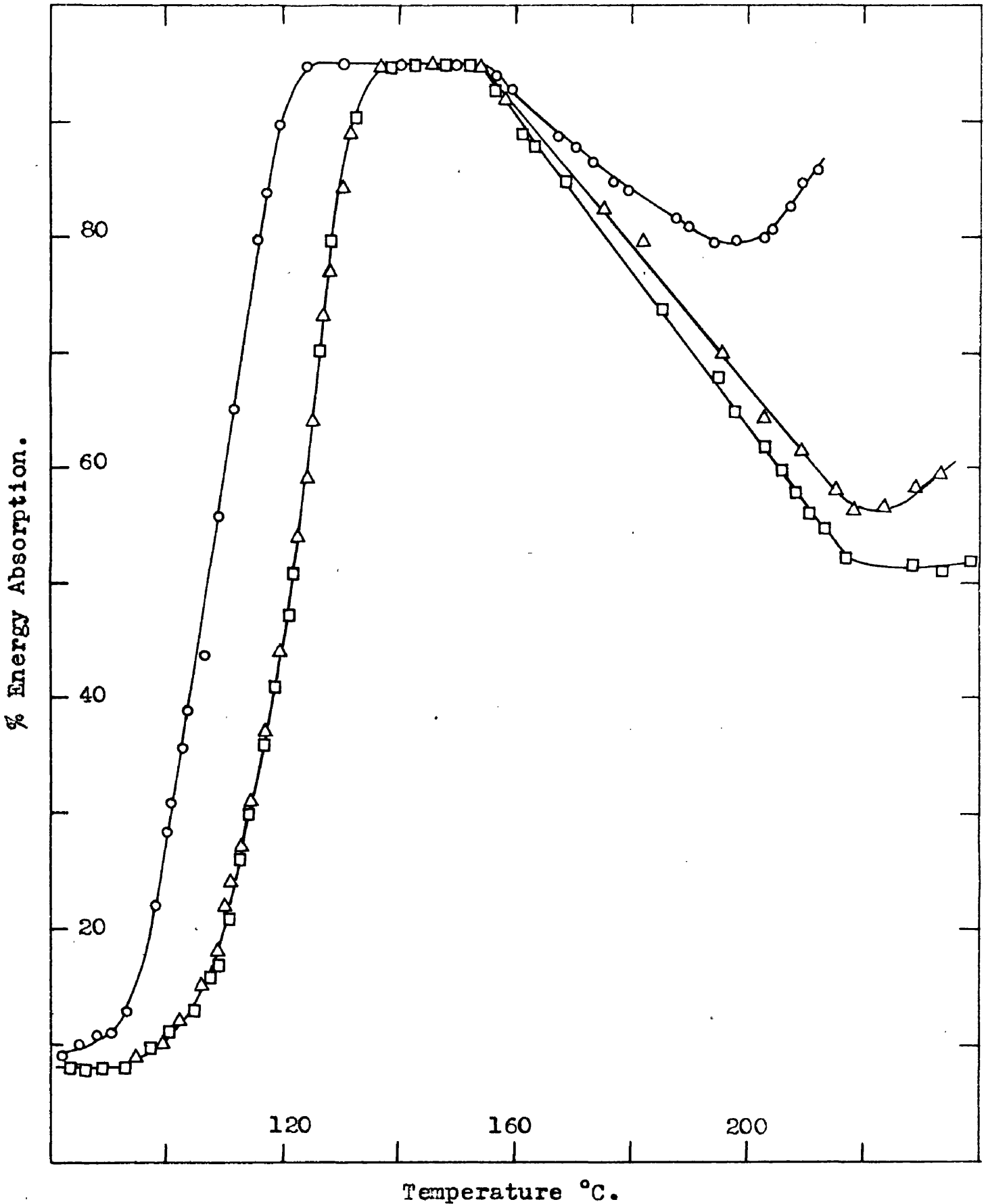

Figure 38.

Energy absorption spectra for polystyrene.

o	-	Specimen DCPJ/3.	Molecular Wt.	195,000
△	-	" Distrene 858.	" "	550,000
□	-	" Emulsion 7A.	" "	1,300,000

molecular weight sample caused the depression of T_m by about 10°C.

The presence of small molecules in a polymer, either molecules of unpolymerised monomer or of added plasticiser, lowers the second order transition temperature by forcing the polymer chains apart and thus reducing the chain-chain interaction. The energy barriers to the rotation of the backbone chain segments are therefore reduced, and on heating the polymer, segmental rotation will commence at a lower temperature. It seems probable therefore, that the presence of residual styrene monomer in the low molecular weight specimen caused the depression of T_m since no plasticisers had been added.

The large displacement of the energy absorption second order peak caused by the presence of relatively small amounts of residual monomer is illustrated by the 90°C displacement from the T_m of completely polymerised methyl methacrylate (Fig.33) to that of an exactly similar polymer containing 6% of monomer (Fig.56, plot R = 0).

A range of poly(vinyl acetate) specimens (Table 18) were examined by ball rebound, and three of the spectra are plotted in Fig.39. The values of T_m obtained do not seem to depend on the molecular weight or even on the degree of branching as indicated by the percentage insoluble content (see Table 22 below).

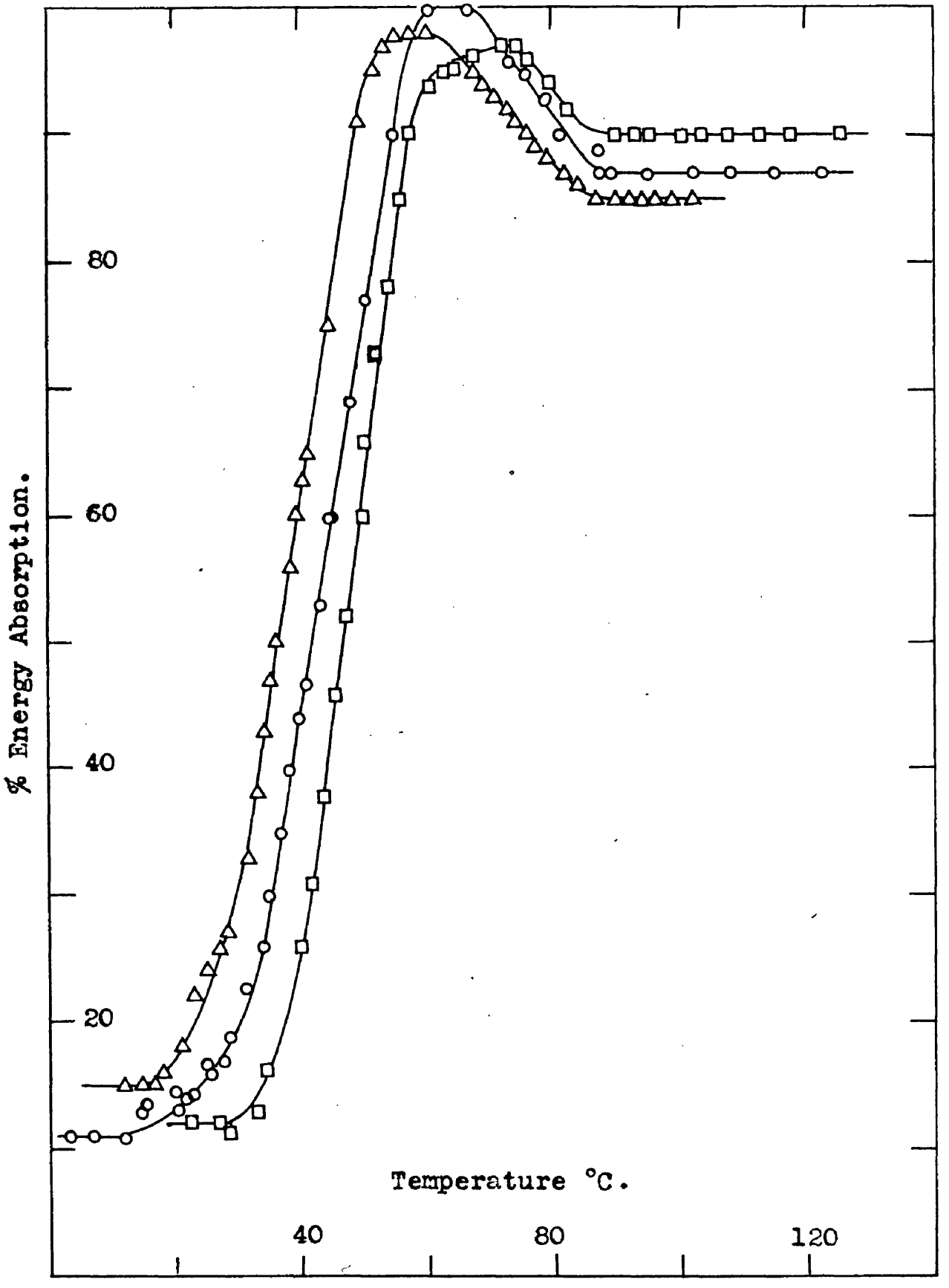

Figure 39 .

Energy absorption spectra for polyvinyl acetate.

△ - specimen 595; o - specimen 498; □ - specimen 660.

Table 22.

Transition temperatures of poly(vinyl acetate) specimens.

Molecular Weight.	Percent Insoluble. (in Ethyl Acetate).	Transition Temp. T_m°C.
41,490	20.6%	60°
79,210	1.1	62
16,730	37.9	70
41,490	4.2	75
43,080	0	86

It seems probable that the spread in the values of T_m was due principally to the presence of the small amounts of emulsifying agents used in the polymerisations. The fact that the solution polymerised polymer (T_m = 86°C) had a much higher transition temperature than the four emulsion polymers, supports this conclusion.

The effect of the presence of crystallinity in a polymer on the shape and position of the second order transition absorption peak is demonstrated in Fig.37. An increasing ratio of isotactic crystalline material to amorphous polymer in the specimens of Ziegler catalysed polypropylene caused a lowering of the peak height. This lowering was slight at first, but the effect became more marked as the last 20% of the amorphous material was replaced. The lowering was due to the fact that there was less energy absorption in the tightly packed crystalline

material. In addition to the depression of the peak, there was also a small but definite increase in the value of T_m as the crystalline content increased which was in agreement with theoretical prediction.

In a crystalline polymer, each chain molecule may pass through several crystalline regions while the parts of the chains lying between these regions have random disordered configurations (amorphous polymer). As such a polymer is heated through its second order transition temperature, rotation of the amorphous segments will occur between the fixed crystalline segments which will thus play a similar role to that of crosslinks in a network polymer. They will tend to tie down the rotating segments by hindering the rotation, and the greater the proportion of crystalline material in the polymer, the greater will be the constraining effect.

The results of the rebound energy investigations on the polypropylenes are tabulated below together with the measured specific volumes and the estimated crystalline content as determined by infrared spectrometry. There is an interesting linear relationship between the specific volumes of the polymers and the maximum energy absorption value observed on the second order transition peak, but since this had no bearing on the immediate problem of resin curing reactions, it was not further investigated.

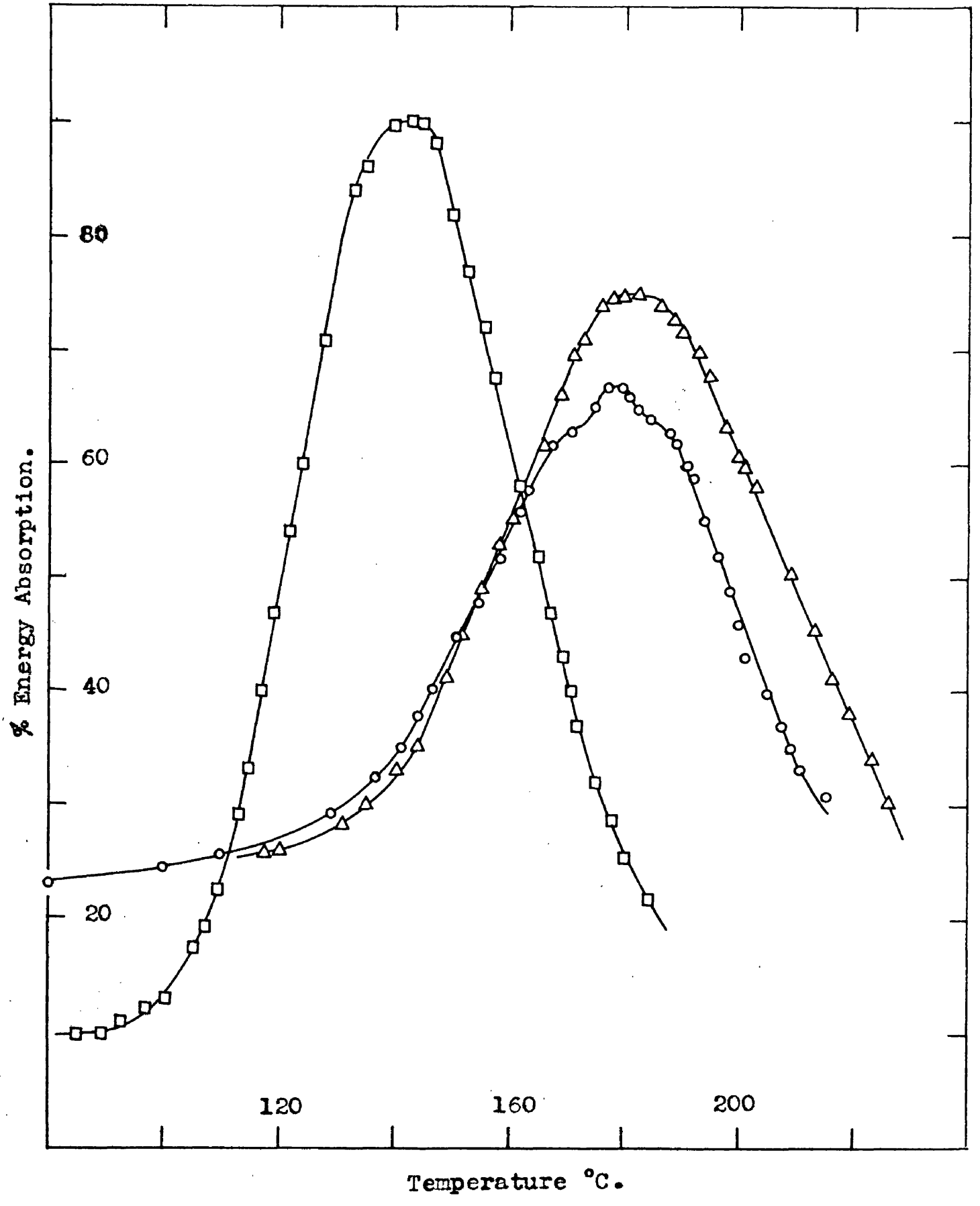

Figure 40.

Energy absorption spectra for a fully cured epoxide/m-phenylene diamine resin.

□ - Resin alone
△ - Quartz filled resin
○ - Resin/glass cloth laminate.

Table 23.

Energy absorption characteristics of polypropylene.

Crystallinity of sample.	Specific volume.	Maximum energy absorption.	T_m °C.
0%	1.177	92.5%	16
5	1.163	90	22
40	1.149	83	21
65	1.133	79	22.5
84	1.125	59	25
90	1.099	43	44
97	1.100	39	30
100	1.068	24	35

Energy absorption spectra of laminated and filled resins.

The addition of a filler or a laminating material to a polymer was shown to have a damping effect on the ball rebound energy absorption characteristics. The absorption level was raised on either side of the second order transition peak while the peak itself was reduced in height due to the internal friction between the filler and the resin. The effects of a glass cloth laminating component and of a silica powder filler on the rebound spectrum of an epoxide resin are illustrated in Fig.40, and Fig.29 shows the effect of incorporating glass cloth into a diallyl phthalate polyester resin.

The secondary absorption maximum in the PMMA spectrum.

The energy absorption curve for poly(methyl methacrylate) (Fig.33) has a well defined shoulder near the base of the second order transition peak. This shoulder, which occurs 70°C lower than the primary maximum, is attributed to the "beta-process" the existence of which has been noted by several workers using both dielectric measurements and mechanical techniques. It has been variously attributed to the presence of the methyl groups attached to the main polymer chain (Staverman[75]), and to rearrangement of the polar carbonyl groups in the side chains (Hoff et al.[76]). Following a study of the mechanical properties of various methacrylate copolymers, Heijboer concluded[77], that two conditions are essential for the existence of the β-maximum:

1) Rotation of the carbomethoxy side group should be possible.

2) The rotation should be subject to steric hindrance by adjacent methyl groups on the main chain.

The β shoulder, which has also been observed to occur in the PEF/MMA polyesters containing high proportions of methacrylate (low R values) (Fig.56), does not represent complete resolution of the secondary relaxation process. The more refined dynamic mechanical techniques which have been used[75,77]. show the presence of the β process by a peak quite separate from the main absorption maximum.

6.4 The Effect of Cure on the Absorption Peak.

Since the temperature at which the ball rebound absorption peak is observed is a measure of the dynamic second order transition temperature of a polymer, the curing of a specimen resulting in a higher T_g will therefore cause a displacement of the peak towards higher temperatures (Figs.41 to 44). Two additional effects on the peak have also been noted. It is generally observed that progressive curing lowers the height of the absorption peak, i.e. the minimum resilience is increased by cross-linking (Figs.41 to 44). Also, there is a broadening of the peak attributed to the widening of the distribution of molecular segment sizes present in the polymer. The broadening varies in extent from system to system, being very evident in the urea-formaldehyde system (Fig.41), and almost entirely absent in the epoxide polymer studied (Fig.44).

Measurements of rate of curing.

Since the position of the energy peak is a measure of the corresponding second order transition temperature, ball rebound measurements of the rate of displacement of the rebound absorption peak (dT_m/dt) provide a means of measuring the rate of curing in a reacting polymer system. The rate of displacement of the absorption peak was followed

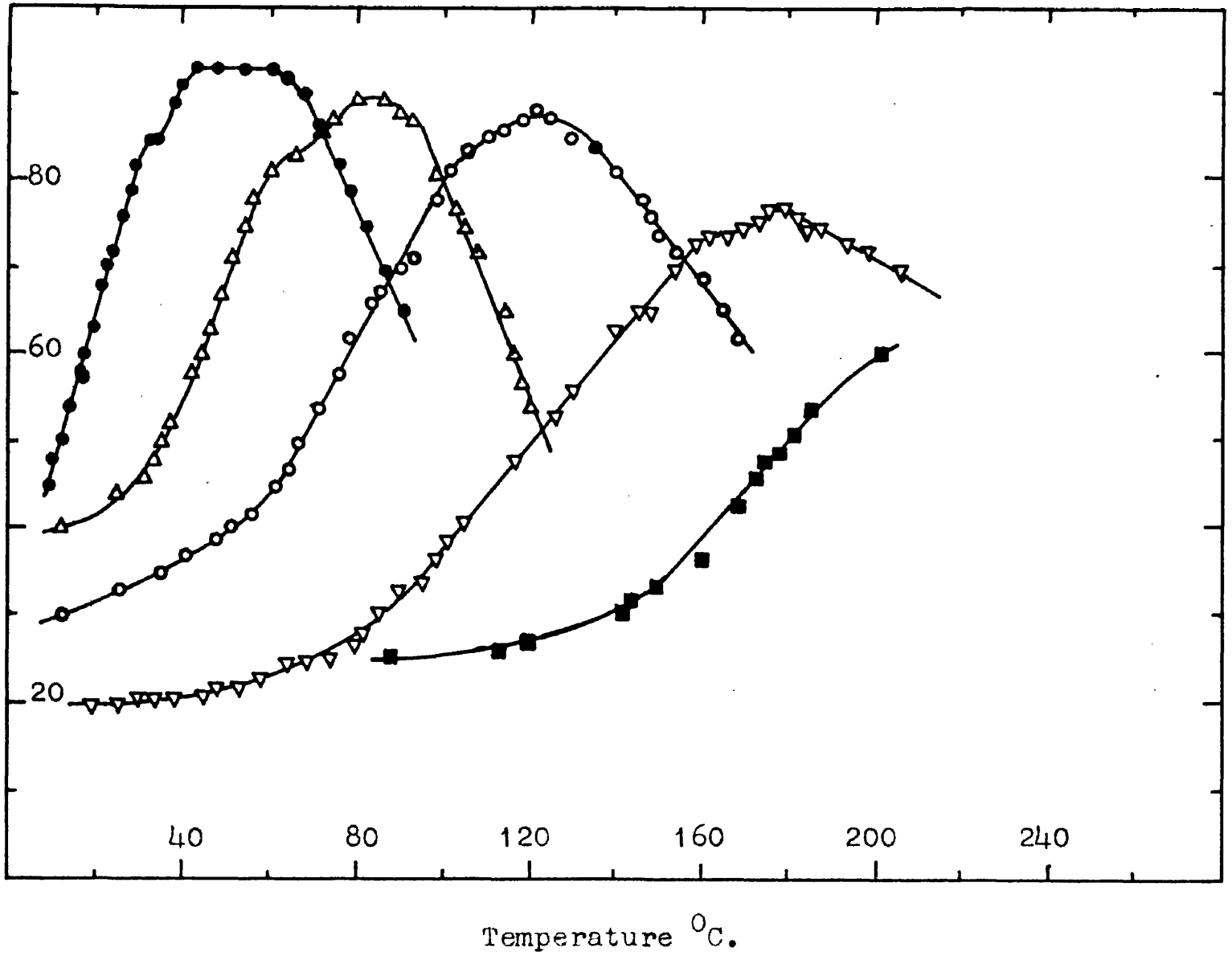

Figure 41.

From left to right successive states of cure of a urea-formaldehyde resin. Note the broadening of the peak with cure.

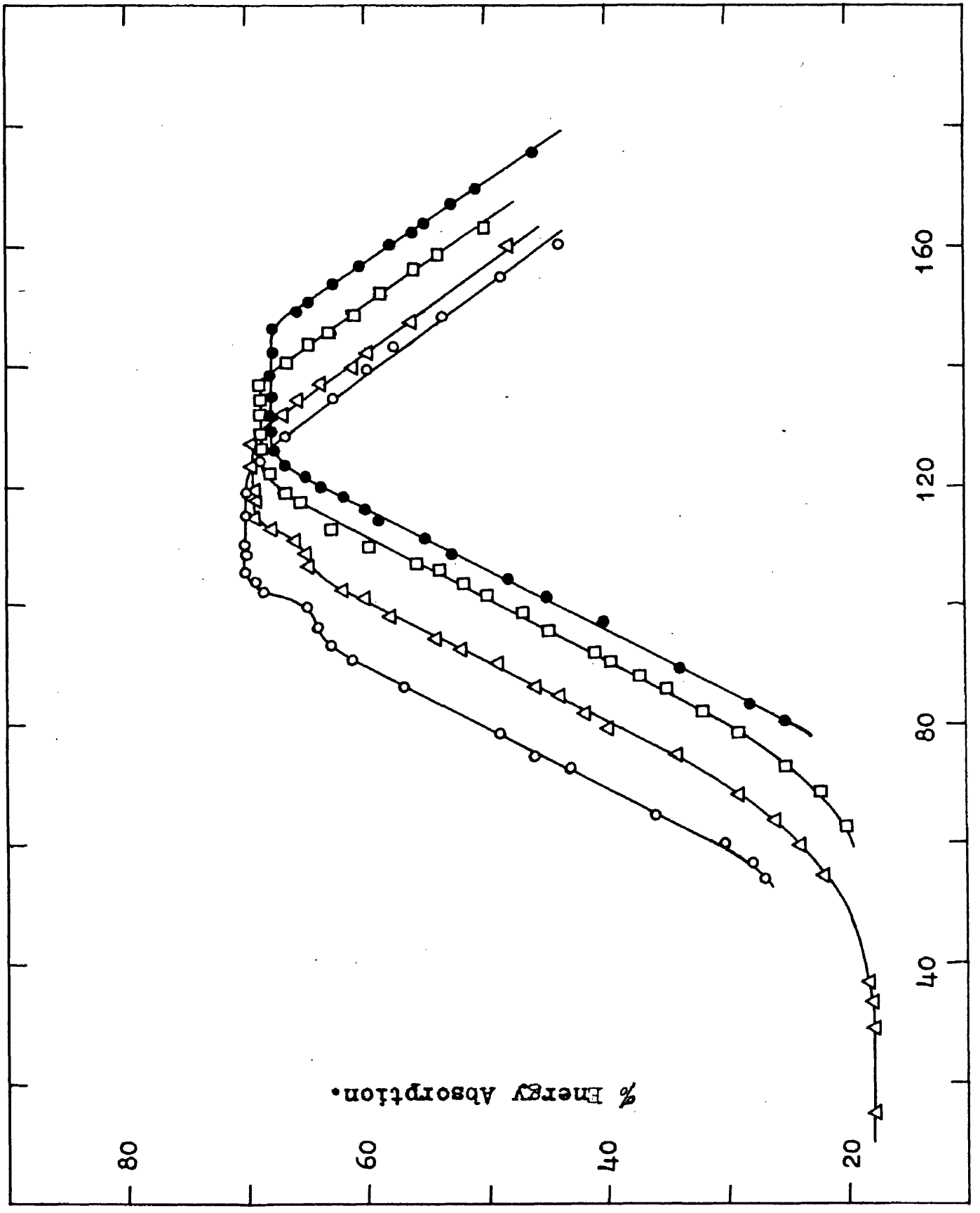

Figure 42.

Successive states of cure of a styrene based polyester/ glass cloth laminate.

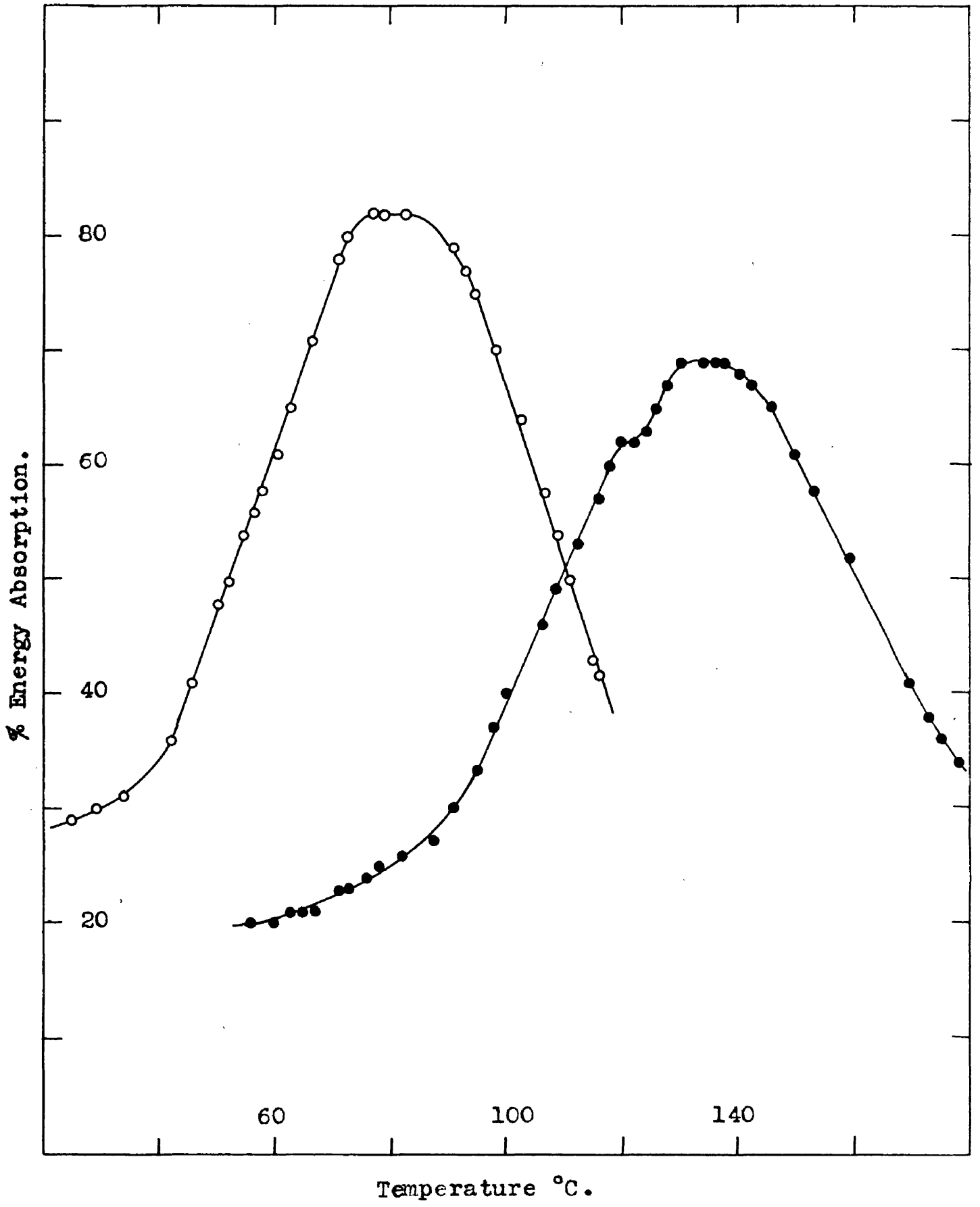

Figure 43 .

Successive states of cure of a phenol-formaldehyde resin.

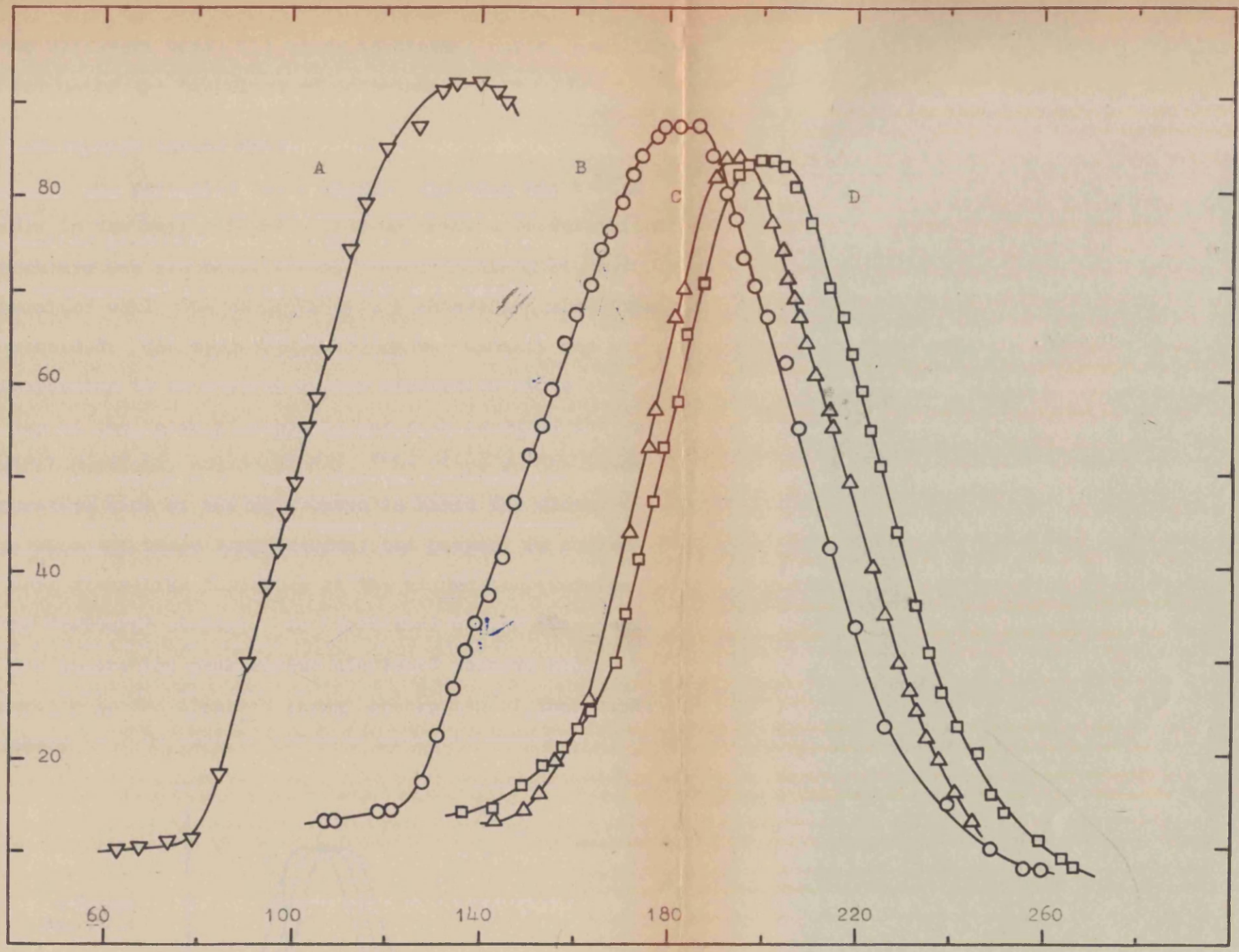

Figure 44. From left to right, successive states of cure of an epoxide/aniline-formaldehyde resin. The peaks do not appear to broaden with the increasing state of cure.

in two different ways; (1) using isothermal curing conditions, and (2) using the "isoelastic" technique.

(1) Isothermal curing rate.

The partially cured polymer specimen was heated rapidly in the ball rebound apparatus until a predetermined temperature was reached. It was then maintained at that temperature while the changing energy absorption with time was recorded. The temperature chosen was usually one corresponding to an initial energy absorption state near the top of the "glassy" slope of the peak curve of the original partially cured polymer. (The slope on the lower temperature side of the peak curve is named the glassy slope since at these temperatures, the polymer is cooler and more glass-like than when at the higher temperatures of the "rubbery" slope.) As isothermal curing proceeded, and the absorption peak became displaced towards higher temperatures, the observed energy absorption of the sample decreased.

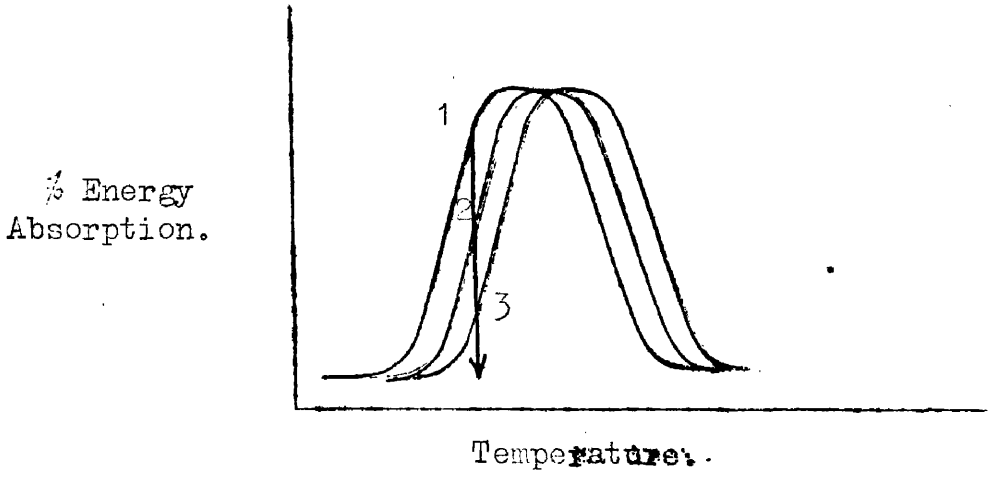

A typical plot of the fall in energy absorption with time of isothermal curing in an epoxide resin system is presented in Fig.45. The heating schedule used in this run is shown graphically in Fig.46, plot I.

Isoelastic curing rate.

As implied by the name, this technique requires that the polymer sample be maintained in a constant elastic state throughout the curing period. The specimen was heated rapidly until the energy absorption peak was reached, and having attained a chosen absorption state, the polymer was maintained there by adjusting the rate of heat input. The curing of the polymer causing the absorption peak to move to higher temperatures tended to lower the energy absorption of the specimen, and heating it resulted in increasing the absorption. By choosing a suitable rate of heat input, the two effects could be balanced so that throughout the curing, reaction occurred in a specimen having a constant physical state. The rate of isoelastic curing was obtained from the rate of movement of the peak curve in the time-temperature plane.

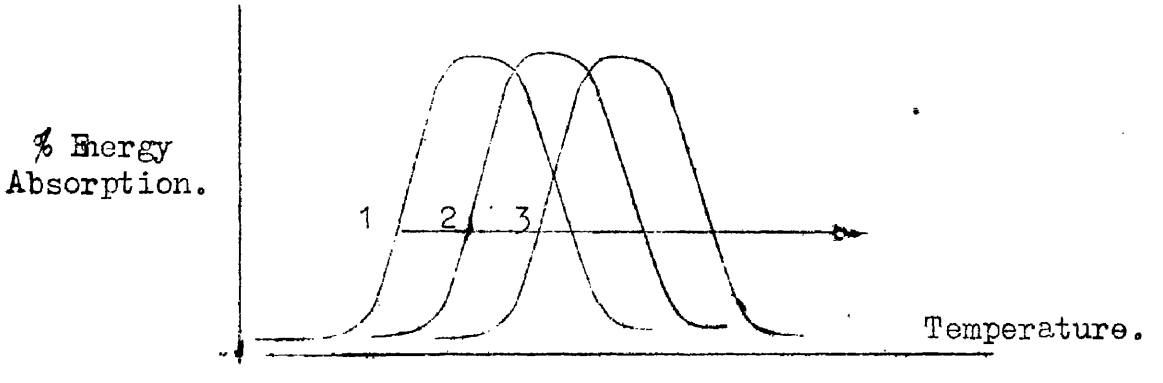

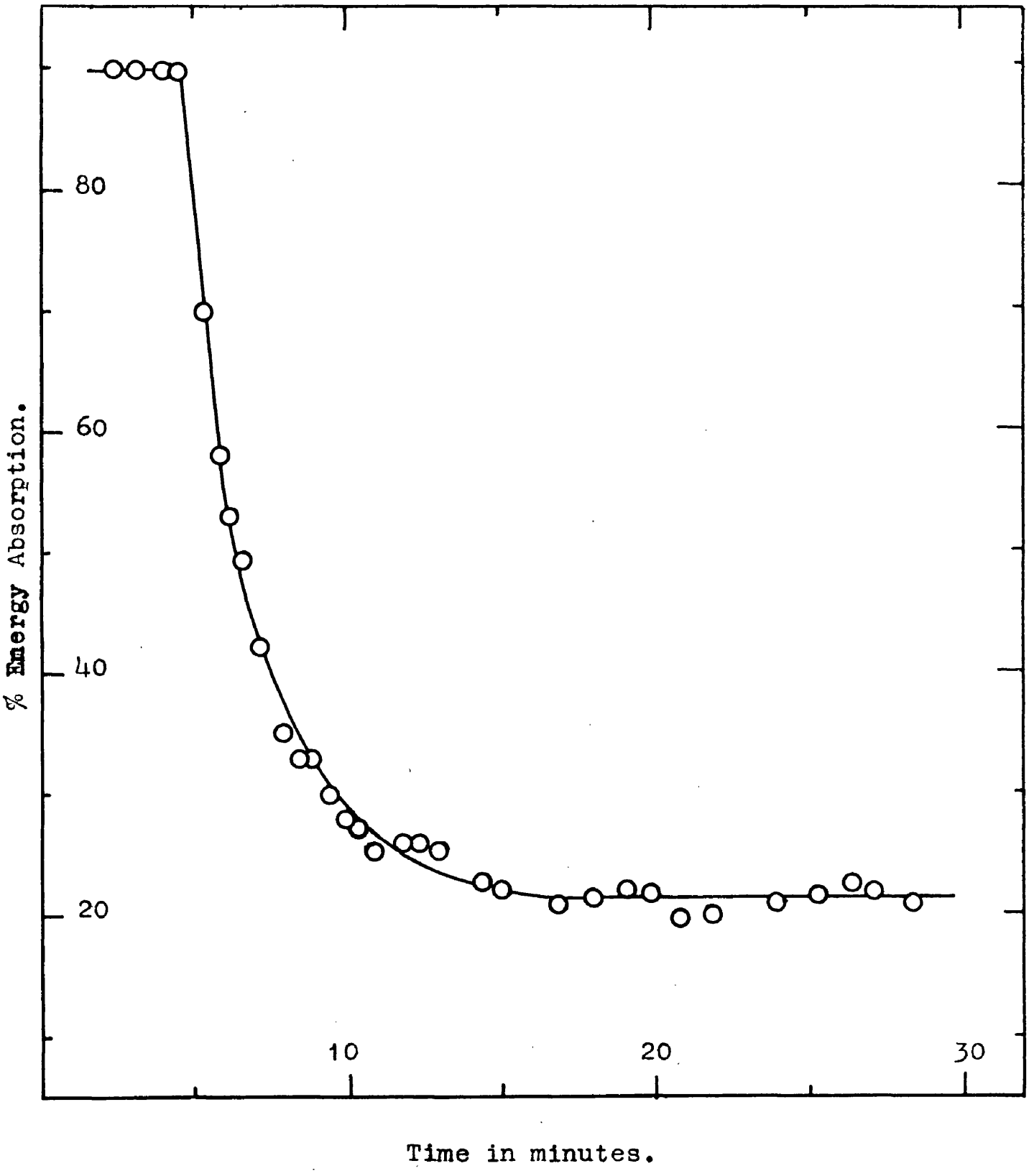

Figure 45.

Isothermal change of energy absorption at 158°C. for an epoxide/aniline-formaldehyde resin.

The success with which a specimen could be held in an isoelastic state is attested by the typical set of results in Table 6 (Appendix). The isoelastic curing rate curve obtained from these results is shown in Fig.46, plot II.

Although the isothermal cure and the isoelastic cure provide different types of information concerning the nature of the curing reaction, they are in fact merely two selected curing schedules in the time-temperature plane cf. Fig.46. Curing schedules are of great importance in the polymer industry, and the two schedules studied in this thesis illustrate the general possibilities for the use of the ball rebound apparatus in this field.

7. Curing Mechanisms.

The objective of this work was to establish the rate of curing as a theoretically intelligible function of the relevant variables. The simplest state of affairs to be hoped for is represented by a "conservative" system. By rough analogy with dynamic theories, this term is used to denote a system in which the curing rate depends on the temperature and on the state of cure, but not on the previous history of the sample, i.e. not on the path in the time-temperature plane by which this state of cure has been reached. It is not expected that all resin systems are "conservative" in this sense, but the epoxide system described below is found satisfactorily to be so.

A bolder treatment postulates that the curing rate is a function only of the internal mobility of the system, i.e.its segmental relaxation rate. This postulate fixes the relation between the state of cure and the temperature for a given rate of cure. The internal mobility of a polymer can be studied independently in terms of the elastic resilience, and if the resilience is kept constant, the mobility, and the curing rate should then be constant. This will be shown to be a successful treatment in a range of different resin systems nearing their curing equilibrium, through the observation of linear "isoelastic" rate plots in the time-temperature plane.

7.1 The Isoelastic Rate Principle.

It is postulated that the curing rate of a polymer system is a function only of its internal mobility, i.e. its segmental relaxation rate. If the internal mobility is held constant by maintaining the elastic resilience of the polymer at a constant level, then linear "isoelastic" curing rates ought to be observed as the curing equilibrium is approached.

Since the principle is quite general, it should be obeyed by any resin system sufficiently near the equilibrium state of cure. This has been successfully demonstrated for a peroxide initiated addition copolymerisation, an acid catalysed condensation polymerisation, and a base catalysed epoxide polymerisation. This last system was chosen for the most extensive study of isoelastic curing because of its convenient experimental characteristics.

That the isoelastic principle is well obeyed by the epoxide/aniline-formaldehyde system is proved by the linearity of the four plots in Fig.47 right up to their (common) equilibrium state, where the curves level off very sharply. The constancy of the isoelastic rates over up to 60°C is very striking when it is remembered that ordinary chemical rates usually more than double over an interval of 10°C. The use of m-phenylene diamine as an epoxide curing agent also gave linear isoelastic rate plots though with a

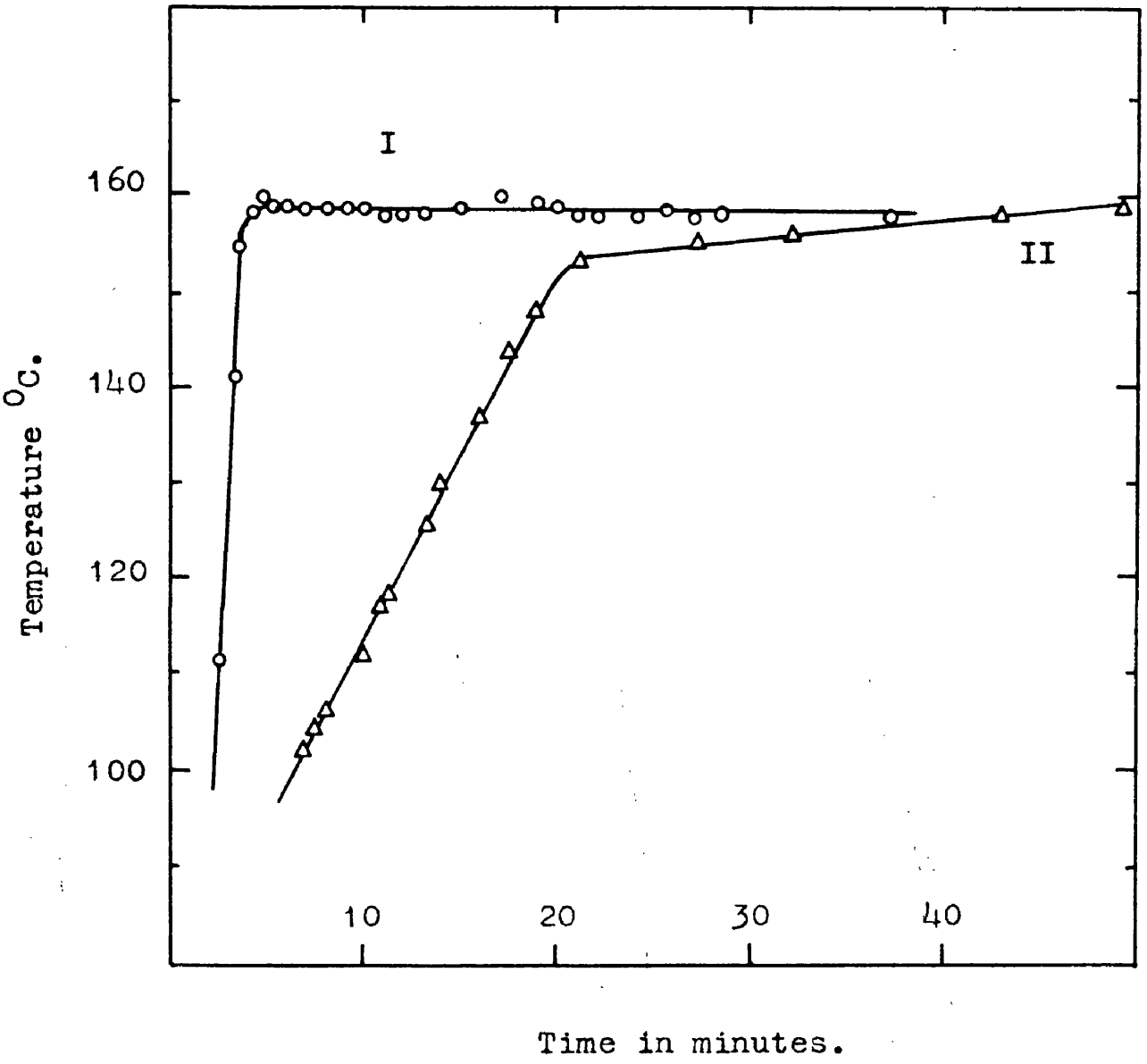

Figure 46.

Two heating schedules for an epoxide/aniline-formaldehyde resin.

I Isothermal run at 158°C.

II Isoelastic run at 22% energy absorption.

Figure 47.

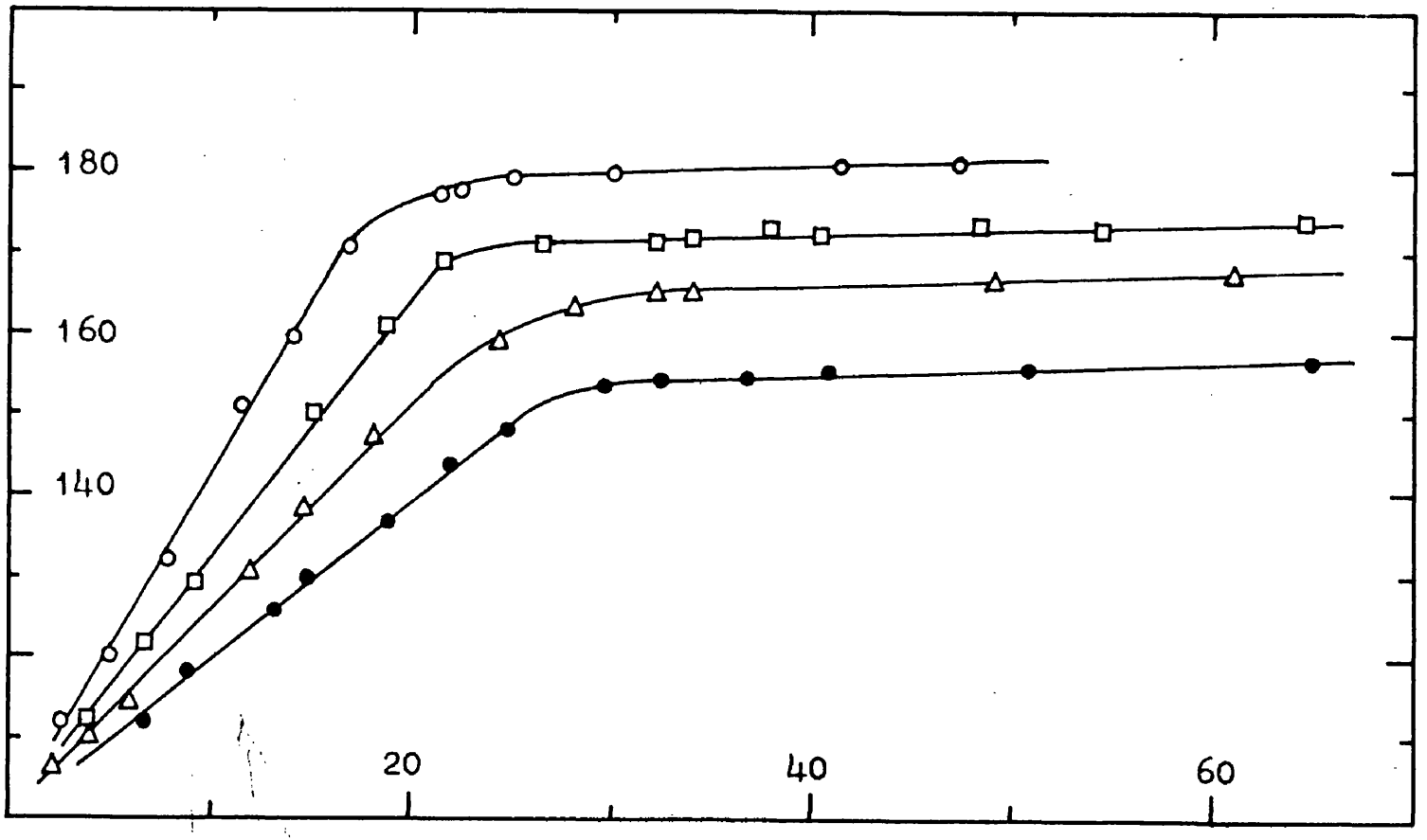

Time in Minutes.

Isoelastic rate curves for the curing of an epoxide/aniline-formaldehyde resin

Energy absorption: o 70%, □ 650%, △ 33%, • 22%.

slower curing rate than did the aniline-formaldehyde resin (Fig.48). The investigation of a urea-formaldehyde system showed that it conformed well to the isoelastic principle over the range covered (Fig.49). It was not possible to follow the curing rate as far as the equilibrium cure state for the U-F system as the specimens always cracked due to shrinkage caused by loss of water before this point was attained. The polyester "contact" resin system for which this work was originally planned was also observed to give linear isoelastic curing rates although experimental difficulties made it impossible to cover such large temperature ranges as in the epoxide system. Curing in these PEF/MMA resins was found to take place through a dual curing mechanism which is discussed in Section 7.4. As the plot in Fig.50 shows, this duality of mechanism did not affect the linearity of the isoelestic curing rate. This is just as expected, since the isoelastic theory invokes no detailed mechanism of curing at all, and in fact, the rate of diffusion outwards of methyl methacrylate (the secondary mechanism) depends on the internal mobility of the system just as much as does the rate of crosslinking (the primary mechanism).

It must be emphasised that the isoelastic rate principle of linear time-temperature rate plots applies only to the final stages of the reaction as the curing system nears its equilibrium (or pseudo-equilibrium). Fig.51 shows the

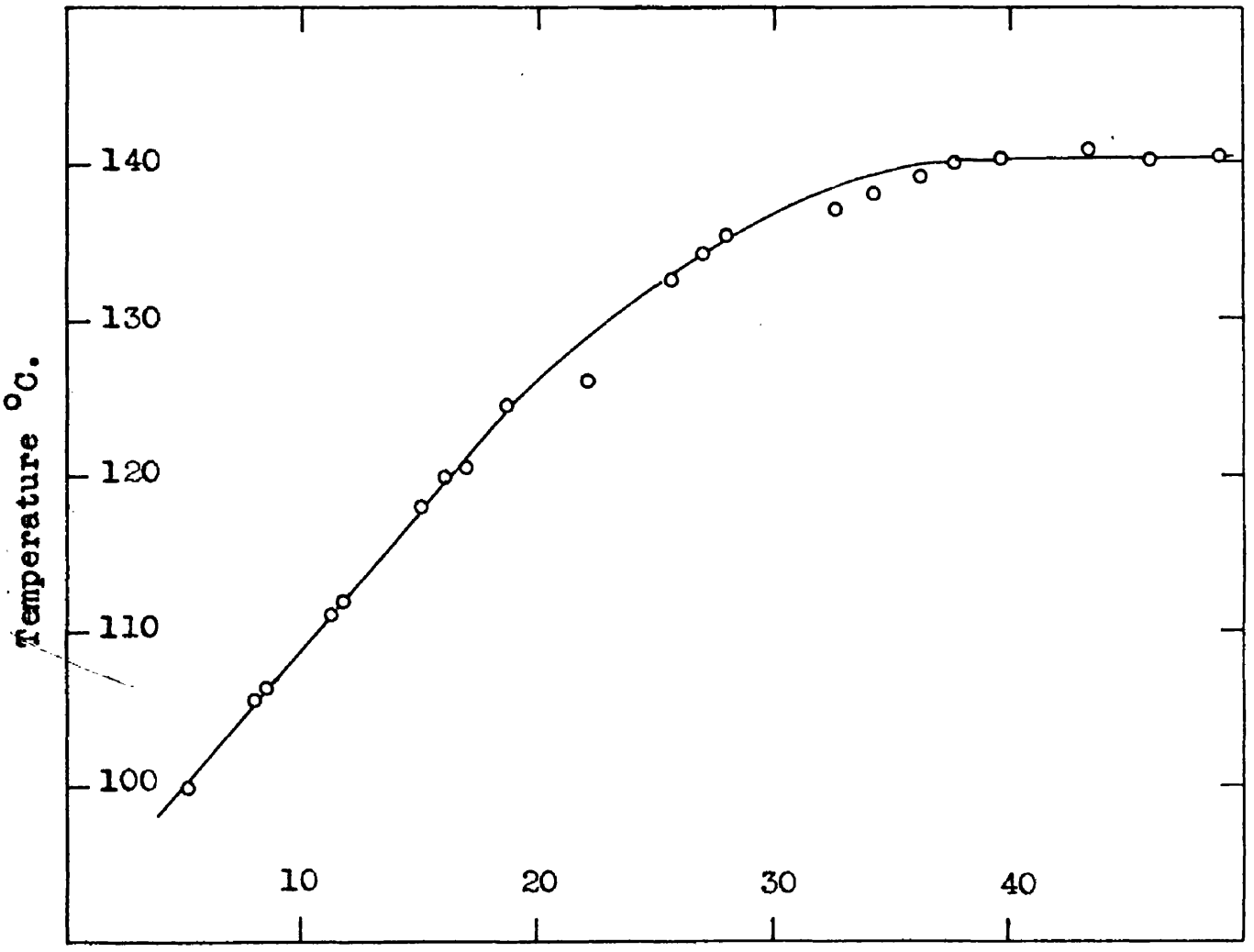

Figure 48.

Isoelastic rate curve for the curing of an epoxide-m-phenylene diamine resin system at 62% energy absorption.

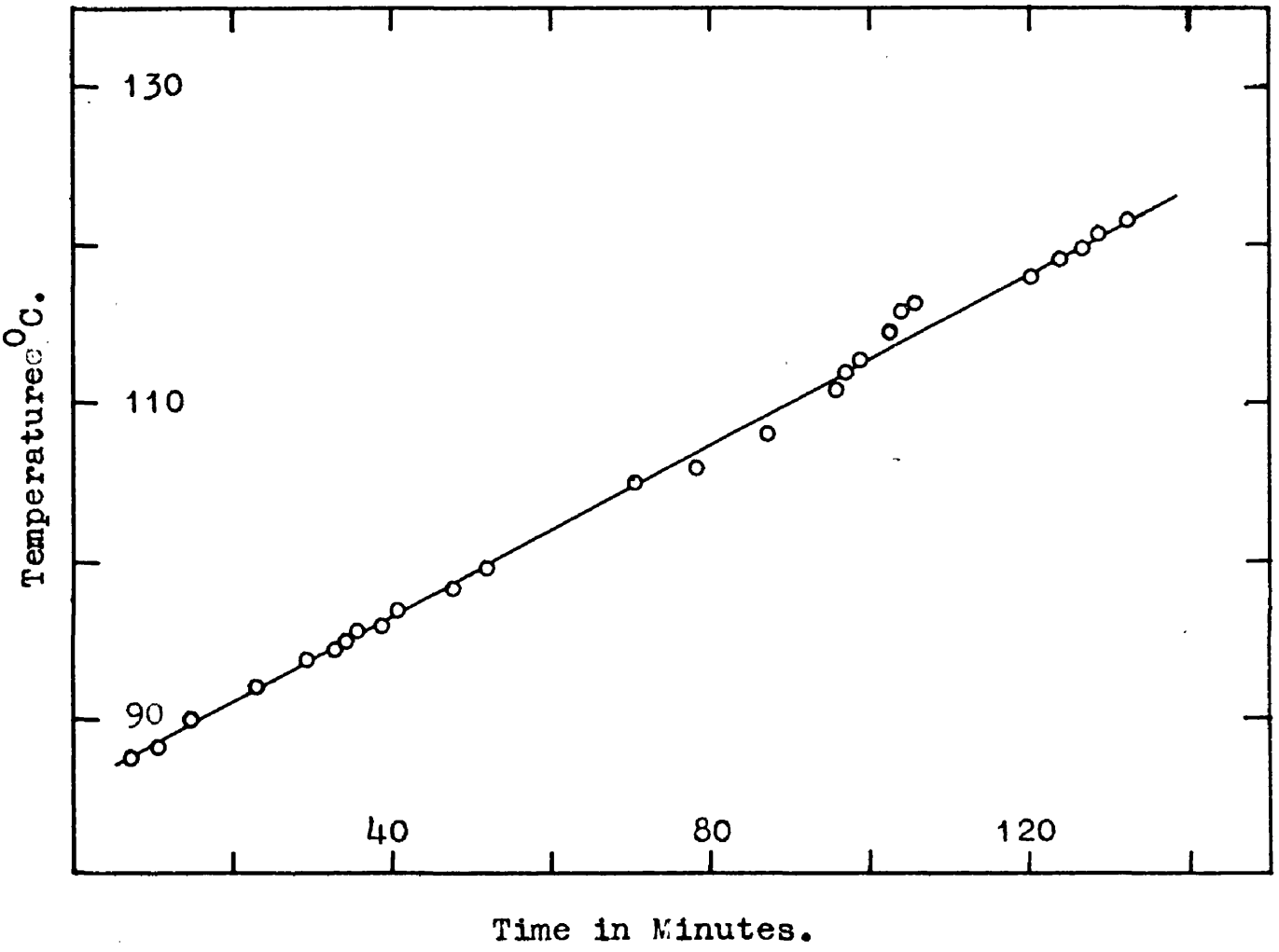

Figure 49.

Linear isoelastic rate plot for the curing of a urea-formaldehyde resin at 74% energy absorption.

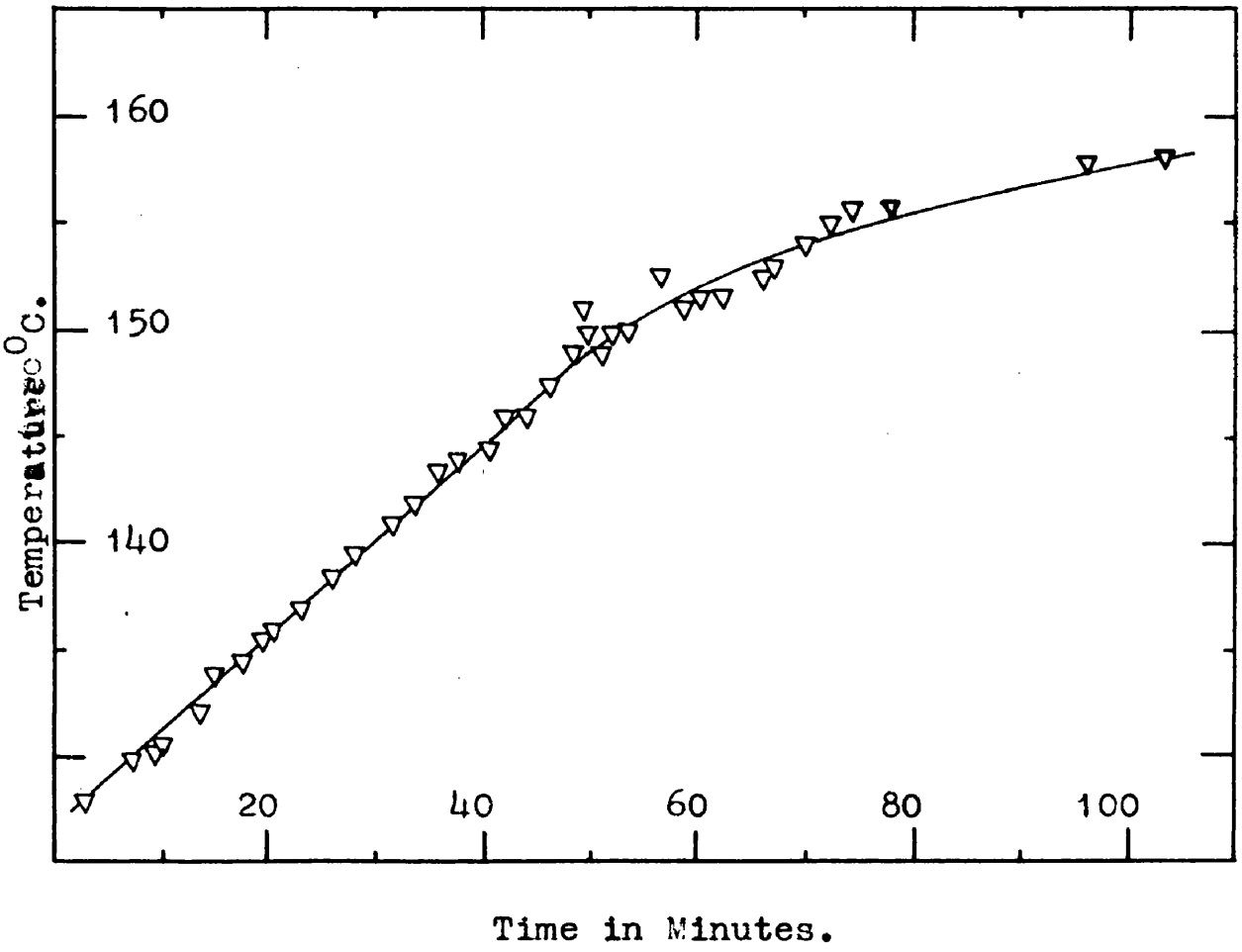

Figure 50.

Isoelastic rate plot for the curing of a model unsaturated polyester resin. (PEF/MMA, R = 1.25) Energy absorption 62%.

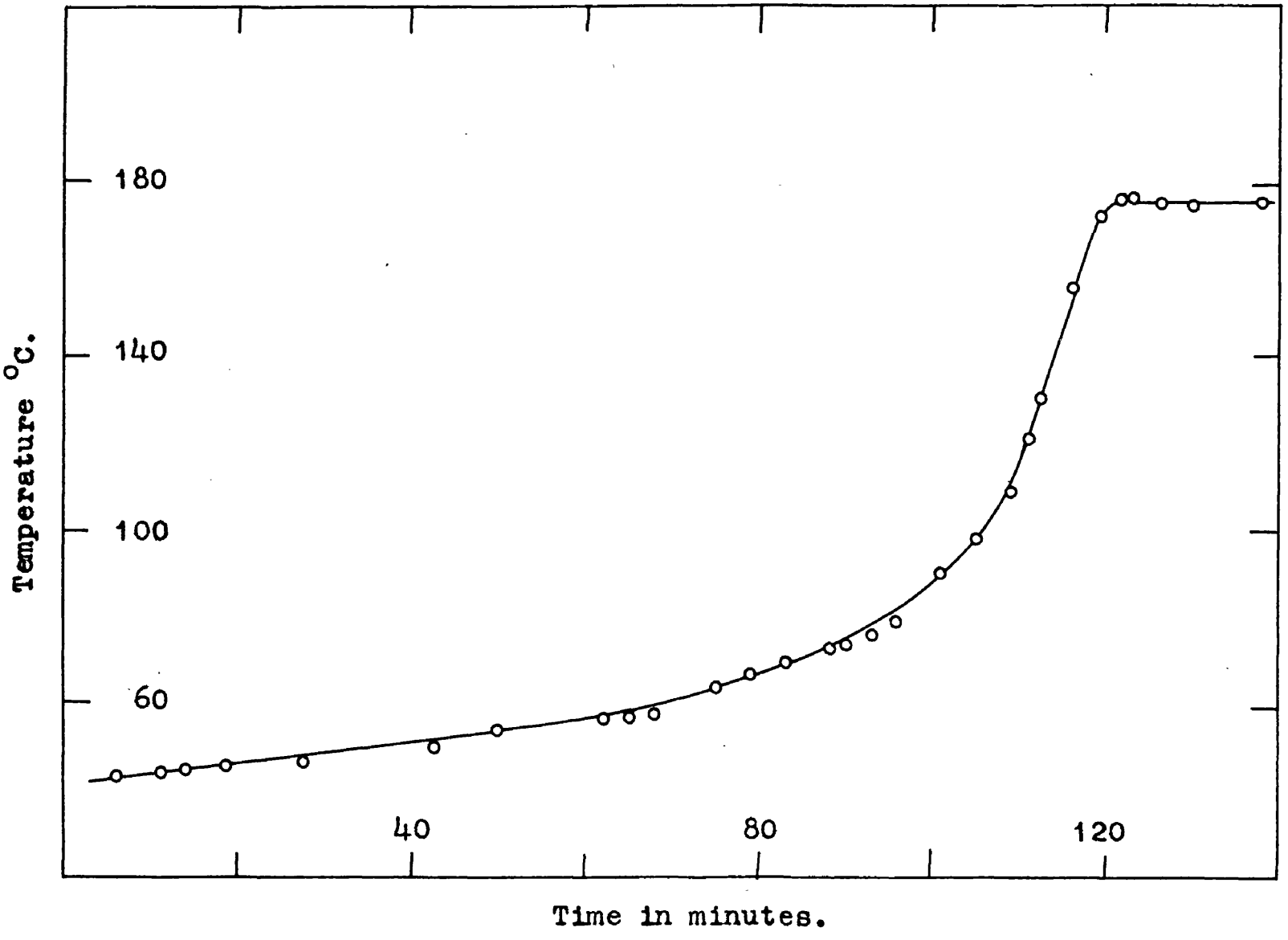

Figure 51. Long range isoelastic rate curve for the epoxide/aniline-formaldehyde curing reaction at 50% energy absorption.

isoelastic rate curve for an epoxide/aniline-formaldehyde curing reaction in which observations were commenced as soon as the specimen became firm enough to be clamped in the ball rebound apparatus, i.e. shortly after the gel point. As in all the other isoelastic runs, a linear curing rate was observed over the last 60°C change in T_m before the equilibrium cure state was reached, but prior to this there was a long period of slow curing at a gradually increasing rate. The reaction mechanisms occurring in this stage cannot yet be explained and further experimental work is required.

The phenol-formaldehyde resin system was the only system studied which did not exhibit a linear isoelastic curing rate terminating sharply at a curing equilibrium. In fact, no equilibrium or pseudo-equilibrium cure state was ever located and no linear isoelastic rate plot could therefore be expected. In the two isoelastic runs shown in Fig.52, the phenol-formaldehyde curing rate was constant over the range 110° - 130°C but then began to increase very rapidly. By the time that the isoelastic temperature had reached 300°C (the maximum temperature measurable on the indicator), the rate of curing was still increasing. This unusual behaviour requires further investigation.

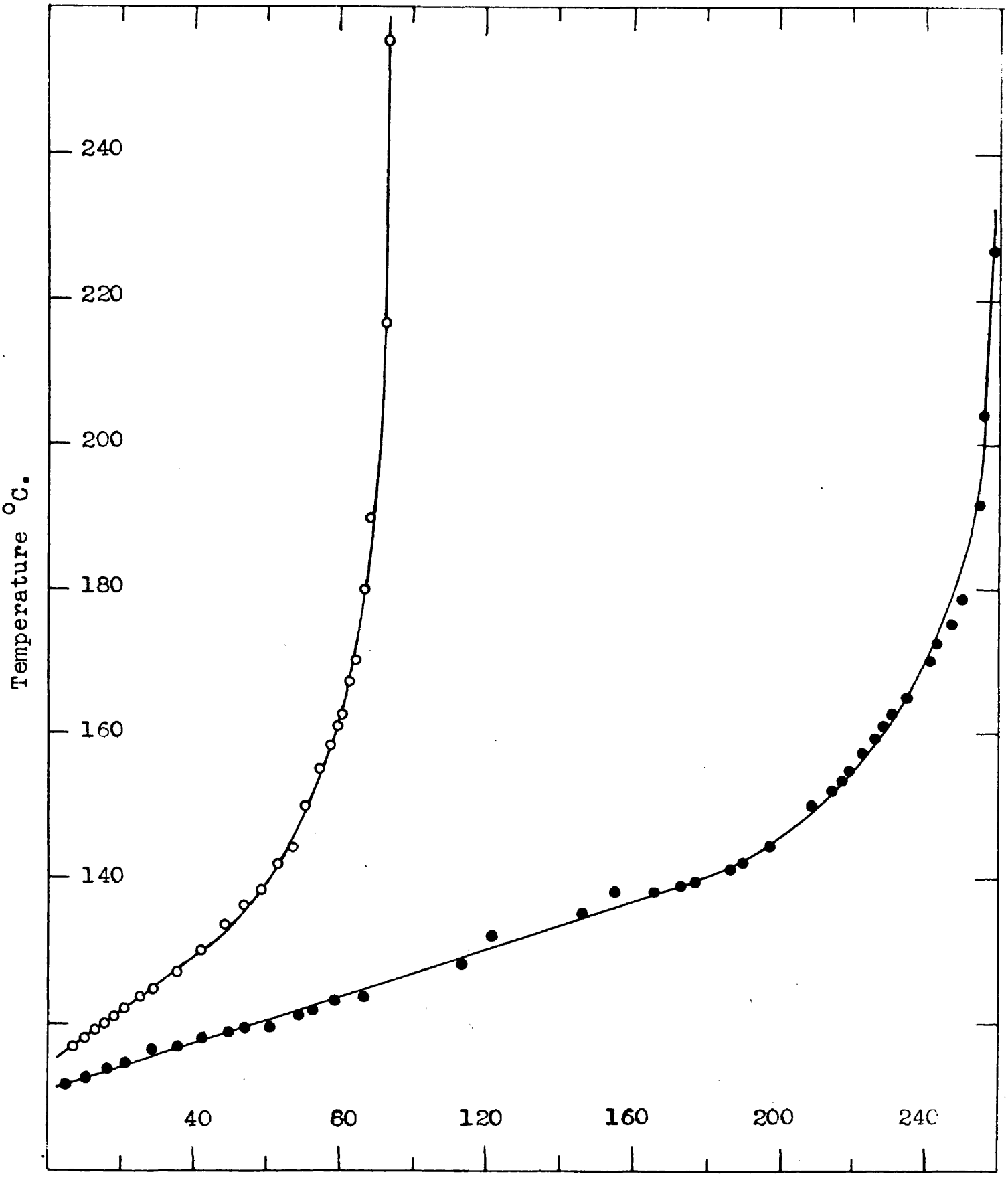

Figure 52 . Isoelastic curing rates for a phenol-formaldehyde system

o - Cure at 40% E.A. on the "rubbery" side of the peak.

● - Cure at 40% E.A. on the "glassy" side of the peak.

7.2 Isothermal Cure as a Relaxation Process.

If curing is a relaxation process, the curing rate (dT_m/dt) should follow a first order or Maxwellian decay[81]. Since $(\partial E/\partial T)_t$ for a given state of cure was a constant between $20 < E < 80$ (E = %energy absorption), i.e. the "glassy" slope of the peak curve was linear over that range, the slope of the isothermal rate curve $(\partial E/\partial t)_T$ was proportional to (dT_m/dt). Therefore, the isothermal rate curve (e.g. Fig.45) should also be a first order plot, and the test for reaction order shown in Fig.53 confirms that Fig.45 does represent a first order reaction. The relaxation time of the curing reaction τ, i.e. the time taken for the displacement from equilibrium to decay to one $e^{th.}$ of its original value, is given as the negative reciprocal of the slope of the first order test plot as τ = 2.5 minutes.

Experimental conditions were not favourable for the direct determination of the activation energy of τ from rate plots like Fig.45 over a sufficiently wide range of temperatures. The linear slope of the peak curve between $20 < E < 80$ covered a temperature range of only 30°C, and the decrease in the observed value of E during an isothermal curing experiment corresponded to a 20° shift in the position of T_m. Therefore, only a 10°C range of curing temperatures was available for direct activation energy determinations. However, an indirect evaluation of the

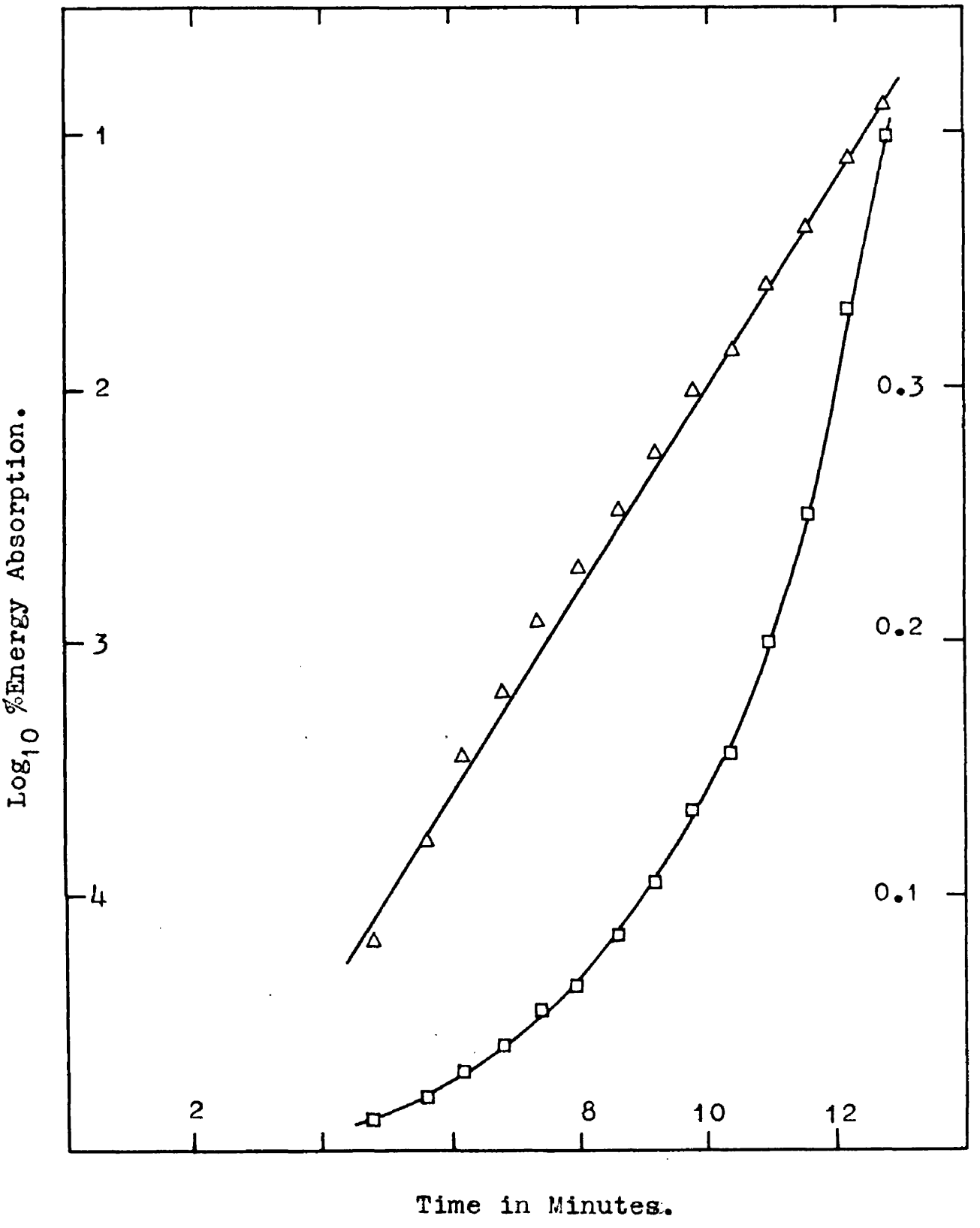

Figure 53.

Test for the order of reaction of figure 45.

△ First order plot - successful (linear).

□ Second order plot - unsuccessful (curved).

activation energy of τ could be made from the isoelastic curing rates in the reactions plotted in Fig.47 by comparison of the rates at different temperatures for specimens at the same state of cure. All the specimens used in the isoelastic curing runs passed through the state of cure represented by curve B, Fig.44 during the reaction. At the moment of passing through this chosen state, every specimen possessed the same energy absorption curve, the same amount of crosslinking, and the same T_m, but they were all at different temperatures and therefore at different energy absorption levels. Fig.54 shows a diagramatic representation of the portions of two isoelastic curing runs commencing from the one common state of cure. From plot B, Fig.44 (which represents the reference state of cure), the energy absorption levels (in fact the isoelastic levels chosen for the runs) in column 1, Table 24 were related to the corresponding specimen temperatures (column 4). These temperatures, together with the isoelastic curing rates (column 2) which were also measured as the specimens passed through the reference state, were then used as the basis for the Arrhenius plot in Fig.55.

Figure 54.

In this schematic representation of two isoelastic runs, the common state of cure through which both specimens pass is arbitrarily placed on the zero time axis. The two curing rates are seen to be:-

Specimen I at 50% energy absorption and $T_1^{\circ}C$,
Isoelastic reaction rate = $\tan (90 - \alpha)$.

Specimen II at 70% energy absorption and $T_2^{\circ}C$,
Isoelastic reaction rate = $\tan (90 - \beta)$.

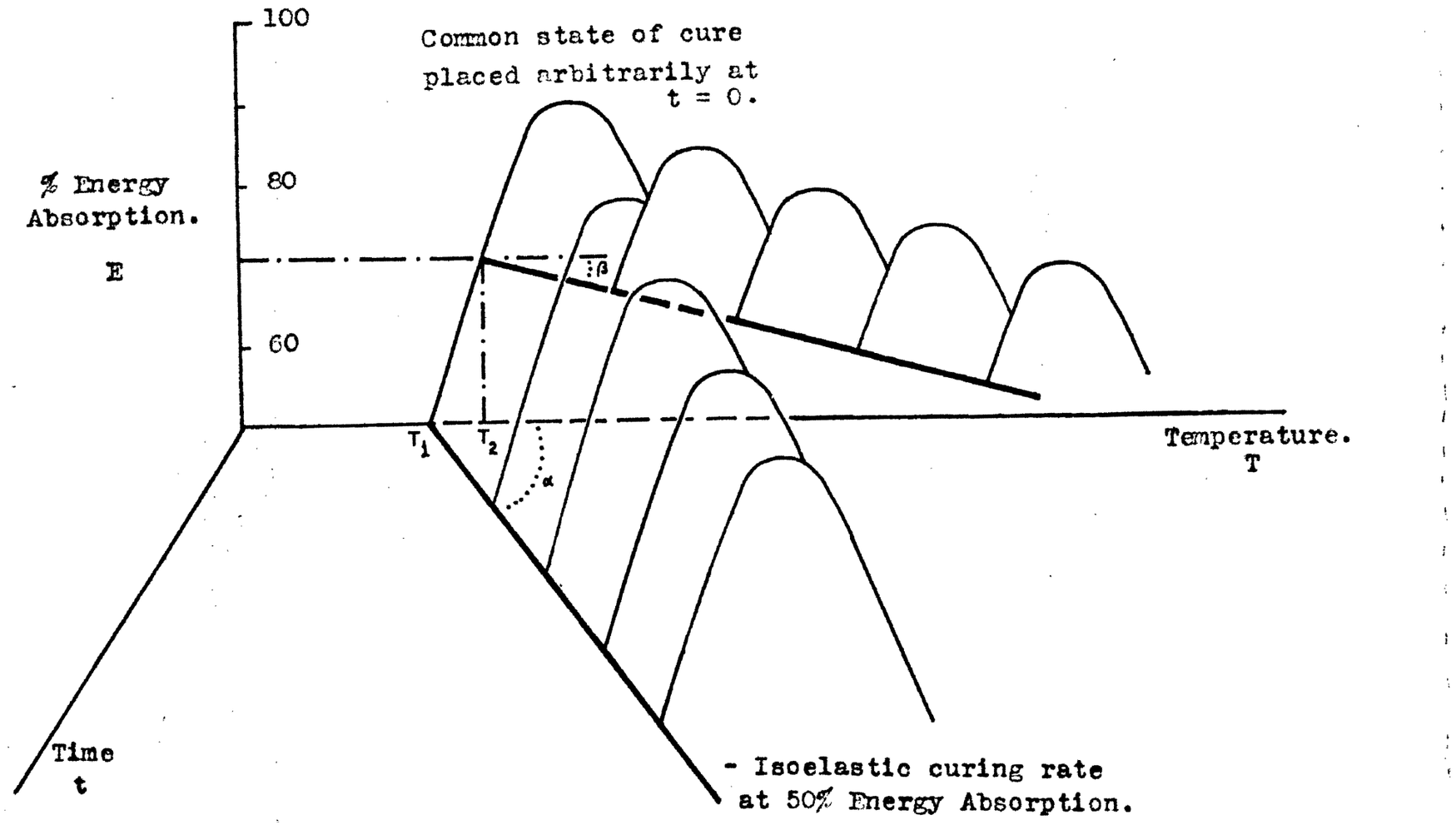
100
80
60
% Energy Absorption.
E
Common state of cure placed arbitrarily at t = 0.
$\overline{\beta}$
T_1
T_2
α
Temperature.
T
Time
t
- Isoelastic curing rate at 50% Energy Absorption.

Figure 54.

Table 24.

Activation energy of epoxide curing.

% Energy Absorption.	Isoelastic Rate.	Log_{10}Rate.	Absolute Temperature.	Reciprocal Temperature.
E	$\left(\frac{\partial T}{\partial t}\right)_E$	$\log_{10}\left(\frac{\partial T}{\partial t}\right)_E$	T°K	1/T°K
22	3.9	0.591	404	0.00247
33	5.4	0.732	410	0.00244
50	7.5	0.875	422	0.00237
62	7.5	0.875	431	0.00232
70	8.2	0.914	436	0.00229

It is observed from Fig.55 that for curing at lower temperatures, the activation energy is fairly high (of the order of 25 Kcals per mole), but it falls sharply at about 20°C below the temperature T_m of the energy absorption maximum of the reference cure state to about 5 Kcals. At some temperature in the region of its second order transition temperature a polymer changes from a rigid glassy material to a rubbery material, and it is suggested that this change in the mechanical properties is the cause of the change in the activation energy of the curing reaction. At higher temperatures, potentially reactive functionalities may diffuse freely through the rubbery polymer, but as the polymer is cooled into the glassy state, the energy barriers to the diffusion of functionalities through the rigid mass

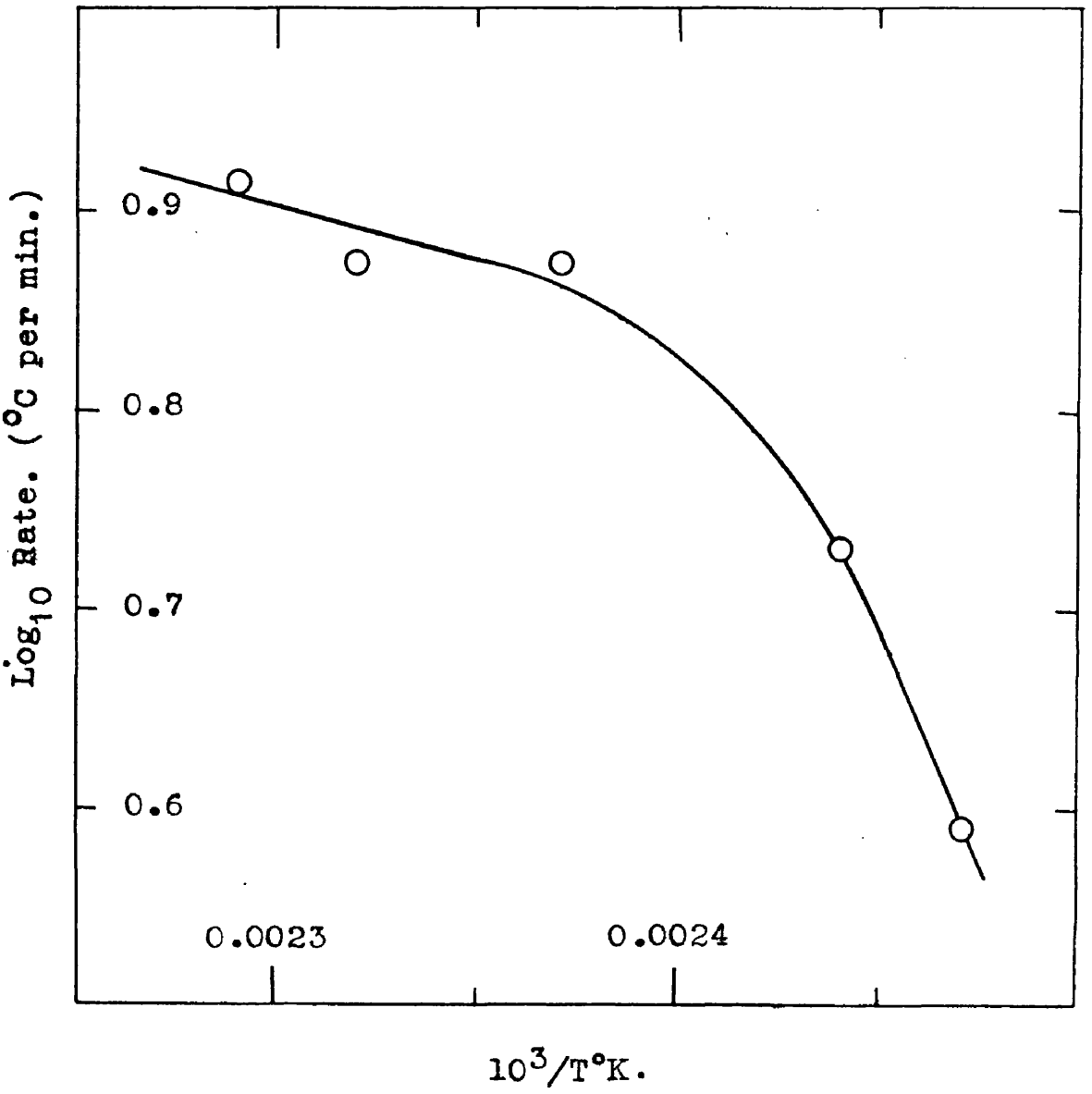

Figure 55 .

Arrhenius plot for the rate of curing of an epoxide/aniline-formaldehyde resin.

are greatly increased. Thus, at the moment at which the curing specimens passed through the reference state, those above the critical temperature were rubbery and presented only low energy barriers to the diffusion of active species, while those at lower temperatures were glassy and had high activation energies of curing.

An activation energy curve of very similar shape to that of Fig.55 has been reported by Russell[82] for the shrinkage during the final stages of the polymerisation of methyl methacrylate.

The position of the change in activation energy is also in qualitative agreement with the measured relaxation time of the curing reaction (τ = 2.5 minutes.). The peak in the energy absorption curve occurs when the segmental relaxation time of the polymer is of the order of one millisecond, i.e. equal to the ball impact frequency (ω). The temperature at which the polymer has a relaxation time of 2.5 minutes will therefore be lower than that at which the peak occurs, i.e. on the glassy slope of the peak curve. This is in fact where the activation energy increase does take place (at E = 40% energy absorption).

7.3 The Conservative Nature of the Epoxide Curing Reaction.

Two samples of epoxide/aniline-formaldehyde resin were subjected to different heating schedules in the time-temperature plane as shown in Fig.46. Plot I shows isothermal curing at 158°C after a rapid initial heating, and plot II a slow linear heating curve levelling off at 158°C. In both cases, the final energy absorption of the specimen was 22% at that temperature. In fact, this same state of cure was, within experimental error (± 2°C), the final state reached in all the cures analysed for the same resin composition. These included the curing reactions plotted in Fig.47, together with the reaction illustrated in Fig.44 of which plot D represents the energy absorption curve for this final state of cure. In any of the samples having this state of cure, irrespective of the heating schedule by which it had been reached, the rate of cure was (practically) zero. The final state thus obeys the condition for a conservative system.

The rate of curing in a conservative system.

In a conservative system, the rate of curing depends only on the state of cure at any moment, and the following law therefore applies to any one state of cure:

$$\left(\frac{\partial E}{\partial t}\right)_T = \left(\frac{\partial E}{\partial T}\right)_t \times \left(\frac{\partial T}{\partial t}\right)_E \qquad (26)$$

The first of the differential coefficients of (26) is the slope of the isothermal rate curve (energy absorption vs. time); the second is the slope of the absorption peak curve (cf. Fig.44); and the third is the slope of the isoelastic rate curve, i.e. temperature vs. time for a specimen held at constant energy absorption. In principle, the three coefficients vary with suitable variables such as E, T, t, or the state of cure. However, the following constancies are observed;

a) $\left(\frac{\partial E}{\partial T}\right)_t$ for a given state of cure is constant between $20 < E < 80$, i.e. the glassy side of the peak curves was linear over that range (Fig.44)

b) $\left(\frac{\partial E}{\partial T}\right)_t$ is practically independent of the state of cure in the epoxide system, i.e. the absorption curve moves parallel to the temperature axis without noticeable change in shape (Fig.44)

c) $\left(\frac{\partial T}{\partial t}\right)_E$ is constant with time over large ranges. (Principle of the isoelastic rate).

A satisfactory experimental verification of equation (26) was demonstrated with the epoxide/aniline-formaldehyde system. Following b) above, values of $(\partial E/\partial T)_t$ were obtained from an accurate drawing of the representative plot D, Fig.44, and the values of $(\partial T/\partial t)_E$, the isoelastic curing rate were experimentally measured at five different energy absorption levels (Fig.47). Because of c) above,

each figure in column three of Table 25 could be taken over a wide range of t (or T) values. The values in the fourth column of the table were least accurately measured, being taken from graphs such as Fig.45, and since theoretically they are products of two constants, they ought themselves to be constant with variations in the temperature at which they were measured. In fact, they appear to vary somewhat with temperature as shown, but the mean value always lay close to that predicted from Equ.(26).

Table 25.

Experimental test for equation (26).

% Energy Absorption.	Slope of Peak.	Isoelastic Rate.	Isothermal Rate.	Equation (26).
E	$\left(\frac{\partial E}{\partial T}\right)_t$	$\left(\frac{\partial T}{\partial t}\right)_E$	$-\left(\frac{\partial E}{\partial t}\right)_T$	$\left(\frac{\partial E}{\partial T}\right)_t \times \left(\frac{\partial T}{\partial t}\right)_E$
22	1.42	3.9	3.5* - 6.7'	5.5
33	1.83	5.4	4.0* - 13.8"	9.9
50	2.13	7.5	19.6	16.0
62	2.25	7.5	21.4	16.9
70	2.67	8.3	23.1	22.2

* - measured at 118°C; ' - at 134°C; " - at 158°C.

The application of Equ.(26) to the epoxide/aniline-formaldehyde system by comparison of columns 4 and 5 of the table is satisfactory considering the inaccuracy involved in reading tangents from rate curves. The "conservative" nature of the system is thus substantially verified.

7.4 Curing in the PEF/MMA Model Polyester System.

It has been shown that following the kink in the linear curing rate in the first stage of the PEF/MMA copolymerisation (Section 4.2), an exponential increase in the rate takes place in the second stage of the reaction and this is in turn followed by a levelling-off corresponding to the final third stage. In the slow third stage, the propagation rate in the polymerisation reaction becomes diffusion controlled and the rate depends on the internal mobility of the system. Dilatometric measurements show that after the rate curve levels off, there is very little further contribution to the total polymerisation present. The appropriate and more sensitive relaxation technique was therefore used for the examination of the final equilibrium (or pseudo-equilibrium) state of cure reached as a function of the PEF/MMA feed ratio R.

It might be thought that, since the reaction rate depends on the internal mobility of the system, polymerisation would generally be arrested at the same mobility or degree of cure irrespective of the feed ratio. The results shown in Fig.56 show that this is true only very approximately since the final degree of cure is spread over 60°C for the range of R values studied. Fig.57, based on the results shown in Fig.56, indicates that the state of cure reached a maximum at a very low R value, i.e. with only a very small

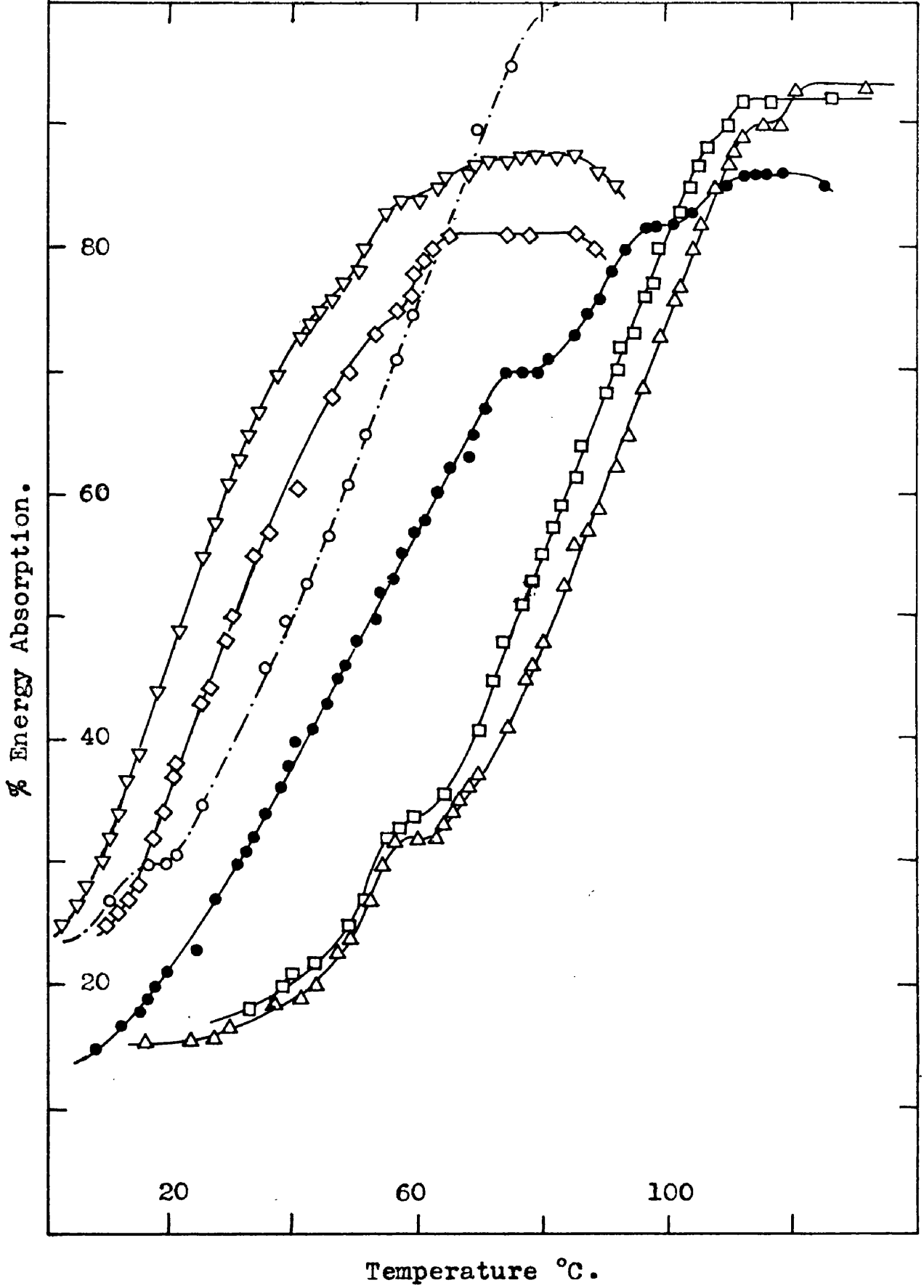

Figure 56. Energy absorption curves for the final state of cure (at 62°C.) of a series of PEF/MMA polyester resins.

o	R = 0	●	R = 0.5
□	R = 0.1	◇	R = 1.25
△	R = 0.2	▽	R = 1.75

amount of fumarate resin initially present. General theories of the second order transition in polymers suggest that the cure should be a function of two parameters. A crosslinking parameter should account for a rise in the value of T_m with increasing branching and crosslink formation, and a plasticisation parameter should account for the lowering of T_m by the presence of residual micromolecules (e.g. MMA monomer) and free PEF chains. Fig.57 therefore suggests qualitatively that at low R values, the degree of cure rises with R because the crosslinking effect predominates, while at high R values, plasticisation due to increasing concentrations of residual condensation chains strongly reduce T_m.

In order to eliminate the suspected effects of after-cure occurring during the measurement of the absorption peaks in Fig.56 (indicated by a rounding-off of the curves at the maximum absorption values), the peak temperature T_m was replaced by the much lower temperature T_{50} in Fig.57. T_{50}, the temperature at which the glassy slope of the peak curve passed through the value E = 50% acts like T_m as a direct measure of the state of cure of a resin.

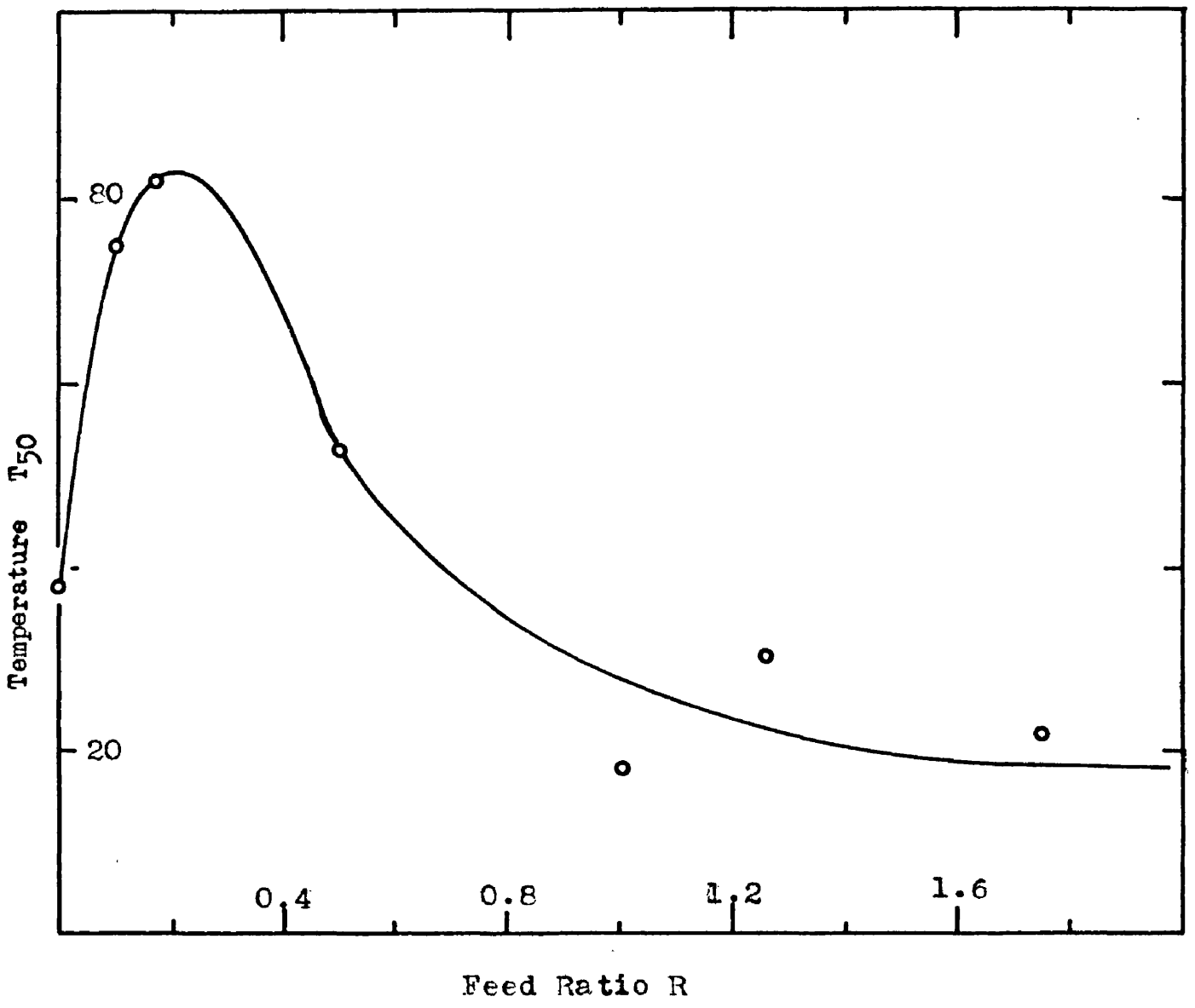

Figure 57. The effect of the PEF/MMA feed ratio on the final state of cure reached (T_{50}) after exhaustive polymerisation at 62°C.

Isoelastic Cure and the Duality of the Curing Mechanism.

Linear isoelastic rate curves were obtained for specimens of PEF/MMA model polyester which had previously been cured to known points near the end of the isothermal polymerisation rate curve at 62°C as measured by density techniques. The after-cure of these specimens was complex since free methyl methacrylate monomer was lost by diffusion and evaporation in the rebound apparatus in the temperature range 120° - 160°C, in addition to the further double bond polymerisation.

The theory of the isoelastic principle is not affected by the duality of the curing mechanism, since no detailed mechanism is invoked at all. In fact, the rate of diffusion outwards of the methyl methacrylate depends on the internal mobility of the system (segmental relaxation rate) just as much as do the rate of crosslink formation and the elasticity.

From measurements of the weight and density of PEF/MMA discs both before and after isoelastic curing runs, the relative contributions of the two mechanisms was assessed. Thus, the disc used for the run illustrated in Fig.50 lost 2.1% in (methyl methacrylate) weight, and its density increased from 1.2913 to 1.3449. These figures corresponded to an after-polymerisation from 30.8% of the unsaturation present in the disc at the beginning, to 44.9% of that

at the end of the isoelastic run (calculation - Appendix page 131).

It has been shown that in PEF/MMA resins initially containing appreciable amounts of fumarate unsaturation ($R \geqslant 0.1$), about 90% of this unsaturation survives unpolymerised after exhaustive heating at 62°C.[83] Relaxation, weight and density observations show that this residual unsaturation is almost entirely inert to further polymerisation even when the specimen is heated to 160°C. For example, a specimen of feed ratio R = 1.25 retained 63% of its unsaturation after exhaustive polymerisation (48 hours) at 62°C, and only a further 3.4% polymerised at 160°C. Similarly, the isoelastic polymerisation of Fig.50 reached a final state with 44.9% of its unsaturation reacted, while a duplicate specimen after exhaustive treatment at 62°C reached 37% reacted unsaturation (calculation - Appendix, page 131).

Appendix.

I. Note on Nomenclature.

It seems to be customary to speak of crosslinking the polyester resin with a monomer such as methyl methacrylate, while occasionally the polyester is referred to as the crosslinker for the methacrylate. In as much as the polyester is the polyfunctional component, it seems preferable to associate it nominally with the crosslinking process, so the latter usage is adopted here.

II. Proof of the proportionality of (rate of flow) to sin(angle of inclination) in a plug viscometer.

Viscometer: 2mm. bore capillary with plug of porosity 45 microns.

Viscous medium: boiled out distilled water.

Table A1.

Angle θ°	Time to flow 3 cm.	Mean Flow Time.
5°↙	47.5, 46.7, 47.6, 47.0 seconds.	47.3 secs.
5°↘	55.4, 55.7, 54.0, 54.9.	55.0
10°↙	24.6, 24.3, 23.6, 23.6.	23.9
10°↘	27.0, 26.6, 27.0, 26.9.	26.9
20°↙	12.6, 12.6, 12.6, 12.6.	12.6
20°↘	13.4, 13.1, 13.8, 13.1.	13.3
40°↙	6.9, 6.9, 7.1, 6.9.	6.9
40°↘	7.5, 7.4, 7.3, 7.6.	7.4

The reading of flow time in Table A1 were taken with the viscometer inclined in both direction as the zero degree setting was not quite accurate. The mean flow times used below demonstrate the good proportionality to 1/sin θ.

Table A2.

Mean angle θ	Sin θ	Mean flow time t	t.sin θ
5	0.087	51.2 secs.	4.46
10	0.173	25.4	4.39
20	0.342	12.9	4.42
40	0.642	7.1	4.50

III. Comparison of viscosities measured with an Ostwald and a plug viscometer.

Plug viscometer: as in II above. Calibration with distilled water gives:-

Viscosity = 5·9. Flow time.Weight.sin θ cpoise.

Ostwald viscometer No.1

Viscosity = 0.004356.Flow time - 2.4/t cpoise.

Ostwald viscometer No.2

Viscosity = 0.04869 t - 2.4/t centipoise.

Solutions of poly(methyl methacrylate) dissolved in MMA monomer containing 4% hydroquinone as inhibitor were measured in the three viscometers above.

Table A3.

Comparison of Ostwald and Plug Viscosity Measurements.

Solution No.	Pure MMA.	No.1	No.2	No.3	No.4
Ostwald No.	1	2	2	2	2
Mean flow time.	97.3secs.	116.5	513	2788	10660
Viscosity cp.	0.403	8.10	25	136	520
Plug:flow time.	2.85	16.7	54.1	250.3	1032
Angle θ	20°	90°	90°	90°	90°
Solution Weight.	0.244	0.256	0.250	0.265	0.244
Viscosity cp.	0.470	8.53	26.6	134.0	496

In Fig.3, the graphical comparison of the two methods of viscosity measurement, the values plotted are 10 times the $\log_{10}$ of the above viscosities.

IV. Justification of Equation 12.

At 62°C, the density of MMA monomer is 0.8979 g/ml, and the molar concentration is therefore

$$(1000 \times 0.8979)100 = 8.98 \text{ moles.l}^{-1}.$$

At 62°C, the density of PEF resin F ($DP_n = 3.92$) was 1.344, and the molar concentration (F) of fumarate double bonds is

$$(1000 \times 1.344 \times DP_n)/(142DP_n + 18) = 9.17 \text{ moles.l}^{-1}.$$

For an equimolar mixture (R = 1) of MMA and resin F, the initial molar concentration is therefore: $F_o + M_o = 9.08$ which value is very little affected by changes in R.

V. The characteristics of the PEF model polyester resins.

The molecular weight of the ethylene fumarate repeat unit $-(-(CH_2)_2 - OOC.CH=CH.COO)-$ is 142 and the end groups HO- and -H add a further 18. The degree of polymerisation of a PEF polymer could therefore be calculated from the molecular weight using the following relationship:-

Degree of polymerisation (DP) = (Mol.Wt. - 18)/142

Table A4.

Resin.	Reaction Time at 190°C.	Mol.Wt. EG[1]	Mol.Wt. C[2]	Density at 300°K.	Refractive Index*
A	90 mins.	505	396	--	--
B	160	550	435	1.3507	1.5087
C	215	710	572	--	--
D	270	876	646	--	--
E	310	1066	955	1.3618	1.5129
F	105	554	430	1.3469	1.5070
G	235	832	810	1.3534	1.5000
H	315	967	820	1.3508	1.5110
J	93	509	434	1.3556	1.5068
N	95	542	584	1.3568	1.5081
I"	320	---	424	--	--

[1] End Group molecular weight; [2] Cryoscopic Mol.Wt.

* Determined at 300°K; " Prepared from ethyl fumarate.

VI. Typical set of readings for a viscodilatometric gelation experiment.

The results are for Run D 13 which is shown graphically in Fig.4, page 14.

PEF resin D, Feed ratio R = 0.96, Temperature 62°C.

Initiator 1.52% methyl ethyl ketone hydroperoxide.

Table A5.

Position of plug meniscus.[1]	Time[2]	Position of open meniscus.[1]	Time.[2]
0.16	2 min.20 sec.	4.22	2 min.35 sec.
0.30	3-00	4.43	3-15
0.40	3-30	4.52	3-45
0.49	4-00	4.60	4-15
0.58	4-30	4.74	4-45
0.66	5-00	4.74	5-15
0.73	5-30	4.81	5-45
0.80	6-00	4.86	6-15
0.88	6-30	4.93	6-45
0.94	7-00	4.97	7-15
1.00	7-30	5.02	7-45
1.05	8-00	5.06	8-15
1.10	8-30	5.09	8-45
1.13	9-00	5.12	9-15
1.22	9-30	5.16	9-45
1.26	10-00	5.19	10-15
1.29	10-30	5.21	10-45
1.305	11-00	5.23	11-15
1.31	11-30	5.235	11-45
1.315	12-00	5.227	12-15
1.33	12-30	5.22	12-45
1.34	13-00	5.22	13-15
1.34	13-30	5.21	13-45
1.34	14-00	5.205	14-15
1.34	14-30	5.195	14-45

[1] The positions of the menisci were read against scales engraved in 0.30 mm. divisions.

[2] Times from immersion of reactants in thermostat at 62°C.

VII. Calculation of the rate of reaction and the conversion at the gel point in a PEF/MMA gelation reaction.

The viscodilatometer to be used was first calibrated for volume by measuring the length of columns of water of known weight. The length of the resin column in the instrument was measured during the induction period and again at the gel point, and using the volume/length calibration, the two volumes V_o (initial) and V_c (at the gel point) were calculated. Assuming that the contraction which occurred was due entirely to the polymerisation of MMA (Section 4.2), the conversion of monomer at the gel point is given by:-

$$\beta_c = K(V_o - V_c)/V_o$$

where $K = (0.2188 + 0.00467.T°C)$[39]. Since the initial concentration of the reactants $(F_o + M_o) = 9$, then if t_c is the gel time in seconds, the rate of reaction is given by:-

$$\text{Rate of reaction} = 9.\beta_c/t_c \ \text{mol.l}^{-1}.\text{sec}^{-1}.$$

Thus for run D 13 (Fig.4), the observed volumes were:-

$V_o = 1.7312$ ml., $V_c = 1.7179$ ml.

The conversion at the gel point was therefore:-

$$\beta_c = 4.04\ (1.7312 - 1.7179)/1.7312$$
$$= 0.03099$$

or as normally expressed 3.099%

and the reaction rate = $(9 \times 0.03099)/(570)$

$$= 4.89 \times 10^{-4} \ \text{mol.l}^{-1}.\text{sec}^{-1}.$$

VIII. Results of gelation experiments.

All runs were performed at 62°C except where otherwise indicated ([1] at 42°C and [2] at 82°C.)

Resin PEF C.

Initiator.	B%	R	G_o mins.	t_c mins.	β_c	Rate.	Rate.$B^{-\frac{1}{2}}$.
MEK	2.35	1.09	19.5	14	4.63%	4.96	3.24
TBHP	3.63	"	21	9	1.16	1.94	1.02
TBHP	4.44	"	69	57	2.50	0.65	0.31
MEK	0.38	0.79	23	17	2.04	1.80	2.92
MEK	1.29	"	20	16	3.42	3.20	2.82
MEK	2.29	"	19	16	4.19	3.92	2.60

PEF resin D

MEK	0.26	1.00	16.5	7.8	0.74	1.40	2.74
MEK	0.86	"	13	6.4	1.11	2.60	2.80
MEK	3.10	"	25	21.8	6.04	4.14	2.36
Thermal		"	105	55	3.37	0.92	--
MEK	0.12	0.96	18.8	10.4	0.99	1.44	4.11
MEK	0.42	"	15	10	1.30	1.94	3.90
MEK	1.52	"	13.5	9.5	3.10	4.89	3.97
TBPB	0.79	"	21.5	9	0.74	1.22	1.38
TBPB	5.00	"	13.5	4.5	0.62	2.05	0.92

PEF resin F.

[2]MEK	0.80	1.00	20.5	18.5	11.0	8.91	9.96
[2]MEK	2.03	0.33	23.0	21.0	25.4	18.12	12.70

PEF resin I (prepared from ethyl fumarate).

MEK	1.57	1.00	--	--	--	2.82	2.24
[2]MEK	1.48	0.33	25	24	28.60	19.32	15.88
[2]MEK	1.44	0.33	25.5	Viscosity run only.			

PEF resin G.

MEK	1.57	0.50	63	59	12.4	3.14	2.51
MEK	1.57	"	69	62	15.0	3.62	2.90
MEK	1.35	1.00	24.3	21.8	4.17	2.87	2.47
MEK	1.56	"	24	22	4.65	3.17	2.54

Results of gelation experiments (continued).

Initiator B%	R	G_o mins.	t_c mins.	β_c	Rate.	Rate.$B^{-\frac{1}{2}}$.
PEF resin J.						
MEK 1.38	1.00	21	17.3	1.91	1.66	1.42
TBHP 2.04	"	86.5	59.5	4.13	1.04	0.73
TBPB 1.80	"	20	14	0.97	1.04	0.78
BZP 1.90	"	6.8	4.1	2.20	8.04	5.83
[1]BZP 2.00	"	31	26	1.10	0.63	0.45
TBPB 1.65	0.91	12	8.3	0.30	0.54	0.42
TBPB 3.60	"	9.8	7.8	0.45	0.86	0.46
TBPB 1.0	"	13.3	9.5	0.45	0.72	0.72
TBPB 0.18	"	28	9	0.68	1.13	2.69
TBPB 0.38	"	17.5	8.8	0.43	0.75	1.22
TBPB 2.64	"	15.7	8.5	0.58	1.03	0.63
PEF resin N.						
MEK 0.11	0.96	12.5	5	0.33	0.98	3.01
MEK 0.23	"	13	7.5	0.49	0.98	2.07
MEK 0.57	"	10	6	0.49	1.22	1.61
MEK 1.10	"	14	11	1.95	2.65	2.53
MEK 1.88	"	20.3	16.8	4.37	3.90	2.85
MEK 0.84	"	13.3	9.3	2.99	4.84	5.31
MEK 1.45	"	16.8	13	3.17	3.66	3.04
HCH 1.95	"	17.5	12.5	1.55	1.85	1.33
HCH 0.46	"	13	7	0.41	0.87	1.28
Thermal	"	37	26.5	1.18	0.67	--
MEK 2.40	0.49	47.2	42.8	11.90	4.16	2.67
MEK 0.68	"	67.5	57.5	10.80	2.81	3.42
HCH 0.62	"	81	69	6.57	1.43	1.81
HCH 1.11	"	78	69	9.87	2.14	2.03
HCH 0.32	"	63	50	3.18	0.95	1.68
HCH 2.33	"	87	81.5	14.40	2.66	1.74
MEK 0.72	"	67	59.5	11.90	3.01	3.55
HCH 0.96	"	77	70	8.59	1.84	1.88
HCH 0.42	"	65	56.5	4.43	1.44	1.81
HCH 1.66	"	90	83	13.80	2.50	1.94
MEK 0.29	"	62	56	6.94	1.86	3.45
Thermal	"	385	373	5.64	0.23	--
MEK 0.89	0.80	29	26	5.17	2.98	3.16
AZBN 0.96	"	14	12	5.13	6.41	6.54
AZBN 0.07	"	17.5	11	0.77	1.05	4.00
MEK 0.88 (+0.0072 CN)	"	50	46.5	19.70	6.36	6.79
Thermal	"	245	45	1.17	0.39	--

Results of gelation experiments (continued)

Gelation of diallyl compounds at 80°C, using 1% BZP initiator.

Monomer.	Overall gel time G_o mins.	Actual gel time t_c mins.	Mean value conversion.
Diallyl Isophthalate	205 215	202 208	14.9%
Diallyl Phthalate.	291 287	287 283	18.5%
Diallyl Terephthalate	156 159	152 154	12.5%
Diallyl Oxalate.	393) By time of 367) bubble rise.	--- ---	20.2%

Methyl methacrylate polymerisations.

Initiator	B%	Temperature °C.	Reaction Rate$_1$ ($mol.l^{-1}.sec^{-1}$)	Rate.$B^{-\frac{1}{2}}$.
MEK	0.83	62	2.86	3.14
MEK	0.76	62	2.49	2.86
MEK	1.56	62	3.18	2.56
BZP	1.94	42	1.29	0.93
BZP	1.90	62	7.85	5.68
TBPB	1.85	62	1.82	0.98
MEK	0.84	62	3.21	3.49
TBHP	1.40	62	0.86	0.73
MEK	1.50	82	4.75	3.80
HCH	2.00	62	2.20	1.56

IX. Calculations of PMF/MMA after-polymerisation.

The following experimental observations were made i) before polymerisation, ii) after polymerisation at 62°C for 75 mins., and iii) after the isoelastic curing run at 62% energy absorption illustrated in Fig.50.

Monomer	i)	ii)	iii)
Specimen Weight.	0.3855g.	0.3855g.	0.3773g.
Density (ρ)	1.1995 g/ml.	1.2913	1.3449
Specific Volume $(V)_{20°C}$	0.8337 ml/g.	0.7744	0.7740
Volume of specimen.	0.3217	0.2981	0.2805

The conversion of double bonds at each stage may be calculated from the specific volumes (V) using Equation (4):

$$\text{Polymerisation at } 20°C = 0.434(V_o - V)/V_o$$

Applying this to the polymer in state ii):

Conversion after 75 mins. at 62°C =

$$0.434(0.8337 - 0.7744)/0.8337$$

$$= 30.80\%$$

Between states ii) and iii), i.e. during the isoelastic run, a loss in weight was recorded for which a correction must be made. Assuming this loss to be attributable entirely to the outward diffusion of MMA monomer, the MMA volume loss was therefore 0.0087 ml. Since the loss of MMA and the polymerisation are independent processes, the loss must be allowed for when calculating the final polymerisation iii).

Therefore the corrected initial volume of the disc is

$$= 0.3217 - 0.0087 \text{ ml.}$$

$$= 0.3130 \text{ ml.}$$

Similarly, the corrected initial weight is

$$= 0.3855 - 0.0082 \text{ g.}$$

$$= 0.3773 \text{ g.}$$

and the corrected initial specific volume is then 0.830ml/g. Using this corrected value of V_o , the calculation of the conversion at stage iii) gives:-

$$\text{Conversion} = 0.434(0.830 - 0.744)/0.830$$

$$= 44.9\%$$

An exactly similar PEF/MMA mixture was polymerised for 48 hours at 62°C, i.e. until measurable reaction at that temperature had ceased. It was then given an isoelastic after-curing schedule exactly similar to that of Fig.50. The following weight and density observations were made, and from them were calculated, in precisely the same manner as above, the conversion of double bonds existing at each stage.

	"Monomer" mixture.	After 48 hrs. at 62°C.	After isoelastic curing.
Weight.	0.4594g.	0.4594g.	0.4449g.
Density.	1.1995	1.3106	1.3390
Conversion.	--	36.7%	42.4%

X. Table A6.

Specimen of the experimental results for an Isoelastic Rate Experiment. Run BE 13. Epoxide resin 828 + 33.5 % aniline-formaldehyde resin. Specimen precured for 10 minutes at 110°C.

% Energy Absorption. E	Time. t	Temp.°C. T	E	t	T
8	3mins - secs 60		21	8-00	106.0
8	3-45	77.3	20	8-15	106.5
10	4-00	81.0	18	8-50	107.9
11	4-20	84.2	20	9-20	109.0
13	4-45	89.5	22*	10-00	112.2
14	5-15	93.5	22.5	10-15	114.5
15	5-40	96.0	23	10-20	115.8
16	5-50	97.5	22*	10-45	116.8
17	6-00	98.2	22*	11-00	118.5
19	6-15	99.6	21	11-30	119.0
20	6-35	101.5	19	12-10	120.0
End of heating-up period			19	12-30	121.5
Isoelastic run begins.			21	13-00	124.2
22*	6-50	102.2	22*	13-10	125.8
22*	7-00	103.5	22*	13-30	127.8
22*	7-15	104.2	22*	13-50	129.0
22*	7-30	105.0	22*	14-00	130.0
22*	7-45	105.8	Run continues thus for a further 58 minutes.		

* Denotes isoelastic points as plotted in Figure 46.

Glossary of Symbols.

B	Initiator concentration in percent.
β	Fractional conversion of the total unsaturation present.
c	Subscript denoting the critical condition (gel point).
DP_n	Number average degree of polymerisation.
DP_w	Weight average degree of polymerisation.
E	% Energy Absorption as measured by ball rebound.
F	Molar concentration of PEF fumarate unsaturation.
k	Reaction rate constant (with appropriate subscript).
M	Molar concentration of methyl methacrylate monomer.
R	Feed ratio- fumarate/methacrylate (= F/M).
r_F	PEF monomer reactivity ratio.
r_M	MMA monomer reactivity ratio.
t	Time.
T	Temperature °C.
T_g	Second order transition temperature (dilatometric).
T_m	Temperature at which maximum energy absorption occurs.
T_{50}	Temperature at which energy absorption E = 50%.
ρ	Fraction of fumarate links incorporated into a methyl methacrylate polymerisation chain.
ϕ	Fraction of fumarate double bonds originally present which have reacted.

References.

1	Ellis.	U.S. patent. 2,195,362 (1936).
2	Morgan (Editor).	Glass reinforced plastics. Iliffe & Sons, London, 1954.
3	Symposium.	Ind.Eng.Chem.,1613-1645, 1954.
4	McMillan.	Ph.D.Thesis, Glasgow University, 1957.
5	Flory.	(a) J.A.C.S., 67, 441, 1945. (b) J.Phys.Chem., 46, 132, 1942.
6	Stockmayer.	(a) J.Chem.Phys., 11, 45, 1943. (b) -"- , 12, 125, 1944.
7	Walling.	J.A.C.S., 67, 441, 1945.
8	Simpson and Holt.	J.Pol.Sci., 18, 325, 1955.
9	Symposium.	Ind.Eng.Chem., 48, 72, 1956.
10	Drummet et al.	Reference 9, page 76.
11	Bennet & Averell.	Chem.& Ind., 936, 1952.
12	Dietz et al.	Reference 9, page 75.
13	Fineman.	Can.J.Research.,25B, 101,1947.
14	Brugel & Farbe.	Lach., 58, 475 & 523, 1952.
15	Leonard.	J.Acoust.Soc.America,12,241,1940.
16	Schultz-Grünow & Weymann.	Koll.Zeit., 131,61, 1953.
17	Zener.	Elasticity and Anelasticity of Metals. Chicago University Press, 1948.
18	Richards & Pratt.	Trans.Far.Soc., 49, 744, 1953
19	Ferry.	Koll.Zeit., 148, 1, 1956.
20	Tobolsky.	J.Appl.Phys., 27, 673, 1956.
21	Müller.	Reference 67, page 215.

22	Stavermann.	Koll.Zeit., 134, 189, 1953.
23	Bueche.	J.Chem.Phys., 22, 603, 1954.
24	Wolf & Schmeider.	Koll.Zeit.,127, 65, 1952.
25	Chuikin.	Zh.Tekh.Fiz., 25, 595, 1955.
26	Alfrey.	Mechanical Behaviour of High Polymers, Interscience, 1948.
27	Maxwell.	Phil.Trans., 157, 52, 1867.
28	Debye.	Polar Molecules, Dover Publications, N.Y., 1955.
29	Reddish.	Trans.Far.Soc., 46, 459, 1950.
30	Menary et al.	J.Chem.Soc., 2232, 1948.
31	Signer & Berneis.	Makromol.Chem.,8, 268, 1952.
32	Umstätter.	Makromol.Chem.,10, 30, 1953.
33	Muskat & Wyckoff.	The flow of homogeneous fluids through porous media., McGraw-Hill, London, 1937.
34	Gordon & Macnab.	Trans.Far.Soc., 49, 31, 1953.
35	Gordon & Roe.	J.Pol.Sci., 21, 27, 1956.
36	Bamford & Dewar.	Proc.Roy.Soc.A., 197, 356, 1949.
37	Carothers & Arvin.	J.A.C.S., 51, 2570, 1929.
38	Brownlie.	J.Sci.Inst., 27, 215, 1950.
39	Bevington et al.	J.Pol.Sci., 14, 463, 1954.
40	Nichols & Flowers.	Ind.Eng.Chem., 42, 292, 1950.
41	Skellon & Wills.	The Analyst., 73, 78, 1948.
42	Peat.	Quantitative Analysis, Vogel. (Second edition) page 332.
43	Baysal & Tobolsky.	J.Pol.Sci., 9, 171, 1952.
44	Matheson et al.	J.A.C.S., 71, 497, 1949.

45	Batzer & Mohr.	Makromol.Chem., 8, 217, 1953.
46	Feuer et al.	Ind.Eng.Chem., 46, 1643, 1954.
47	Flory.	Principles of Polymer Chemistry. Cornell University Press, New York, 1953., page 320.
48	Gordon et al.	Trans.Far.Soc., 52, 1012, 1956.
49	Jacobsen & Stockmayer.	J.Chem.Phys., 18, 1600, 1950.
50	Bellamy.	Infrared spectra of complex molecules. Methuen, London, 1954.
51	Brauer et al.	Modern Plastics, 34, 153, 1956.
52	Mackay & Melville.	Trans.Far.Soc., 45, 329, 1949.
53	Simpson & Holt.	J.Pol.Sci., 18, 335, 1955.
54	Stockmayer.	J.Chem.Phy., 11, 45, 1943.
55	Morris & Schnurmann.	Nature, 160, 674, 1947.
56	Trommsdorf et al.	Makromol.Chem., 1, 169, 1948.
57	Smith & Norrish.	Nature, 150, 336, 1942.
58	Gordon et al.	J.Pol.Sci., 18, 497, 1955.
59	Cass & Burnett.	Ind.Eng.Chem., 46, 1619, 1954.
60	Vale.	Reference 2, page 41.
61	Simpson et al.	J.Pol.Sci., 10, 489, 1953.
62	Gordon.	J.Chem.Phys., 22, 610, 1954.
63	Haward.	J.Pol.Sci., 14, 535, 1954.
64	Flory.	J.A.C.S., 63, 3083, 1941.
65	Stockmayer.	J.Chem.Phys., 12, 125, 1944.
66	Walling.	J.A.C.S., 67, 441, 1945.
67	Symposium.	Das Relaxationsverhalten der Materie., Koll.Zeit., 134, 1953.
68	Trommsdorf.	Makromol.Chem., 13, 76, 1954.

69	Barr.	Reference 9, page 72.
70	Jenkel & Klein.	Z.Naturforschung, 7a, 619, 1952.
71	Edgar.	J.C.S., 2638, 1952.
72	Bishop.	J.Appl.Chem., 6, 256, 1956.
73	Tillet.	Proc.Phys.Soc.B., 67, 677, 1954.
74	Bunn & Howells.	Nature, 174, 549, 1954.
75	Staverman et al.	Proc.2nd.International Conf. Rheology., New York, 1954.
76	Hoff et al.	J.Pol.Sci., 18, 161, 1955.
77	Heijboer.	Koll.Zeit., 148, 36, 1956.
78	Dilke.	Private communication.
79	Walter & Redding.	J.Pol.Sci., 21, 551, 1956.
80	Fox & Flory.	J.Applied.Phys., 21, 581, 1950.
81	Symposium.	Reference 67, page 3.
82	Russell.	Private communication.